Couplage d’une agression électromagnétique à un réseau d’antennes de type actives

Effects of jamming on active antenna arrays

Direction des applications militaires
Centre de Gramat
Vulnérabilité des systèmes et efficacité des armements

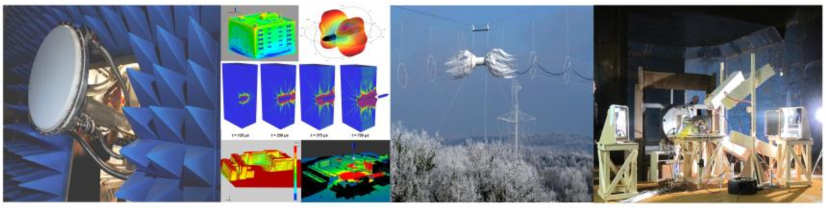

GELIS Gabriel

Maître d’apprentissage : DIOT Jean-Christophe, CHAULOUX Antoine
Ou Responsable de stage
Tuteur enseignant (ENSIL-ENSCI) : ZANINETTI Jacques
Advisor (Polito) : PIRINOLI Paola

Dates de stage : 11/03/2019 au 09/09/2019
Formation suivie : Electronic & Telecommunications /Embedded Systems
Etablissement : ENSIL-ENSCI + Politecnico di Torino

Stage effectué au CEA/Gramat

Double degree with ENSIL-ENSCI in Limoges and Il Politecnico di Torino.

Visa de l'entreprise		
Entité	**date**	**visa**
Maitre d'apprentissage ou Responsable de stage NOM Prénom	26/08/2019	
SERE Chef du laboratoire LMFP RIBIERE-THARAUD Nicolas	04/09/2019	Nicolas Ribière-Tharaud Chef du Laboratoire Micro-ondes de Forte Puissance
Responsable de l'unité de communication et affaires publiques (UCAP) : PUECH Roland	26/08/2019	Roland Puech CEA/Gramat/UCAP

Diffusion :

- Maître de stage : 1 ex
- Tuteur enseignant : 1 ex
- Le stagiaire : 1 ex
- UCAP : 1 ex

Acknowledgements

First of all, I would like to say thank you to Sir. TORTEL Stéphane the service chief and Mr. RIBIERE-THARAUD Nicolas to have welcomed me to their unity and laboratory.

I would like to thank my advisor, Dr. Jean-Christophe DIOT, for his support, his patience and his advices during my internship.

I also want to show my gratitude for my second advisor Dr. Antoine CHAULOUX who followed and assisted me when I needed it. His devotion for his job taught me lots of things.

Then, I thank my office colleague who I could talk with and asked questions about the thesis. His job's passion made me understand how to run it.

Moreover, I would like to say thank you to the people who I may forget and who was close to me during these six months.

Hence, thanks to everyone I reached my goal to properly write my thesis as well as my report in perfect conditions.

Abstract

Radiating antennas are usually designed in order to operate within a particular frequency range strongly dictated by the application it belongs to. However it appears that when considered across very wide frequency ranges (ie various decades), antennas may exhibit unexpected behaviors such as substantial radiation patterns or reflection coefficient variations. It is then conceivable that an antenna exposed to electromagnetic field signal out of its operational frequency range may present dramatically high gain. In other words the antenna might not filter this signal. This *out-of-the-band* aspect needs to be studied.

Keywords: Microstrip antenna; Patch Antenna; Radiation patterns; Wideband Patch Antenna;

Content

Introduction

The CEA/Gramat studies vulnerabilities of electronic equipment potentially exposed to electromagnetic perturbations. Electromagnetic waves may interact with the system through different inputs. Antennas could be one of them it is as a consequence necessary to evaluate the probability an electromagnetic signal can flow through this input as function of different parameters (frequency, spatial position, antenna topology …)

The first chapter is dedicated to the antenna theory. This bibliographical overview aims to list the important antenna characteristics. Within those features the realized gain, the adaptation and the bandwidth are of interest. This overview also enables to enumerate the existing antennas. In this project the involved antennas are the ones called patch antennas.

The next chapter is devoted to simulations and realizations about single patch antennas and their array disposition. Moreover, in this section the single patch antennas are listed and one of them is chosen. The same methodology is indeed applied for the array arranging. For both single antenna and antenna arrays their raised issues are depicted. Finally, to prepare the statistical approach arrays are deeply discussed.

The last chapter is pledged to the statistical study. The selection of faithful arrays enables to examine the filtering capabilities within broadband frequency ranges. Results are observed with respect to the different arrays, different gain threshold and different illumination angle.

1. PRESENTATION DE L'ORGANISME

1.1 LE CEA

1.1.1 GENERALITES

Le CEA (Commissariat à l'Energie Atomique et aux Energies Alternatives) est un établissement public industriel et commercial (EPIC) de droit privé. Ce statut lui permet d'avoir des activités avec différentes sociétés privées ou publiques tout en étant financé par l'état français.

Le CEA a été créé en 1945 sous l'ordonnance du général Charles De Gaulle. Il a pour but de réaliser les recherches sur le nucléaire et la maîtrise de l'atome. Il intervient ainsi dans quatre grands domaines de recherches : la défense, les énergies décarbonées, les technologies pour l'information et la santé, et la recherche fondamentale.

Il existe 9 centres de recherche CEA répartis sur le territoire français (Figure 1) (le centre Paris-Saclay comprend les sites de Saclay et de Fontenay aux Roses). Certains de ces centres sont rattachés à la DAM (Direction des Applications Militaires) et d'autres sont liés aux applications civiles. Six PRTT (Plates-Formes Régionales de Transfert Technologique – (Hauts de France-Lille ; Grand Est-Metz ; Provence-Alpes-Côte d'Azur-Cadarache Gardane ; Occitanie-Pyrénées Méditerranée-Toulouse ; Nouvelle-Aquitaine-Bordeaux ; Pays de la Loire-Nantes)) appartenant au Pôle Recherche Technologique du CEA (CEA Tech) ont été créées en région, elles se rajoutent aux deux « bases arrières » historiques du CEA Tech de Saclay et de Grenoble.

1.1.2 LES DIRECTIONS OPERATIONNELLES DU CEA

Ces 9 centres travaillent au profit de quatre directions opérationnelles (cf. Figure 1) :

La DEN : Direction de l'Energie Nucléaire dont les travaux se rapportent aux systèmes nucléaires du futur, à l'optimisation du nucléaire industriel et au développement et à l'exploitation d'outils expérimentaux et de simulations (centre de Paris Saclay, Cadarache et Marcoule),

La DRT : Direction de la Recherche Technologique, qui se concentre sur les micro et nanotechnologies, les nouvelles technologies de l'énergie et les nanomatériaux ainsi que sur les systèmes numériques intelligents (centre de Grenoble),

La DRF : Direction de la Recherche Fondamentale qui réalise la recherche des effets et applications du nucléaire au médicale (radiothérapie, marquage biomoléculaire,…) et qui effectue la recherche fondamentale (centre de Paris Saclay : site de Saclay et site de Fontenay aux Roses),

La DAM : Direction des Applications Militaires qui est le pôle Défense et Sécurité du CEA. La DAM travaille sur les armes nucléaires, la matière nucléaire et l'impact sur l'environnement, la sécurité et la non-prolifération ainsi que sur la défense conventionnelle (centres DAM/Direction Ile de France (DIF), Cesta, Valduc, Le Ripault et Gramat).

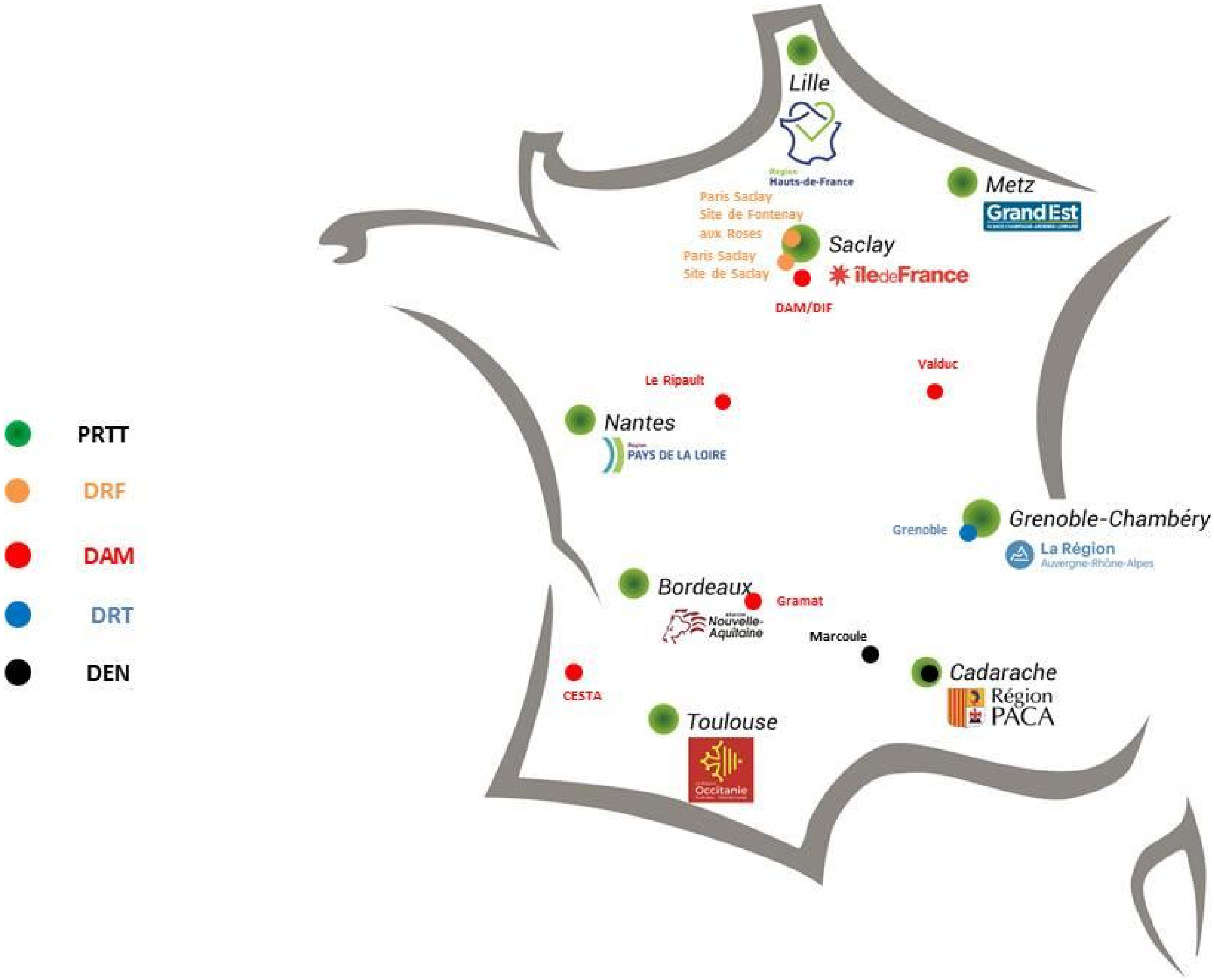

Figure 1 : Carte des centres CEA et des PRTT

1.1.3 LE CEA EN CHIFFRES (EXTRAIT DU DOCUMENT « LE CEA EN CHIFFRES - DONNEES 2018 »)

Le CEA comprenait en 2018, 19 925 collaborateurs dont 16 096 salariées CDI (contrat à durée indéterminée), 1 015 salariés en CDD (contrat à durée déterminée), 1 181 doctorants, 170 post-doctorants, 1 138 alternants et 325 autres salariés.

Les ressources financières sont de 5,3 milliards d'euros (1,8 Md€ activités défense, 2.2 Md€ activités civiles et 1,3 Md€ opérations assainissement et démantèlement).

Les partenariats académiques sont mis en œuvre via 46 UMR (Unité Mixte de recherche, 4 UMS (Unités Mixtes de Service), 1 USR (Unité de Service et de Recherche), 54 accords-cadres avec les écoles et universités et 5 alliances thématiques de recherche (Aviesan (Alliance nationale pour les sciences de la vie et de la santé), Ancre (Alliance nationale de coordination de la recherche pour l'énergie), Athena (Alliance nationale des sciences humaines et sociales), Allistene (Alliance des sciences et technologies du numérique) et Allenvi (Alliance nationale de recherche pour l'environnement).

Le CEA est le seul organisme de recherche français au top 100 mondial des acteurs de l'innovation (Classement Clarivates), le 1er organisme de recherche déposant des brevets en Europe (Source Office Européen des Brevets) et le 1er organisme de recherche déposant de brevets en France (Source INPI (Institut National de la Propriété Industrielle). En 2018, 704 dépôts de brevets prioritaires ont été enregistrés sur une famille active de 6700 brevets. 70% des 211 start-ups créées par le CEA depuis 1972 et 79% des 148 start-ups créées depuis l'an 2000 sont en activité.

Enfin, le CEA a émis 5 045 publications scientifiques en 2018.

1.2 LE CEA/GRAMAT

1.2.1 L'HISTOIRE DU CENTRE

C'est en 1946 que le site de Gramat, situé au sein du parc naturel régional des causses du Quercy dans le Lot, est retenu pour implanter, dans le gouffre de Bèdes, des bancs d'essais de propulseurs de grande puissance (V2), essais qui n'ont jamais eu lieu.

En 1956, le site devient le polygone d'expérimentations de la section atomique de la DEFA (Direction des Études et Fabrication d'Armement) et accueille les premiers essais liés au fonctionnement détonique des armes nucléaires.

En 1959, le site devient le CEG (Centre d'Etudes de Gramat), dépendant de la DGA (Délégation Générale pour l'Armement). En 1965, les études de durcissement mécanique puis électromagnétique débutent. À partir des années 1970, le centre s'ouvre sur le domaine des armes conventionnelles.

C'est en janvier 2010 que le CEG de la DGA a rejoint le CEA. Il devient ainsi le neuvième centre du CEA et le cinquième centre de la DAM.

Le site s'étend aujourd'hui sur 325 hectares et emploie 260 salariés ainsi que des stagiaires, apprentis, thésards et sous-traitants. Il est le centre de référence pour l'étude de l'efficacité des armements et de la vulnérabilité des systèmes aux effets des armes conventionnelles et nucléaires.

1.2.2 DOMAINE D'ACTIVITE

Les activités du CEA/GRAMAT se concentrent autour de trois domaines :

- Le nucléaire de défense (50%)
- La défense conventionnelle (45%)
- La sécurité globale (5%)

Dans chacun de ces cas, le centre est spécialisé dans l'étude de la vulnérabilité des armes et systèmes de défense.

Le nucléaire de défense vise à étudier les effets du rayonnement, du souffle, du flash thermique et des agressions électromagnétiques d'origine nucléaire.

Les recherches en défense conventionnelle permettent le développement des compétences en physique des explosifs, détonique, balistique terminale et en vulnérabilité des structures. Dans le domaine électromagnétique, elles ont pour but d'évaluer l'impact des menaces futures que pourraient représenter les AGREMI (Agressions électromagnétiques intentionnelles).

Enfin, la sécurité globale a pour objectif d'étudier la sécurité des infrastructures civiles ou militaires face aux actes malveillants, aux accidents ou aux catastrophes naturelles.

1.2.3 ORGANISATION DE L'ENTREPRISE

Le DEA (Département Effets des Armes) constitue l'organe principal de production technique du centre et est divisé en différents services, lesquels sont sous divisés en différents laboratoires.

Along my internship I was integrated to the SERE service inside the LFMP Laboratory (The High Power Microwaves Laboratory)..

2. INTRODUCTION ABOUT ANTENNAS

This first chapter deals with the general definition of antennas. From the bibliography passing through some public papers a range of antennas is studying. By the end only one antenna is selected to be produced. This antenna is decided on some expectations extracted by the antenna's characteristics.

2.1 WHAT IS AN ANTENNA?

An antenna is basically defined as an electrical transformer: either it transforms electrical energy to electric/magnetic fields or it receives electric/magnetic fields and converts them to electrical variables – current/voltages. Therefore, an antenna relies on the « principle of reciprocity »: it can either emit or receive signal.

A relevant question would be: «how does the mechanism of radiation work? ». An illustration – based on a single wire – will be taken to properly explain this functionality.

Cylindrical conducting wires may be characterized by its motion of electric charges as well as its creation of current flow.

$$l.\frac{dI_z}{dt} = lq_l\frac{dv_z}{dt} = lq_l a_z$$

Where: $l\ is\ the\ length\ of\ the\ wire\ (meters)$;

$q_l\ is\ the\ charge\ per\ unit\ length\ \ (coulomb/m^2)$;

$I_z\ is\ the\ current\ in\ the\ wire\ defines\ as\ q_l v_z\ (ampere)$;

$a_z\ is\ the\ acceleration\ defines\ as\ \frac{dv_z}{dt}\ (meters/sec^2)$;

$v_z\ is\ the\ uniform\ velocity\ (meters/\sec)$;

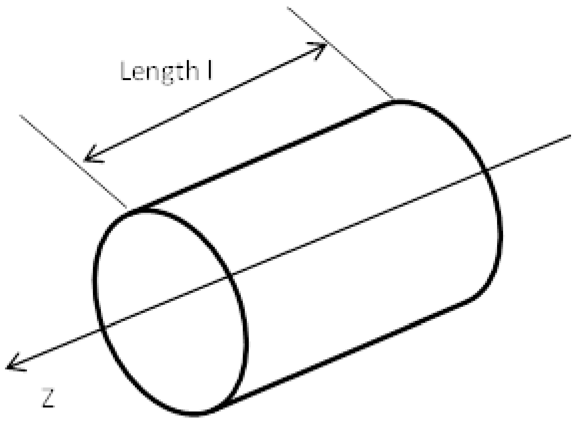

Figure 2: Conducting wire

Note: the axis z is defined along the wire.

The previous equation is the relation between current and charge which states if it needs a time-varying current or an acceleration to create radiations.

Therefore, if the charge q_z is not moving along the wire, the current I_z is not created and then there is no radiation.

Then, if the charge q_z is moving with a uniform velocity there is no radiation if the wire is straight and infinite. However there is radiation if the wire is curved, bent or discontinuous.

Finally, if the charge q_z is oscillating in a time-varying, even the wire is straight a radiation exists.

2.2 ANTENNA FROM CIRCUIT VIEW

An antenna is composed of a resistance and a reactance. Therefore its complex impedance is equal to R + j .X; note the fact that the R and the X are both depending on the frequency.

Here is the equivalent circuit for an antenna:

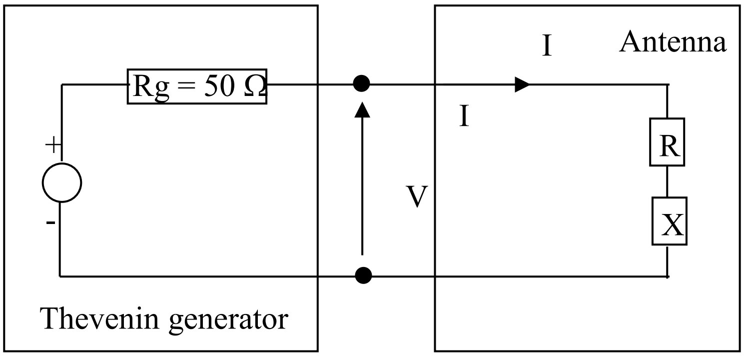

Figure 3: Figure of circuit view antenna

P_g: power from the generator

$P_g = \frac{1}{2}EI^*$ more precisely: $P_g = Re(E_g)$

This power is delivered to the charge (antenna) and also in its inner resistance.

P_a: power which is accepted by the charge

$P_a = \frac{1}{2}VI^*$ where $P_a = \frac{1}{2}\frac{E^2(R+jX)}{(R_g+R)^2+X^2}$; therefore P_a is maximum where X=0 and R=R_g

P_i is the incident power: this is the power provided to an adaptive charge – no reflection

P_r is the reflected power by the antenna

Impedance at high frequency

At high frequency, the input impedance cannot be measured.

Therefore measured impedance is expressed with the reflection coefficient and the characteristic impedance by the transmission line – between the generator and the charge.

Thus, we obtain: $Z = Z_c \frac{1+S_{11}}{1-S_{11}}$ where generally Z_c is equal to 50Ω.

Moreover the reflection coefficient S_{11} can be expressed with the reflected power by the incident power: $|S_{11}|^2 = \frac{Reflected\ power}{Incident\ power}$

Consequently, the reflection coefficient can be derived in dB

$$|S_{11}|_{dB} = 10\log(|S_{11}|^2) = 10\log\left(\frac{P_r}{P_i}\right) \text{ or } |S_{11}|_{dB} = 20\log(|S_{11}|) = 20\log\left(\frac{V_r}{V_i}\right)$$

The antenna is considered as well adapted when $10\log(|S_{11}|^2) < -10\ dB$ or greatly adapted when $10\log(|S_{11}|^2) < -20\ dB.$

The ratio between the maximum voltage over the minimum one is defined as the Voltage Standing Wave Ratio – VSWR where VSWR = $\frac{1+|S_{11}|}{1-|S_{11}|}$

The efficiency which links the accepted power and the incident power thus: $Pa = Pi\,.\,v$

But $P_r = \rho^2 P_i = |S_{11}|^2 P_i$ then $v = \frac{P_a}{P_i} = \frac{P_i - P_r}{P_i} = 1 - \rho^2 = 1 - |S_{11}|^2$

And therefore the v represents the adaptation efficiency and then deals with the adapation losses.

Bandwidth:

It is defined where the $|S_{11}|$ parameters is less than –10 dB.

It can also be expressed with two frequencies – the maximum and the minimum one: Δf

Or this bandwidth may be derived compared to the center frequency: $\frac{\Delta f}{f_0}$

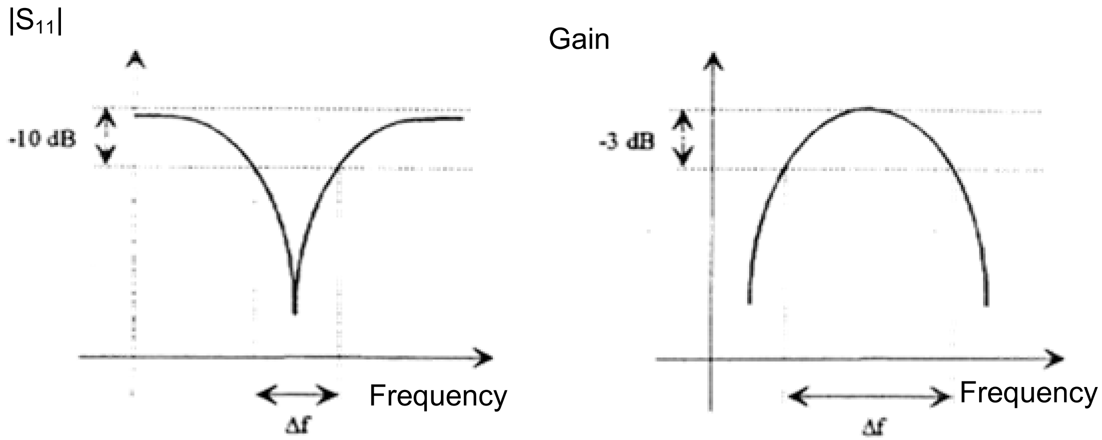

Figure 4: Bandwidth circuit/radiation

. From the circuit view the S_{11} parameter must correlate with the realized gain from the radiating view.

2.3 RADIATION CHARACTERISTICS

Farfield pattern

The expression of the electromagnetic farfield pattern for a surface current of $\vec{J}(M,r)$ for spherical, surface and line distributions have been established previously – see appendix 1.

The expression is related to a source point because we are considering the farfield conditions, indeed far away from the source, spheres look like planes.

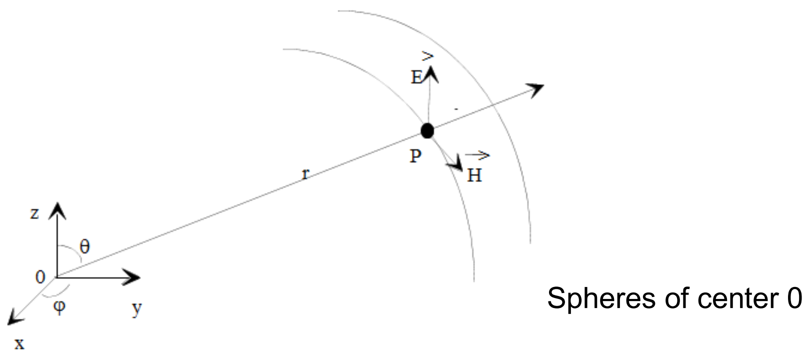

Figure 5: Point source

Moving away from the source the electromagnetic field decreases in 1/r and also depends on the θ and φ angles. Therefore the electromagnetic field can be expressed with two vectors:

$$\vec{e}(x,y,z,t) = \vec{e}(P,t) => \vec{E}(x,y,z) = \vec{E}(P)$$

$$\vec{h}(x,y,z,t) = \vec{h}(P,t) => \vec{H}(x,y,z) = \vec{H}(P)$$

These two vectors belong to a wave plane and are perpendicular to the propagation direction and each other. It means that the considered field is locally a plane wave.

Characteristics about radiated power

1. The Poynting Vector

The Poynting Vector is defined as $\vec{P} = \frac{1}{2}\vec{E} \wedge \vec{H}^*$ where its direction is the same as the propagation one.

Therefore, the total radiated power is equal to the Poynting Vector flow across a closed surface around the source. As an example, Fig 6 depicts a sample of sphere locally considered as a plane wave.

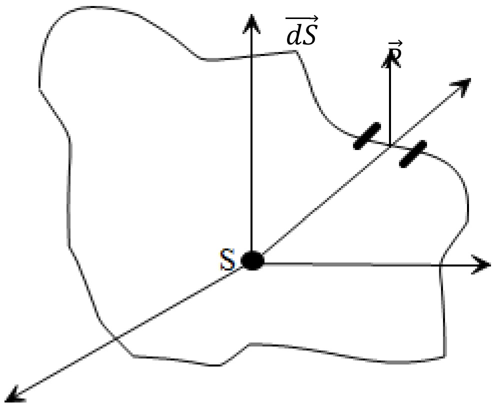

Figure 6: Source and Poynting Vector

Hence, the radiated power may be defined in two different ways:

Using the Poynting Vector

$P_r = \iint_{sphere} \vec{P} \cdot \vec{dS} = \iint_{sphere} |\vec{P}| dS$ where $|\vec{P}| = \frac{1}{2}|\vec{E} \wedge \vec{H}^*| = \frac{1}{2}\frac{E^2}{\eta} = \frac{1}{2}\eta H^2$

Mathematically

$P_r = \iint_{sphere} \frac{dP}{dS} \cdot dS = \iint_{sphere} dP_s \cdot dS$ where $\frac{dP}{dS} = dP_s = surface\ density\ power$

2. The Surface Density Power

Considering the two previous relations we thus obtain:

$$dP_s = |\vec{P}| = \frac{1}{2}|\vec{E} \wedge \vec{H}^*| = \frac{1}{2}\frac{E^2}{2\eta} = \eta\frac{H^2}{2}$$

Consequently, dP_s depends on R because both E and H also depend on it. Hence it is really interesting to use this formula to characterize an antenna. To design an antenna the electromagnetic fields are indeed frequently exploited.

3. The Spherical Density Power (DP)

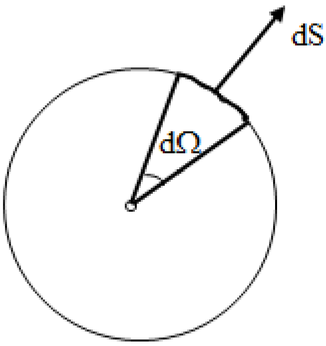

Figure 7: Angle solid

In order to facilitate the calculations, the total radiated power is represented by surface unit herself defined by a solid angle unit.

$$P_r = \iint_{4\pi\ steradian} dP_\Omega \cdot d\Omega = \int_{sphere} dP_S \cdot dS$$

But, $d\Omega = \frac{dS}{R^2}$

$$P_r = \iint_{4\pi\ steradian} dP_\Omega \cdot d\Omega = \int_{sphere} dP_S \cdot R^2 \cdot d\Omega$$

$$dP_\Omega = R^2 dP_S \ with \ dP_S = R^2 \cdot \frac{E^2}{2\eta}$$

Furthermore, $E^2 = \frac{e^2}{R^2}$ the field consequently depends on R which is not the case for$dP_\Omega = \frac{e^2}{\eta}$

Hence, dP_Ω depends on θ and φ, that is why density power is mainly used to characterize the antenna's radiation.

It expresses the radiated energy in a given direction: $dP_\Omega(\theta, \varphi)$

Efficiency

The efficiency for an antenna is defined as $\frac{P_r}{p_a} = \frac{G_{intrinsic}}{D}$; the efficiency is equal to 1 when the antenna is lossless and the gain is thus equal to the directivity.

The realized gain, takes into account the adaptation, can be defined as:

$$G_{realized}(\theta, \varphi) = \frac{dP_{\Omega}(\theta,\varphi)}{\frac{P_g}{4\pi}} = \left(1 - {S_{11}}^2\right) \cdot G_{intrinsic} \text{ since } P_a = \left(1 - {S_{11}}^2\right) \cdot P_g$$

Power budget

The power budget considers all the losses between a receiver and a transmitter. It is known as Friis formula.

Conditions: Farfield; Lossless; Narrowband signal

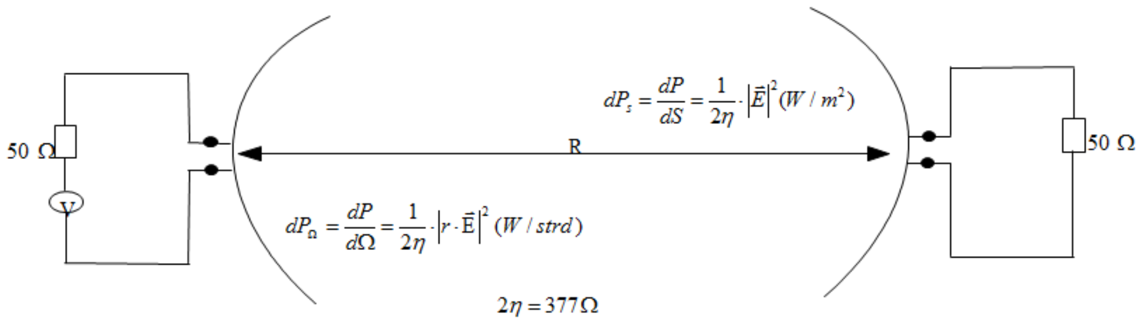

Figure 8: Link between a receiver and a transmitter

$$P_{RX} = P_{TX} \cdot g_T \cdot g_R \cdot \chi \cdot Af_S \cdot A_{add}$$

Where $P_{RX}$is the available power at RX

P_{TX} is the emitted power $\quad g_T \text{ and } g_R$ are the gains of the antennas

X is the depolarization loss which is equal to $|\widehat{p_T} \cdot \widehat{p_R}|^2$

Af_S is the free-space loss equal to $\left(4\pi\frac{R}{\lambda}\right)^{-2}$

A_{add} are the additional losses :

- Atmospheric absorption
- Fading
- Diffraction by obstacles
- Ground reflection

Then with our conditions - $\chi = 1\ and\ A_{add} = 1$ - the previous equation becomes:

$$P_{RX} = P_{TX} \cdot g_T \cdot g_R \cdot Af_S$$

Therefore, with $Af_S = \left(4\pi \frac{R}{\lambda}\right)^{-2}$ the Friis formula is:

$$P_{RX} = \left(4\pi \frac{R}{\lambda}\right)^{-2} \cdot P_{TX} \cdot g_T \cdot g_R$$

The EIPR - Effective (equivalent) Isotropically Radiated Power – represents the radiated power that could have been radiated in an isotropic way.

$EIRP = g_T \cdot P_{TX}$ where g_T is the realized gain and P_{TX} is the radiated power.

2.4 CHARACTERISTICS OF ANTENNAS

Such a sophisticated device offers many different performances that are characterized following parameters here summarized.

2.4.1 RADIO-FREQUENCY BANDS

The Radio-Frequency band represents the operating frequency spectrum where the antenna is used. For microwave domain there are 7 different bands.

Here it is the list:

- L-band : 1-2 GHz
- S-band : 2-4 GHz
- C-band : 4-8 GHz
- X-band : 8-12 GHz
- Ku-band : 12-18 GHz
- K-band : 18-26 GHz
- Ka-band : 26-40 GHz

.

2.4.2 BANDWIDTH

The antenna bandwidth represents the frequency band where the antenna operates: within this band the performances of the antenna have to remain as constant and as satisfactory as possible. Usually this band is defined as a percentage of the carrier/center frequency.

One can consider a carrier frequency equal to 5 GHz with 30 percent bandwidth. It means the frequency bandwidth is equal to 1.5 GHz around 5 GHz = 3.5 – 6.5 GHz.

It exists two kinds of bandwidth; the first one is defined for the gain at – 3 dB where the radiated power is linearly divided by two, then the second bandwidth is defined by the adaptation (at least – 10 dB in the case of the present study). For the narrow band applications it needs to meet these two previous conditions to guarantee the good functionality of this antenna.

2.4.3 DIRECTIVITY/GAIN/POLARIZATION

The directivity D of a non-isotropic source is the ratio between its radiation intensity in a given direction over an isotropic source. In mathematical form it gives:

$$D = \frac{U}{U_0} = \frac{4\pi U}{P_{rad}} \; where \; P_{rad} \; represents \; the \; total \; radiated \; power \; (W)$$

In other words the directivity is the capability of the antenna to concentrate the radiated power in a given direction. This is computed without any losses.

The gain G of an antenna is an actual or realized quantity which is defined as the ratio between the radiation intensity over the total input power. This means the gain is always less than the directivity because it takes into account input losses.

Mathematically the gain is equal to:

$$G_{axis} = \frac{E^2 \cdot 4\pi \cdot d^2}{Z_0}$$

where E^2 is the normalized power pattern

Z_0 is the intrinsic impedance of space : $Z_0 = 120\pi = \frac{\mu_0{}^{1/2}}{\varepsilon_0} = 377\ \Omega$

D is the distance (in farfield conditions)

The polarization of an antenna is the electric field orientation with respect to the propagation direction. There are linear, circular and elliptical polarizations.

The linear polarization describes the electric-field (magnetic-field) vector at a given point in space where this vector is always oriented in a same direction at every period of time.

The circular polarization describes the electric-field (magnetic-field) vector at a given point in space where this point traces a circle as function of time.

The elliptical polarization describes the electric-field (magnetic-field) vector at a given point in space where this point traces an elliptical curve as function of time as well.

2.4.4 RADIATION PATTERN LOBES

A radiation pattern can be composed – depending on which antennas are used – of several kinds of lobes. There are mainly three types of lobes: the main, the side and the back ones.

The main lobe is the lobe in the axis propagation direction where the side and back ones can be differently oriented.

Generally a lobe is stated in a spherical space with the z-axis which is usually the direction of the propagation and two angles called theta and phi.

Therefore, an additional characteristic might be defined: the beamwidth. It is the angular range within the radiated power is greater or equal to half maximum power.

2.4.5 SIZE CONSTRAINTS

The size of the antenna is usually dictated by its frequency. The lower the size the higher the frequency is.

2.4.6 FEEDING TECHNICS

There are different ways to energize an antenna. Some are cumbersome others are easy to implement. It is an important process step that antenna designers may pay a lot of attention to.

The possible feeding technics will be detailed in the 3.5.1 part.

2.4.7 ANTENNA EFFICIENCY

The antenna efficiency takes into account all losses as reflection losses, conductivity losses, dielectric losses…

Finally, the formula for the total efficiency is:

$e_0 = e_{cd} * (1 - |\Gamma|^2)$ *where* Γ *is the reflection coefficient at the input terminal*

2.4.8 POWER RANGE - µW/GW

Antennas can be exposed or used to radiate very high power. The type of power directly influences the design of the antenna:

- Continuous power may induce high temperatures, fully metallic structures are consequently preferred;
- A pulsed power may lead to dielectric breakdowns. The type of materials is then determinant as well as electromagnetic field values inside of the antenna.

2.5 PATCH ANTENNA

Many kinds of antennas can be conceived. This study only focuses on patch elements.

2.5.1 FUNDAMENTALS AND REVIEWS

A classical patch antenna has usually four common features:

- A very thin flat metallic layout called the patch;
- A dielectric substrate characterized by its dielectric constant and thickness;
- A ground plane which is larger than the patch;
- A feed which provides the radiofrequency power;

The use of patch antenna is becoming more common due to the fact it is easy to be manufactured. Furthermore, it is very robust because it usually has rigid dielectric substrate.

Finally, the main advantage of patch antenna technology is the price as cheap materials are often convenient for realizations.

The patch is radiating thanks to the side effects where in that case need to be maximized. The thickness of the substrate, therefore, should be as high as possible but still in a given interval: usually $0.003*\lambda < h < 0.05*\lambda$; where h represents the thickness. However the dielectric constant ε_r should be as low as possible. Hence, a tradeoff between the thickness of the substrate and its dielectric constant has to be defined.

Consequently, to feed the antenna it exists several ways:

- Microstrip line
- A Coaxial Probe
- A Stripline
- A Coupled Aperture
- CoPlanar Waveguide (CPW)

The microstrip feeding is the cheapest method to feed a patch antenna, in fact the antenna is considered as a transmission line. This impedance line is defined with its width, the thickness and the dielectric substrate. Therefore, this line is chosen after choosing the specifications for the patch antenna while the impedance is equal to 50Ω. Then, it remains to select where to put this line because the point will define the excited mode of the antenna.

The coaxial probe feeding offers several advantages, the probe is settled behind the system which can be easily accessed and the wire is reinforced which avoids certain losses, this is true for thin thickness substrate. On the contrary, for high thickness the induction of the probe seriously affects the bandwidth. Moreover, probes could lead to other problems related to drilling holes and soldering which may disrupt the adaptation.

For the coupled aperture the power transport is realized by an aperture and therefore the aperture positioning with respect to the feedline is difficult to find, this is mainly true in small dimensions. Moreover, the adaptation is also a real problem, in fact the ground plane which contains the aperture can add a parasitic charge and therefore could create mismatch.

The CPW – CoPlanar Waveguide – offers the possibility to have in the same layout the feedline and the ground plane which is an advantage when designing flexible structure for instance. In that feeding case the coupling is ensured by an open circuit at the CPW termination.

Finally, the stripline which is a line settled between two different substrates. The radiation of the line is hence reduced by setting a high dielectric constant for the underneath substrate and a low thickness. On the contrary, for the patch radiation which concerns the upper substrate, the permittivity has to be low and its thickness should be high.

See appendix 2 to better know how these feedings are done.

Generally, a common patch antenna does not have a wideband; in fact, in literacy for simple patch antenna the bandwidth does not exceed 5% of the center frequency. However, by changing the antenna feeding it might be possible to readjust the necessary bandwidth. This point will be discussed in the chapter called “Wideband Patch Antenna”.

2.5.2 EXAMPLE: SIMPLE PATCH ANTENNA – DESIGN

Taking a simple patch antenna it allows understanding how a patch antenna works. Hence, to design a patch antenna, it needs to determine the length and the width of the patch, as well as the positioning of the feedline. The thickness of the substrate is deduced directly from the length and the width.

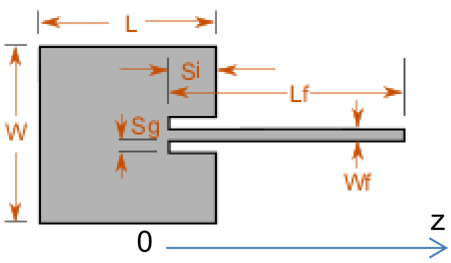

Figure 9: Simple patch antenna

First of all, there are two input resistances to define, the first one is defined as z = S_i and the other one is at z = 0. Therefore, the relation which links these two magnitudes:

$R_{in}(z = S_i) = R_{in}(z = 0) \cdot cos^2(\frac{\pi}{L} \cdot S_i)$ with L the length of the patch

Let's design an antenna with available materials on market. Hence, the thickness h is a multiple of 0.8 mm, then the permittivity $\varepsilon_r = 4.7$ - which is a FR4 material, and finally the center frequency is $f_0 = 3\ GHz$

The first parameter which has to be computed is the width of the patch:

$W = \frac{c}{2f_r} \cdot \sqrt{\frac{2}{\varepsilon_r+1}}$; thus W = 28.64 mm; where c is the light velocity in vacuum

$\varepsilon_{eff} = \frac{\varepsilon_r+1}{2} + \frac{\varepsilon_r-1}{2}\frac{1}{\sqrt{1+12\cdot h/W}} = 4.11$ where h = 1.6 mm

$\frac{\Delta L}{h} = 0.412 \cdot \frac{(\varepsilon_{eff}+0.3)\cdot\left(\frac{W}{h}+0.264\right)}{(\varepsilon_{eff}-0.258)\cdot\left(\frac{W}{h}+0.8\right)} = 0.46$ -> hence ΔL = 0.73 mm

L = L_{eff} - 2ΔL = $\frac{\lambda_g}{2} - 2\Delta L = 21.6\ mm$ where $\lambda_g = \frac{c}{f_r\sqrt{\varepsilon_{eff}}}$

This input resistance at z=0 is: $R_{in}(z = 0) = \frac{1}{2G}$ where $G = \frac{W}{120\cdot\lambda_0}\left(1 - \frac{1}{24}\left(\frac{2\pi h}{\lambda_0}\right)^2\right) = 0.0025$

Thus: $R_{in}(z = 0) = 203\ \Omega$ and $R_{in}(z = S_i) = 50\ \Omega$

Therefore S_i = 7.22 mm

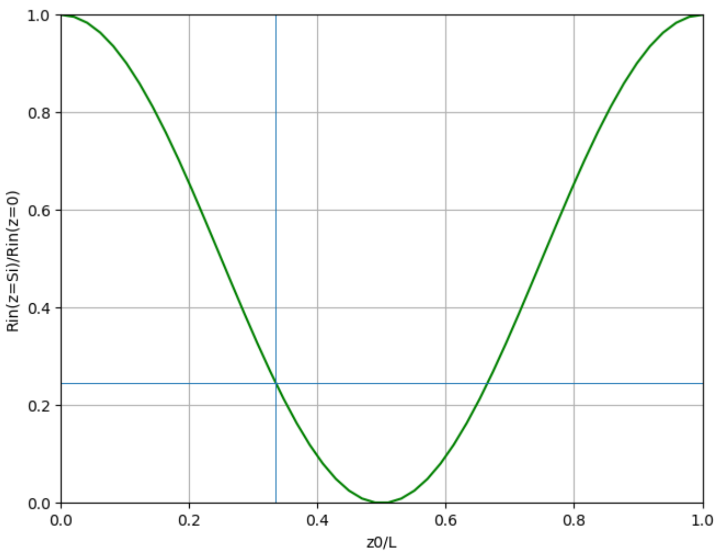

Figure 10 : Inset Feed determination

Using a simulation tool, after designing this simple patch antenna, it is possible to obtain its performances in terms of S_{11} parameter and gain/directivity.

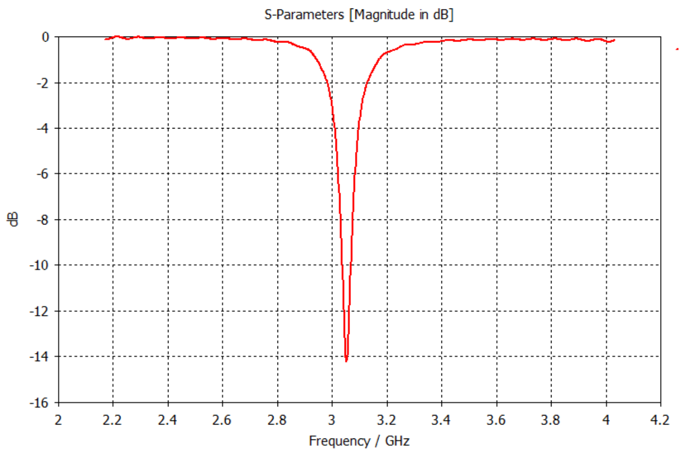

Figure 11 : S11 parameter

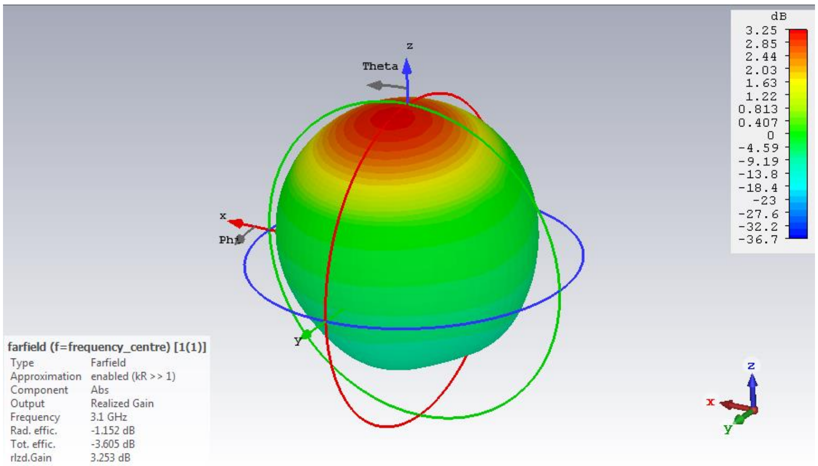

Figure 12 : Farfield at center frequency - 3.25 dB

As it can be observed with the previous model of simple patch, the bandwidth for a very simple is very low. In the example, the bandwidth is 1% of 3 GHz which is very low.

2.5.3 WIDEBAND PATCH ANTENNA – BIBLIOGRAPHY – LISTINGS OF EXISTING ONES

In this chapter, the list of wideband existing patch antenna is done: therefore the center frequency will not correspond to the desired one. It is only a way to show what exists in terms of performance and technology. These standard antennas are adapted to the required center frequency to be used in simulation and to be realized.

2.5.3.1 STUB ANTENNA

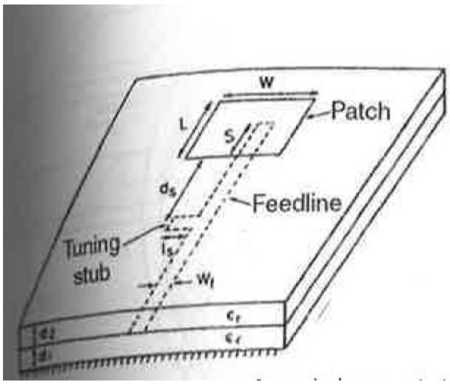

Figure 13: Stub patch antenna

In this antenna there are two stubs, the one is settled at the end of the microstrip just below the patch and the second one is orthogonal to the feedline. The first one may allow centering the adaptation on the Smith chart and the second stub is generally used to obtain a wide bandwidth.

With the same thickness for both substrates and a permittivity equal to 2.2 the literacy gives a bandwidth from 3.375 GHz to 3.855 GHz which represents 13 percent of the center frequency.

By changing the values of these thicknesses and this permittivity the bandwidth of this antenna can be improved still at the same center frequency to 20 percent.

2.5.3.2 A CPW PATCH ANTENNA

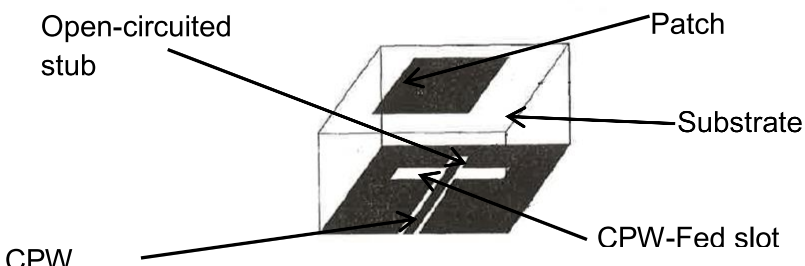

Figure 14: CPW patch antenna

This antenna is composed of only one ground plane which acts as a reflecting ground plane. Into this ground plane there is a cross section aperture used to insert the coplanar waveguide. Therefore, it only needs one substrate which can be assimilated as air medium. At 3.4 GHz, the literacy shows that the bandwidth is almost 36 percent.

2.5.3.3 STACKED SLOT-COUPLED PRINTED ANTENNA

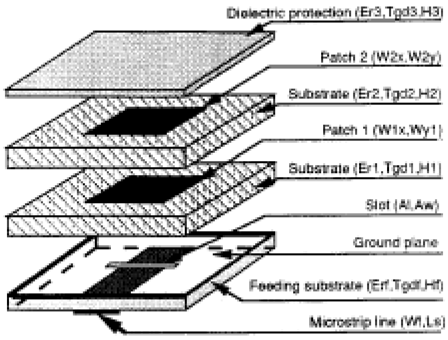

Figure 15: Stacked slot aperture antenna

The stacked slot aperture antenna is composed of two patches, an aperture and a microstrip.

The literacy gives a bandwidth of 26 percent – from 4.6 GHz to 6 GHz. Regarding the directivity, it was settled around from 7.6 to 9 dB.

This antenna is often used as an element in arrays from broadband antennas.

2.5.3.4 A WIDE BAND ANTENNA WITH SLOT IN THE FEEDLINE AND IN THE GROUND PLANE

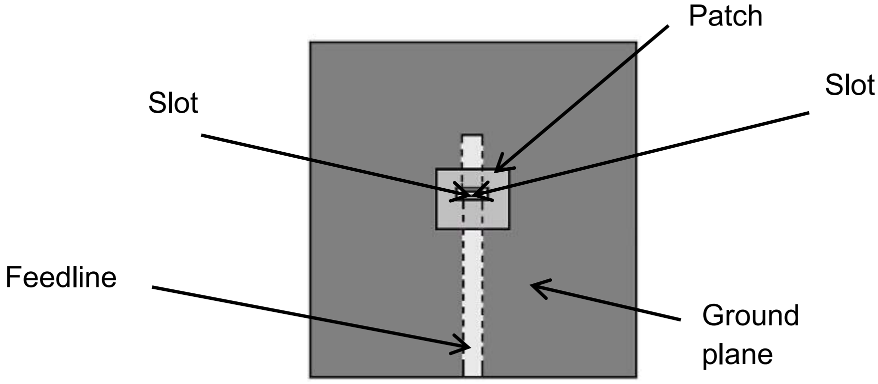

Figure 16: Two slots patch antenna

This kind of antenna is made of two slots; the first one is in the microstrip feedline and the other one is into the ground plane. This technique allows reaching up to 30 percent of bandwidth which is higher than the single patch antenna.

2.5.3.5 AN APERTURE-COUPLING MICROSTRIP ANTENNA

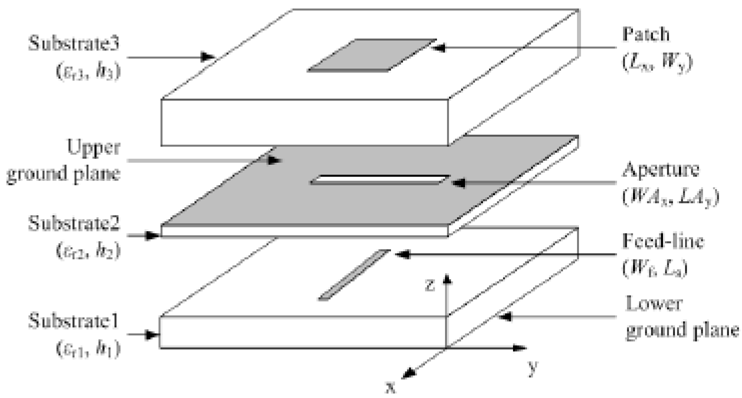

Figure 17: Aperture-coupling patch antenna

The idea in this case is to add vias around the feedline and the aperture to increase the coupling between the patch and the slot. In the publication it was said there are two different structures to be adopted to place the vias. However for the required design only few vias of the previous structure are added to the simulation. The structure of these two via technique is depicted here.

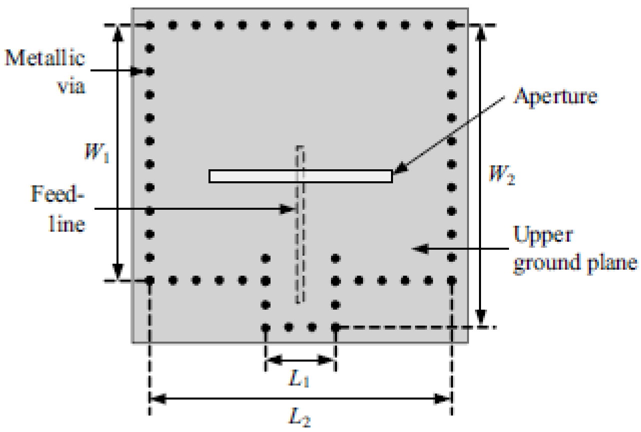

Figure 18: T-shape

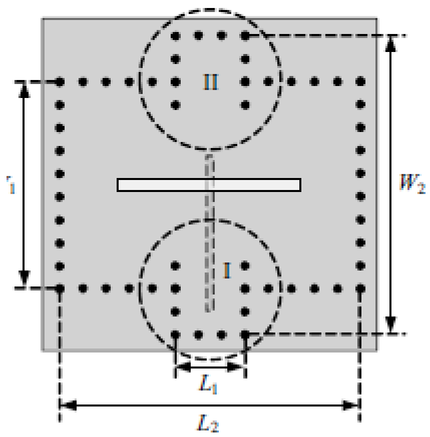

Figure 19: Cross-shape

The paper informs with this technique it is possible to reach a bandwidth from 8.26 GHz to 13.41 GHz which corresponds to a bandwidth of almost 50 percent.

This designed antenna may be easily fabricated and it is compact which is interesting for a patch antenna.

2.6 CONCLUSION ABOUT ANTENNAS

Patch antennas can be designed according to various different ways. Diverse simulations were conducted to reproduce the excepted behaviors and to provide relevant information for the study. All of these are presented on the next of the document.

3. ANTENNA DESIGNS AND REALIZATIONS

In this chapter the requirements for the single antenna are derived. Then, with respect to these expectations one single antenna is selected. Moreover, the array's prerequisites are going to be set and then several arrays are analyzed. The picked array is either used or not to run the statistical study – discussed in the fifth chapter.

3.1 SINGLE PATCH ANTENNA

3.1.1 REQUIREMENTS

To design the single antenna several requirements have been set by using the main characteristics of a generic antenna. Those requirements are presented below:

Gain: in the propagation axis – and at least 7 dB in realized gain

Bandwidth: 600 MHz around 3 GHz which is approximately 20% - within S-band

Center frequency: around 3 GHz

Radiated power: more or less the same in the whole bandwidth +/- 2 dB

Used substrates: standard ones – thickness: multiple of 0.8 mm; permittivity: 4.7 (FR4)

Feeding way: coaxial probes connected behind the antenna in a perpendicular way

Compact and planar antenna: 5cm x 5 cm for the substrate dimensions

The antenna has to be compatible with active antenna array

Impedance adaptation: 50 Ohms

3.1.2 SIMULATED ANTENNAS – CHOSEN ANTENNA

3.1.2.1 WIDEBAND EXISTING ANTENNAS

In this section the existing antennas found in literacy in paragraph 3.5.3. are adapted and simulated at the required frequency. Hence, a frequency scale is done to fully adapt these antennas.

Moreover, the goal is only to find the satisfied requirements and not to find the right feeding way. That is why this section is only focused on the performance in terms of S_{11} parameters and the radiated patterns for each found antenna.

It is enlightened why certain antennas are kept and why some others are dismissed.

The idea is therefore to take the previous found antennas and to apply as said before a frequency scale. Basically this operation consists in multiplying by a coefficient each dimension of the antenna. For instance if the initial antenna works at 10 GHz and it needs to work at 3 GHz, the multiplication coefficient is 10/3. In fact decreasing the frequency increases the characterized lengths.

The simulations for the found antennas are carried out using CST Microwave software that enables to design and simulate electromagnetic projects.

3.1.2.1.1 Wideband patch antenna: double apertures

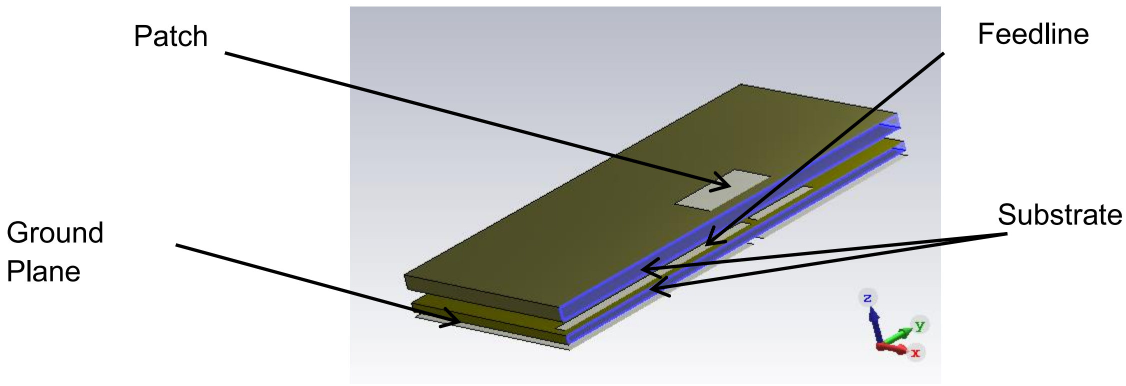

Figure 20: View of double aperture patch antenna

This antenna is called double apertures because it has a first aperture on the ground plane and a second one in the feedline: the feedline is therefore made of two pieces.

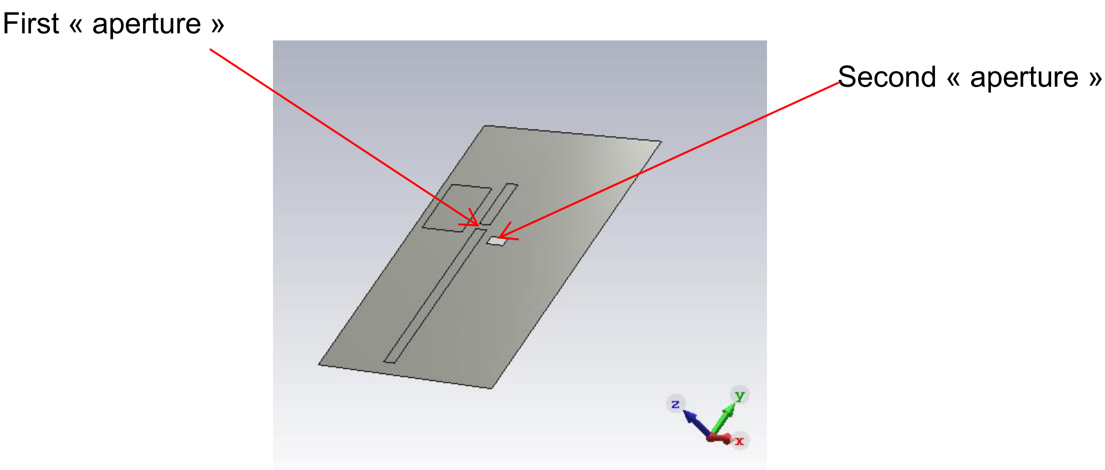

Figure 21: Double aperture antenna

By running the simulation the S_{11} parameters can be found as well as the radiated patterns.

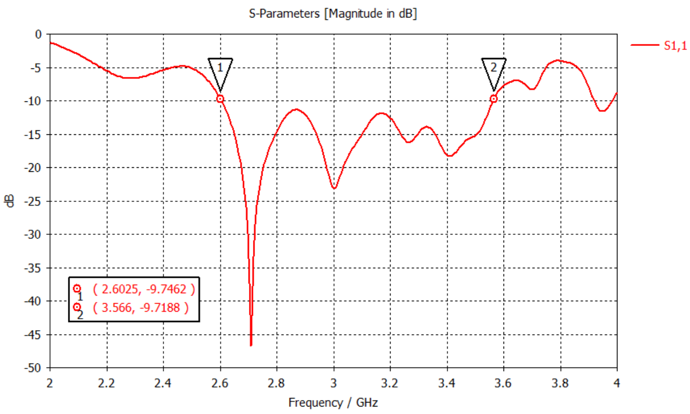

Figure 22: S11 parameters - Within 2-4 GHz band

The bandwidth is from 2.6 GHz to 3.5 GHz which corresponds to 900 MHz around 3.1 GHz and therefore it is 30% of the center frequency. So far this result is acceptable in terms of reflection coefficient performance.

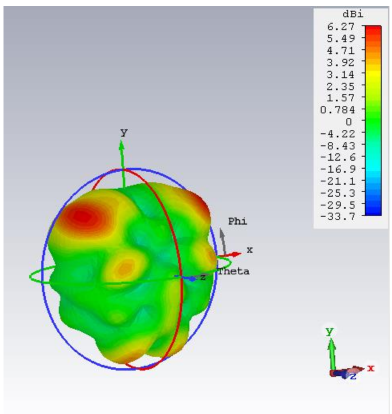

Figure 23: Farfield diagrams at 3.1 GHz

The radiated pattern at the center frequency is not acceptable at all, in fact there are two lobes in y-axis and there is no radiation in z-axis. Hence, this designed antenna is dismissed for the whole study as it is not filling all the requirements.

As seen previously, the S_{11} parameters were completely well adapted within a large bandwidth. However the radiated pattern was not adapted to the center frequency. Consequently, when the S_{11} parameters are adapted to a desired bandwidth, it doesn't mean the electromagnetic fields is correct.

The reason behind these results still has to be explained. In fact the encountered problems cannot be easily justified. More simulations indeed have to be derived to better understand where these consequences come from. The purpose of the job was not to solve problems as this one but was to find correct antenna which follows all the requirements.

3.1.2.1.2 Stub patch antenna

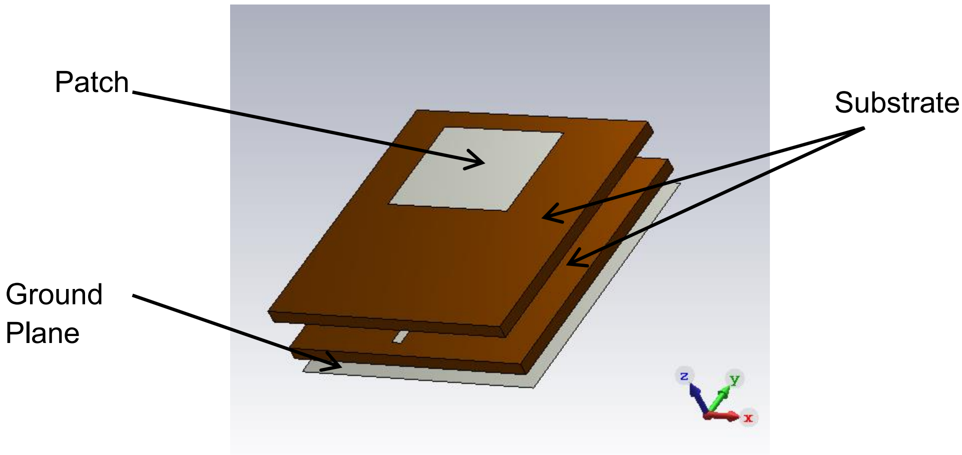

Figure 24: Stub patch antenna

This designed antenna is named as "stub patch antenna" because the feedline has a stub in its structure. Basically stub is an appendice added to a microstrip line to create a resonant mode.

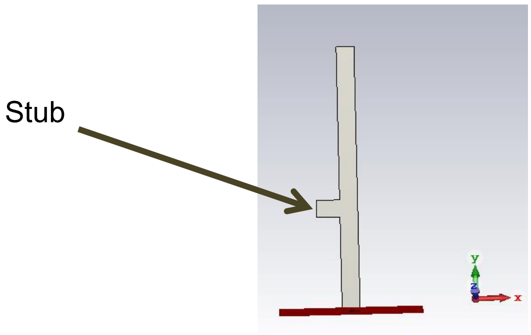

Figure 25: Microstrip with stub

The following picture shows the S_{11} parameters.

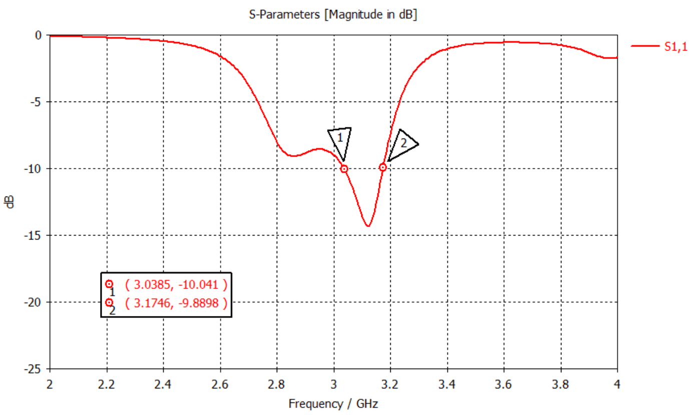

Figure 26: S11 parameters

The encountered problem with this antenna is the narrow bandwidth. As seen in the above picture the bandwidth goes from 3.04 GHz to 3.17 GHz which corresponds to a percentage of 4.2%. This percentage is clearly not enough. Moreover, after running some kind of optimization – by taking +/- 10% of each dimension – this bandwidth has not been improved.

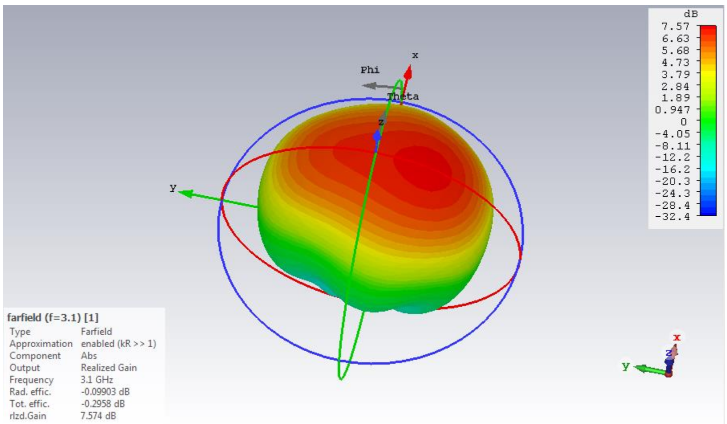

Figure 27: Farfield diagram at 3.1 GHz

The radiated pattern for the stub patch antenna at the center frequency is relatively correct.

The main radiation is not made in the propagation axis there is a little angle between the z-axis and the propagation axis.

Once again, in terms of performance this antenna is not retained for the final design, the requirements for the S_{11} parameters are not satisfied and the criteria regarding the radiated pattern is not much verified as well.

3.1.2.1.3 The CPW patch

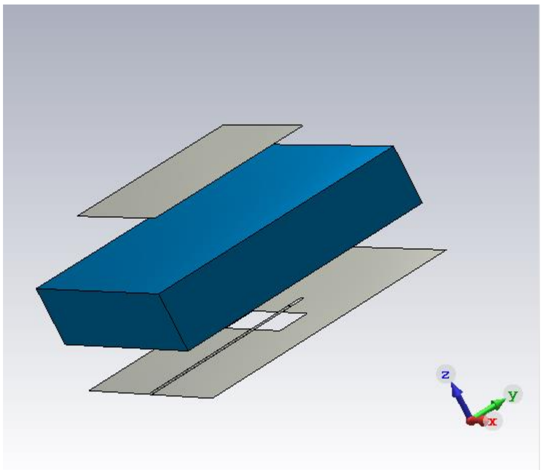

Figure 28: The CPW patch antenna

The denomination CPW is used for CoPlanar Waveguide. Inside a ground plane there is the insertion of a microstrip with a cross section aperture. The following picture shows this CPW technology.

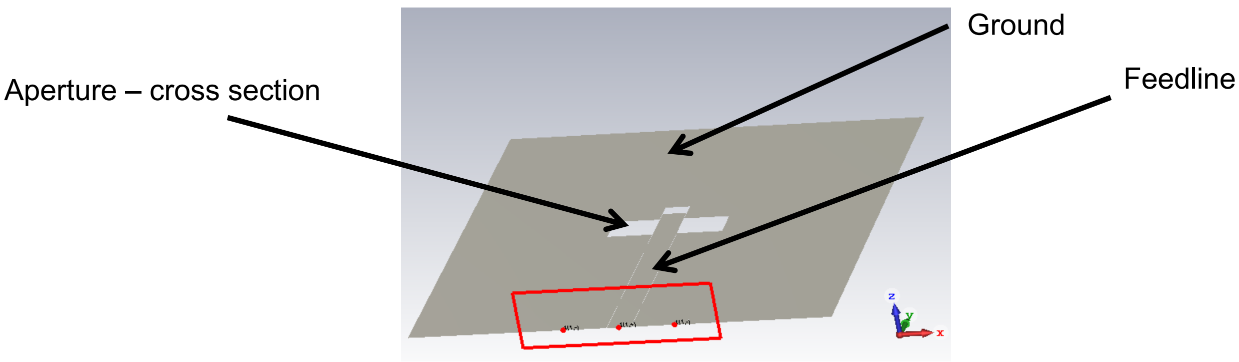

Figure 29: CoPlanar Waveguide technique

In this above picture, the red square represents the port to feed the CoPlanar Waveguide.

The three points are there to properly supply the system. They define the potential to apply to the ground plane and to the feedline. In this case the ground plane has negative potential and the feedline has the positive one.

The gap between the feedline and the ground plane enables to improve the coupling with the patch and the feedline. Hence this gap is really useful for the functioning of the antenna.

The following picture displays the S_{11} parameters.

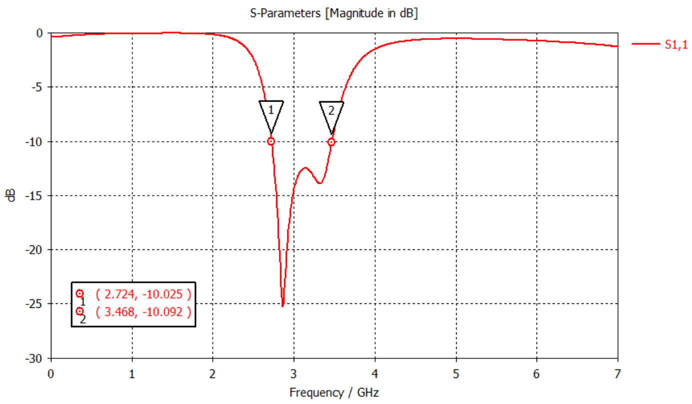

Figure 30: S11 parameters CPW antenna

The bandwidth for the CPW patch antenna is established from 2.72 GHz to 3.47 GHz. The whole bandwidth is therefore equal to 740 MHz which represents a percentage of 24% to the center frequency.

To simplify the study only the radiated pattern at 3.1 GHz is shown. For the other frequencies of radiated patterns only their values are indicated.

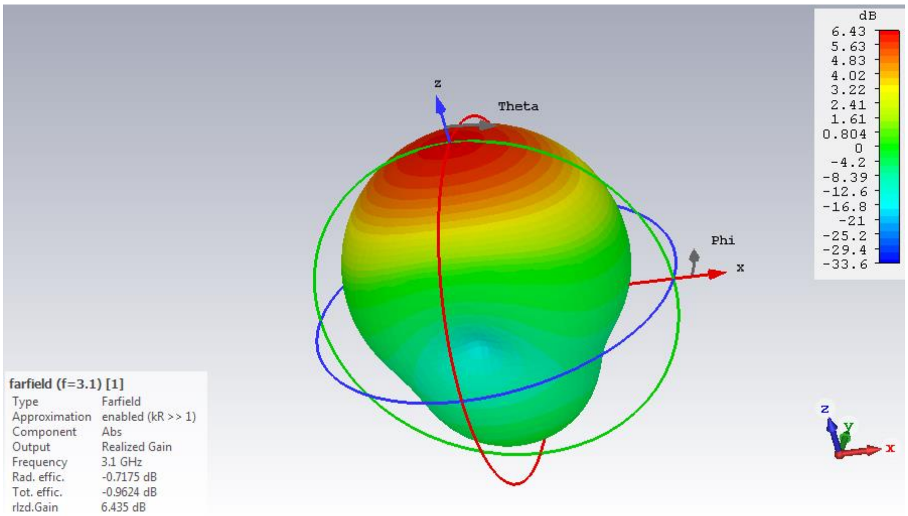

Figure 31: Farfield at 3.1 GHz

The radiated pattern is in z-axis with a value at least equal to 6.43 dB which respects the requirements.

Frequency (GHz)	2.7	2.8	2.9	3	3.2	3.3	3.4
Gain (dB)	5.092	5.952	6.278	6.352	6.587	6.696	6.608

Table 1: Radiated patterns - CPW

This design – the CPW patch antenna – is saved for the final realization. Within the bandwidth the radiated patterns is in z-axis and their values are higher than 5 dB. Moreover, the S_{11} is correct and corresponds to 24% to the center frequency.

3.1.2.1.4 The double patch with aperture and microstrip patch antenna

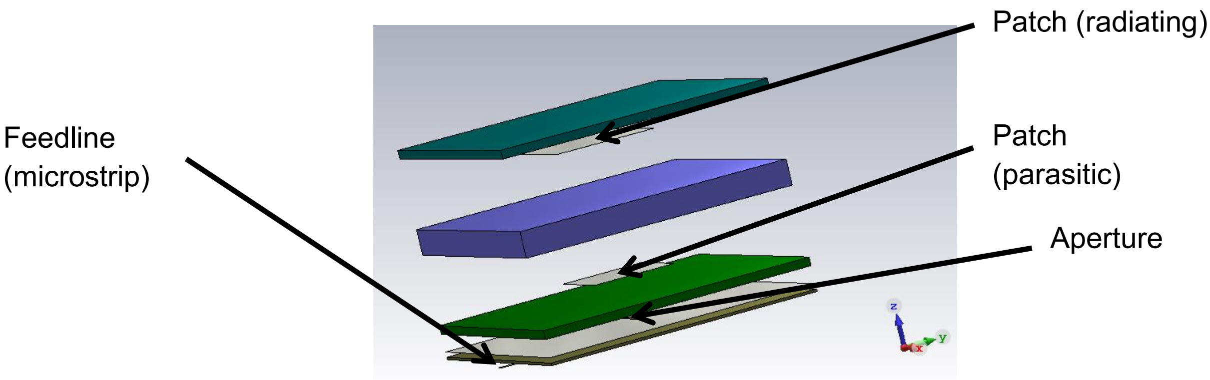

Figure 32: The double patch antenna

The double patch antenna is composed of two different patches. The first one is feeding by a microstrip through an aperture and the second one is feeding by the coupling of the first one.

Moreover, the first patch is also known as the parasitic one and the second patch is called the radiating one.

The following picture shows the S_{11} parameters.

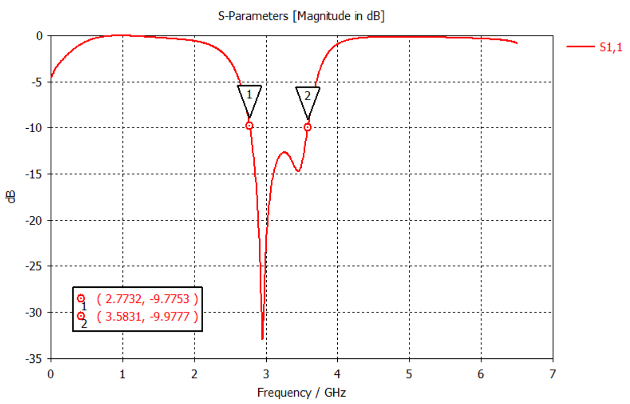

Figure 33: 211 parameters for double patch antenna

The bandwidth for this kind of antenna is settled from 2.77 GHz to 3.56 GHz, which corresponds to 26% of the center frequency. This value is thus acceptable for the final design.

Let's check the radiated pattern at 3.1 GHz. As done before, the radiated pattern values for the following frequencies are shown in a Table 2: Radiated patterns – Double patch microstrip antenna.

The following diagram is the one corresponding to the center frequency.

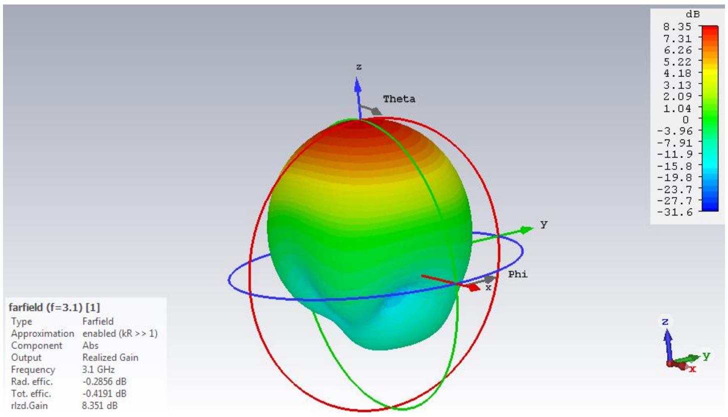

Figure 34: Farfield diagram at 3.1 GHz

The radiated diagram is showing 8.35 dB for the realized gain which is clearly enough to be acceptable. Furthermore, the radiation is done in the propagation axis, thus, the angle between z-axis and this propagation one is quasi null.

Frequency (GHz)	2.7	2.8	2.9	3	3.2	3.3	3.4
Gain (dB)	6.798	7.679	8.164	8.342	8.440	8.583	8.791

Table 2: Radiated patterns – Double patch microstrip antenna

Within the bandwidth, from 2.77 GHz to 3.56 GHz, the whole radiated patterns are at least equal to 7 dB for the realized gain, and moreover the S_{11} parameters are correct and correspond to 26% of the center frequency. Therefore, this proposal is kept for the final design.

3.1.2.1.5 Aperture patch antenna

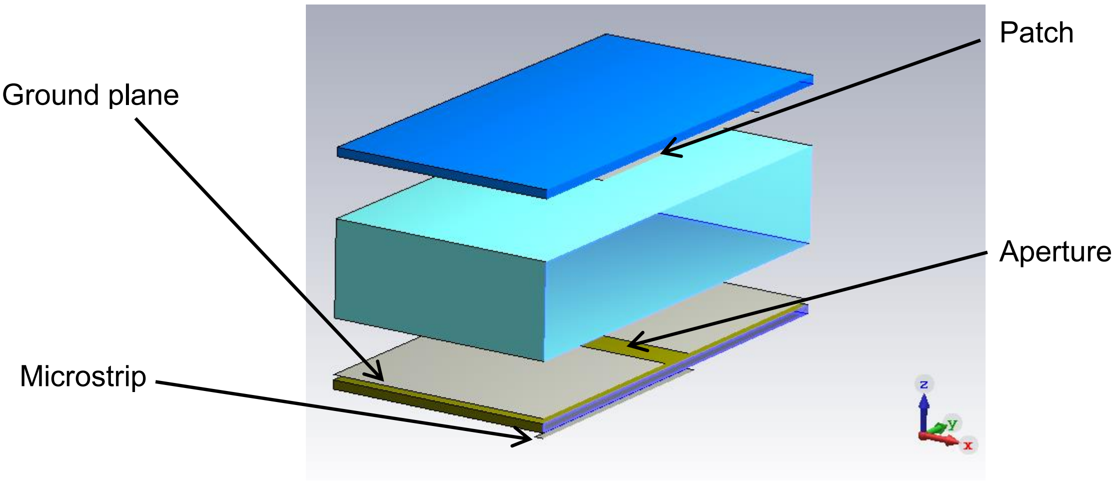

Figure 35: Aperture patch antenna

This patch antenna is composed of a microstrip, a ground plane with an aperture and a patch. The radiation is due to the coupling with the aperture and the microstrip.

The following picture shows the S_{11} parameters.

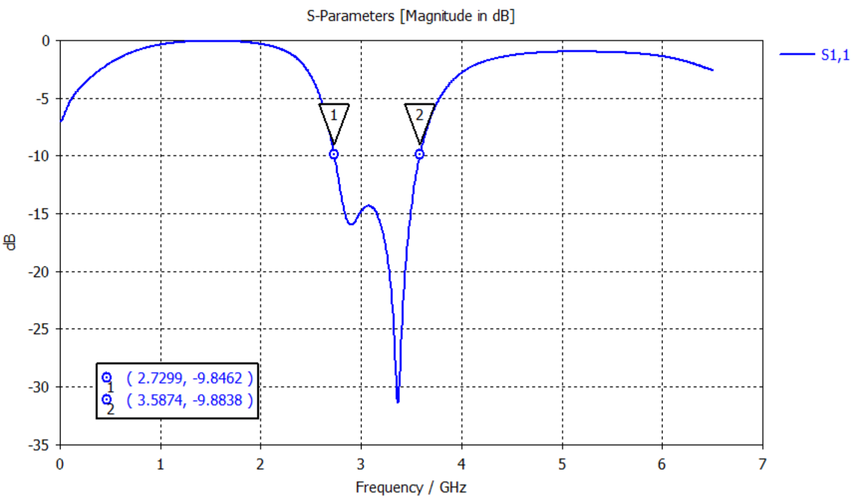

Figure 36: S11 parameters

The bandwidth is defined from 2.73 GHz to 3.59 GHz which corresponds to 28% of the center frequency. This band is acceptable with respect to the requirements.

The following diagram is showing the radiated pattern at 3.1 GHz. For the other frequencies as before the list of values of radiated pattern will be done.

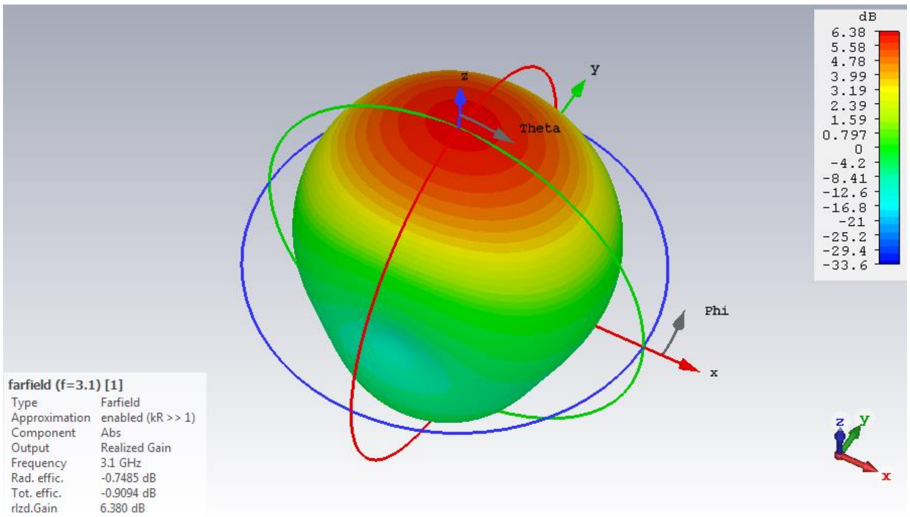

Figure 37: Farfield diagram at 3.1 GHz

The radiated diagram is showing 6.38 dB for the realized gain which is enough for the requirements. Moreover the radiation is done in propagation axis.

Frequency (GHz)	2.7	2.8	2.9	3	3.2	3.3	3.4	3.5
Gain (dB)	4.81	5.624	6.020	6.222	6.541	6.668	6.671	6.452

Table 3: Radiated patterns – Aperture patch antenna

Within the bandwidth, from 2.73 GHz to 3.59 GHz, the whole radiated patterns are at least equal to 5 dB for the realized gain. Moreover the S_{11} parameters are correct and correspond to 28% of the center frequency.

Furthermore, this design can be improved by adding the right feeding way and some vias around the feedline. This will be derived in the next paragraphs.

3.1.2.1.6 Aperture patch antenna with improvements

This kind of antenna is the one chosen to be realized, therefore in this paragraph only its structure is shown. For the rest of explanation it is done in the following parts.

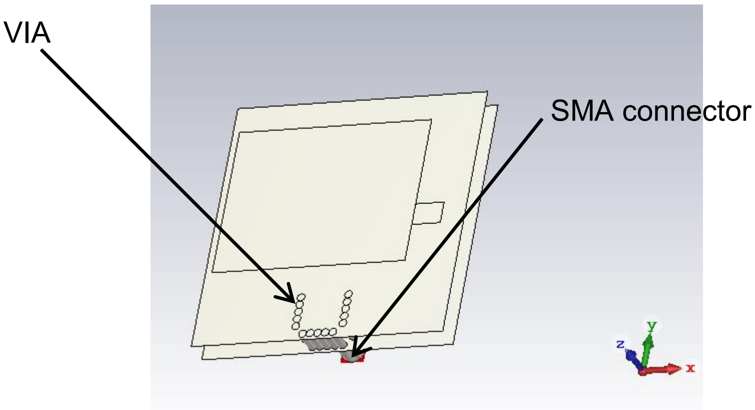

Figure 38: Aperture antenna with improvements

The idea of these vias is to funnel the electromagnetic field along the stripline. Moreover, the SMA connector is installed here to be closer with the reality and the final realization.

The antenna for the realization has to be fed with a coaxial connector; therefore the antenna is taken without any vias and adapted with the coaxial feeding. This kind of feeding is necessary because it needs to feed the antenna in a perpendicular way and behind it. Hence, the only way is to use coaxial connector.

3.1.2.2 WITHOUT VIA – SIMULATION

The design is kept as before but there is the suppression of each via, and then an optimization is running to better know which parameters – among 6 useful ones - have an influence on the S_{11} parameters.

The simulation of each parameter is done by taking for each parameter more or less 10 percent of their values.

During the simulation only three characteristics are studied: the center frequency, the percentage of the bandwidth and the minimum value within this bandwidth. Analyzing those three characteristics the influence of each parameter is thus defined.

The curves, done using a Python script, are showed in the appendix part: it does not bring any more information at this point.

The optimization has been done to better understand which parameters among the 6 useful ones have an influence. Therefore, there are two parameters which affect the three interested antenna characteristics. The first one is the width of the patch also called Wx which affects each characteristic and the second one is the length of the aperture also named as LSy which affects the minimum value at center frequency.

Despite this previous optimization, it was not possible to improve the antenna to reach the requirements. Therefore, the second option was to add a certain amount of vias to make the contact between the two ground planes in order to improve performances.

3.1.2.3 FINAL CHOSEN ANTENNA – CHARACTERISTICS – WITH 15 VIAS

In literacy, as previously said, the antenna works properly with 15 vias positioned all around the feedline as well as around the core of the connector.

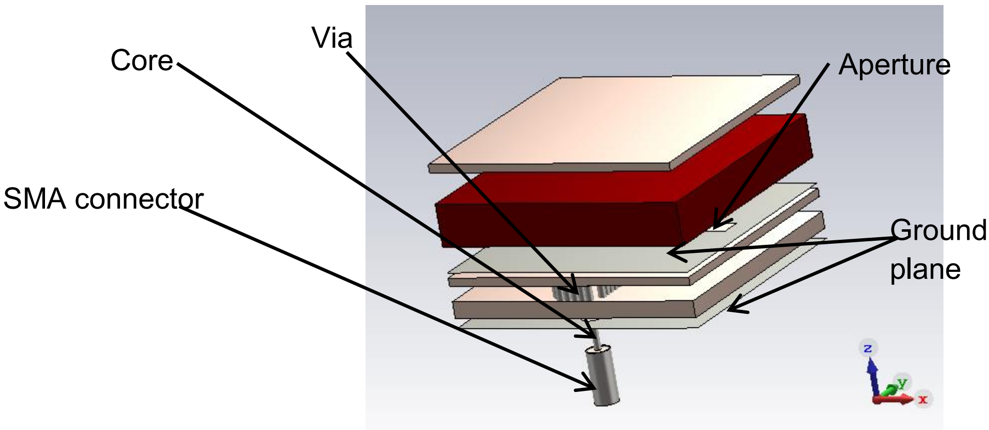

Figure 39: Final chosen antenna

First of all, let's check the performance in terms of S_{11} parameters and radiated power.

Thus, the following picture displays the S_{11} parameters.

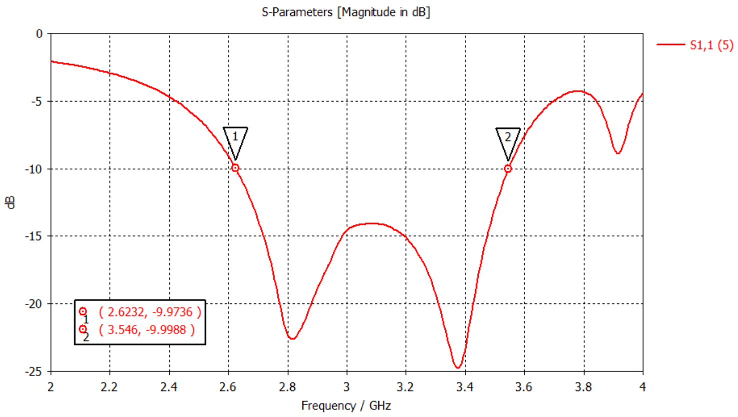

Figure 40: S11 parameters for 15 vias

The bandwidth is from 2.62 GHz to 3.55 GHz which represents 930 MHz and then it gives a percent of 30% of the center frequency.

Here it is the radiated pattern at 3.1 GHz.

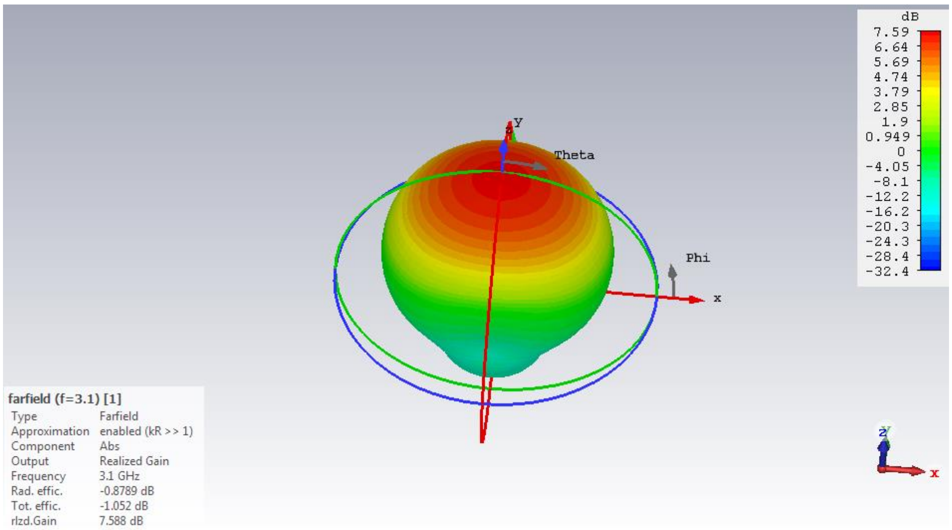

Figure 41: Farfield diagram at 3.1 GHz

The value of the realized gain is equal to 7.588 dB. This gain is settled in the propagation axis as well as along the z-axis. This value is widely acceptable to pursue the study.

Frequency (GHz)	2.6	2.7	2.8	2.9	3	3.2	3.3	3.4	3.5
Gain (dB)	6.279	6.871	6.840	7.331	7.415	7.780	7.898	7.850	7.307

Table 4: Radiated patterns - Aperture antenna with improvements

Within the bandwidth, from 2.62 GHz to 3.55 GHz, the whole radiated patterns are at least equal to 5 dB for the realized gain. Moreover the S_{11} parameters are correct and correspond to 30% of the center frequency.

As said previously, this current design is the final one to be realized and compared to the simulation. The arising question is thus, whether these 15 vias are feasible or they might imply some issues.

However, adding 15 vias and realizing those vias in reality is not feasible. Hence the option is to check with less vias. The first idea is to try with 5 vias and then with 3 vias. The two following paragraphs are examined these techniques with their comparisons by the end.

3.1.2.4 WITH MECHANICAL VIAS – SIMULATION

3.1.2.4.1 With 5 vias

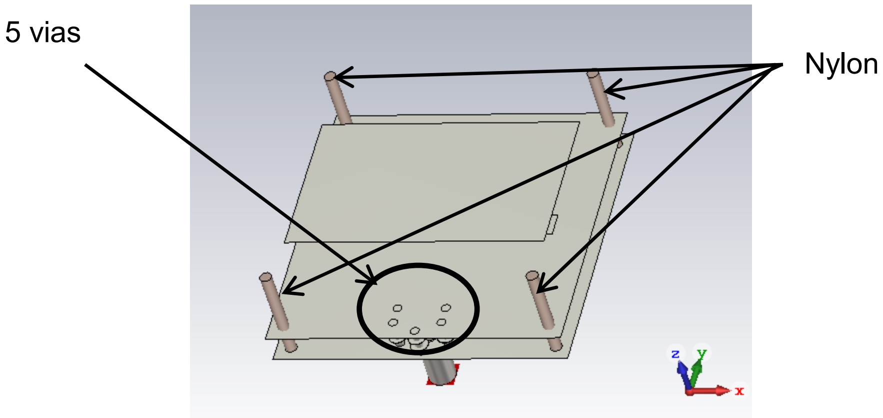

Figure 42: Aperture patch antenna with 5 vias

The first option was to add 5 vias and to check whether the performances are better. The same optimization like for the non vias antenna is indeed developed. The optimization to this method might be found in the appendix number 4. In this paragraph it is only portrayed the performance after running the optimization in terms of bandwidth and radiated patterns.

The following picture is presenting the S_{11} parameters.

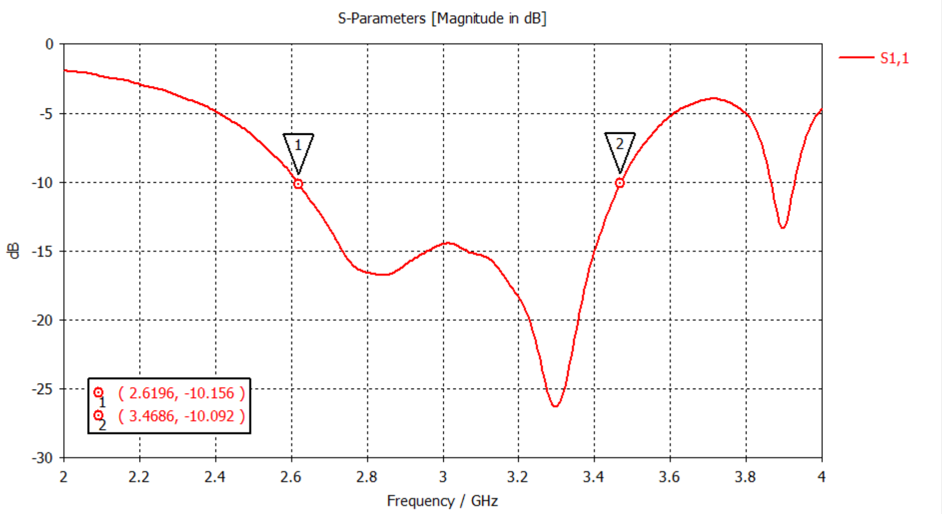

Figure 43: S11 parameters for 5 vias

The bandwidth goes from 2.62 GHz to 3.47 GHz which corresponds to a band of 850 MHz and it is 27 percent of the center frequency. The required value had to be higher than 20-25%, therefore with this 5 vias patch antenna the first objective is respected.

Then, the following picture shows the radiated pattern at the center frequency. For the other frequencies, only the value for the realized gain will be given.

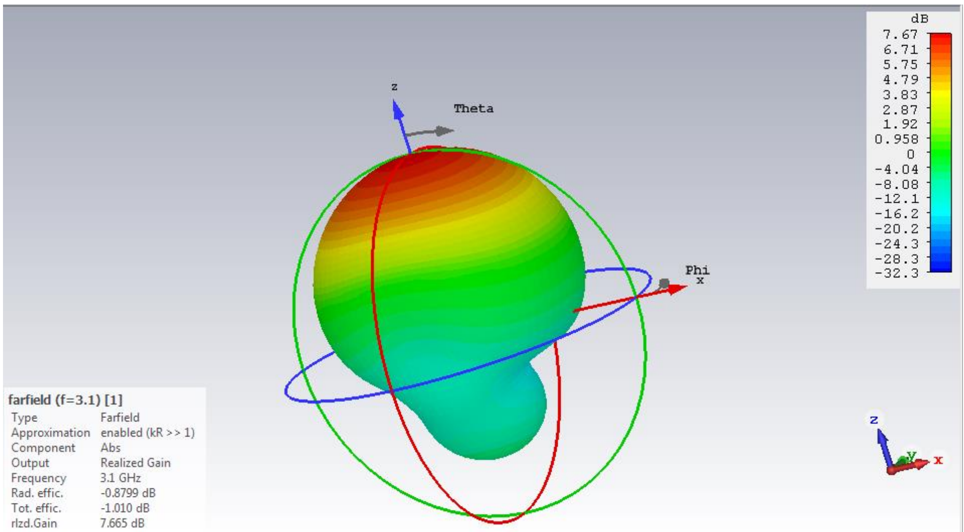

Figure 44: Farfield diagram at 3.1 GHz

The realized gain at the center frequency is equal to 7.67 dB which is higher than the required one. Moreover, this gain is radiated in the propagation axis which is joined with z-axis.

Frequency (GHz)	2.6	2.7	2.8	2.9	3	3.2	3.3	3.4	3.5
Gain (dB)	6.329	6.933	7.138	7.402	7.400	7.858	7.926	7.601	6.421

Table 5: Radiated patterns - 5 vias patch antenna

All these radiated patterns from 2.6 GHz and 3.5 GHz are done in the propagation axis even though this is not printed. It has been checked on CST these patterns were well radiated in z-axis.

The 5 vias patch antenna meets our requirements. The following arisen question would be: is it possible to use less vias and still keeping the same performances?

Therefore the next paragraph deals with the patch antenna with 3 vias.

3.1.2.4.2 With 3 vias

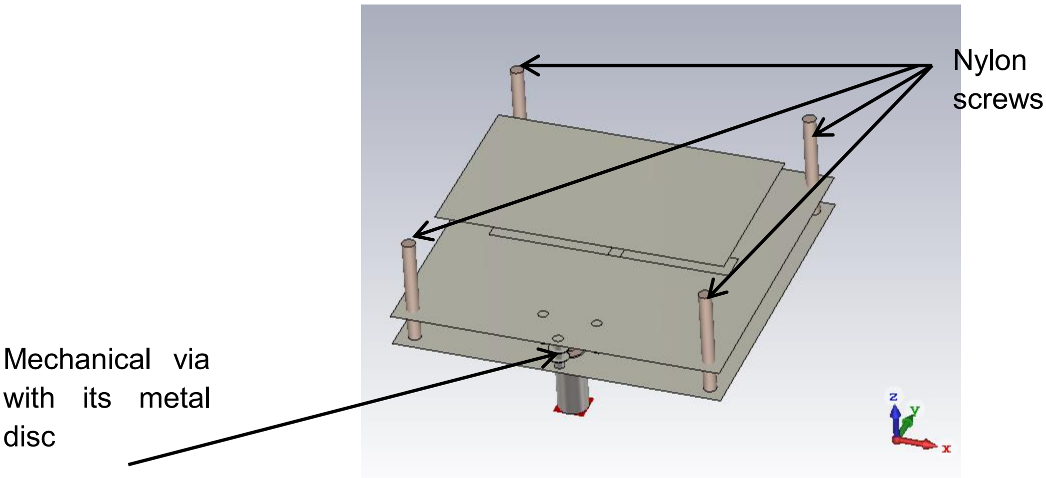

Figure 45: Aperture patch antenna with 3 mechanical vias

The following picture shows the S_{11} parameter for the 3 vias patch antenna.

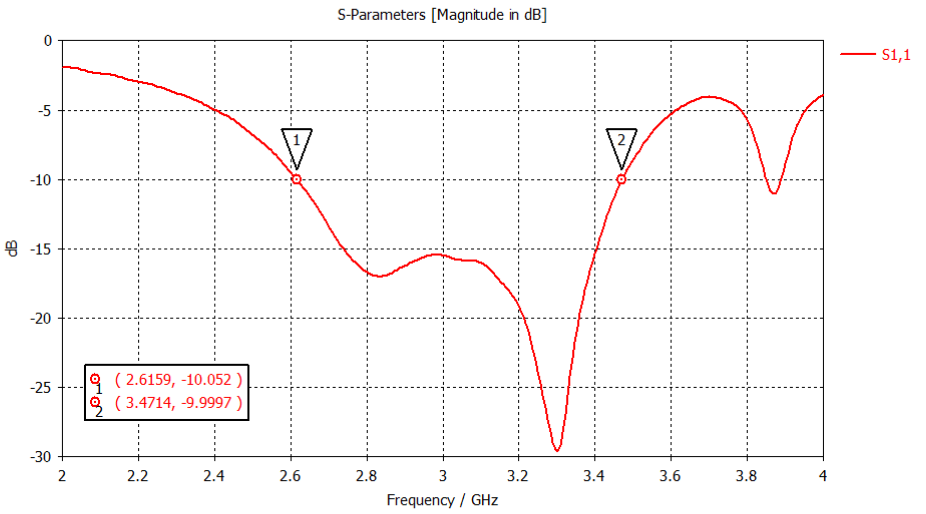

Figure 46: S11 parameter for 3 vias

The bandwidth goes from 2.62 GHz to 3.47 GHz which corresponds to the same value as found for the 5 vias patch antenna.

Then, the next picture shows the radiated pattern at the center frequency.

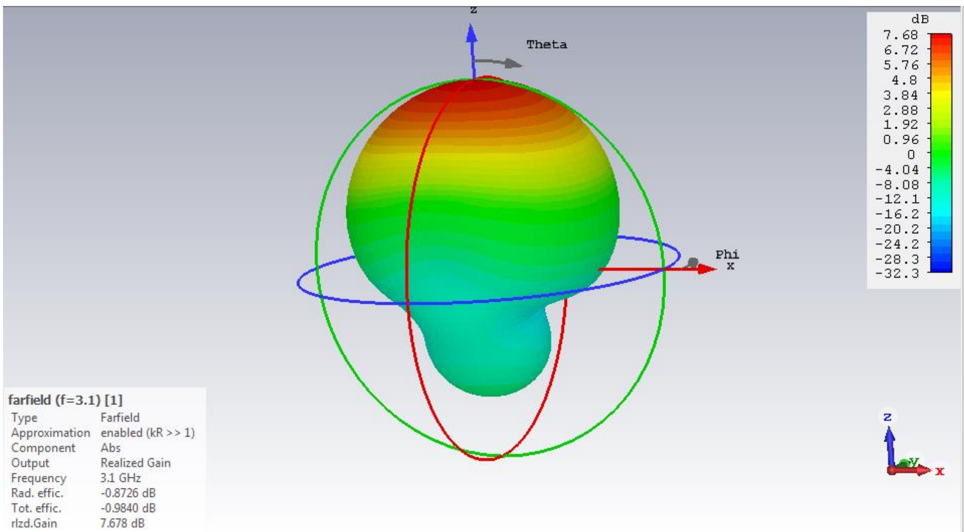

Figure 47: Farfield diagram at 3.1 GHz

The realized gain at the center frequency is equal to 7.68 dB which is higher than the required one. Moreover, this gain is radiated in the propagation axis which is joined with z-axis.

Frequency (GHz)	2.6	2.7	2.8	2.9	3	3.2	3.3	3.4	3.5
Gain (dB)	6.347	6.970	7.215	7.444	7.456	7.901	7.954	7.604	6.380

Table 6: Radiated patterns - 3 vias patch antenna

All these electromagnetic fields from 2.6 GHz and 3.5 GHz are radiated in the propagation axis even though this is not printed. It has been checked on CST these patterns were well radiated in z-axis.

3.1.2.4.3 Comparison between 3 and 5 vias

First of all, in terms of radiated pattern the same result has been found either with 3 or with 5 vias. There is a little difference of 0.01 dB which represents a few reflection losses.

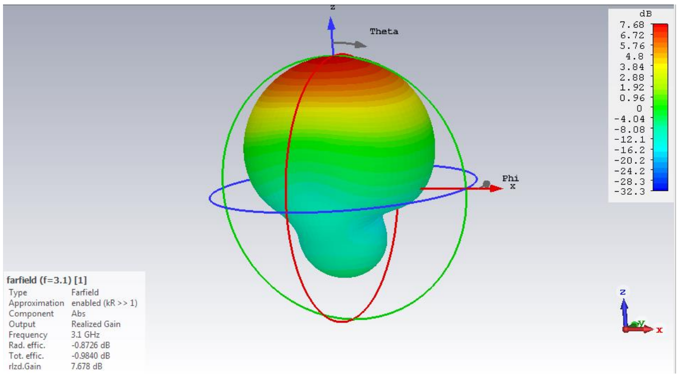

Figure 49: Farfield diagram at 3.1 GHz - 3 VIAS

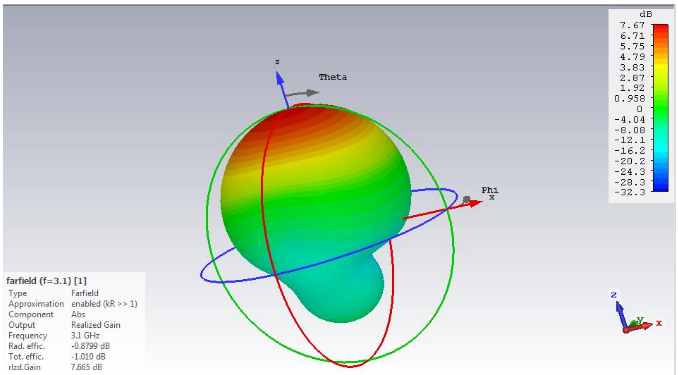

Figure 48: Farfield diagram at 3.1 GHz - 5 VIAS

Secondly, the following picture is showing the comparison of the two S_{11} parameter of each kind of used vias.

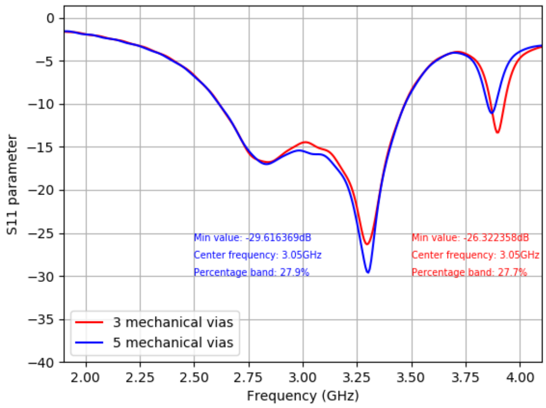

Figure 50: S11 comparison - 3/5 VIAS

In one hand the shape of the curve in both cases is the same. In the other hand, for the minimum value within the bandwidth is better with 5 vias. Finally, for the bandwidth and the center frequency there is no difference between them.

Consequently, as it is simpler to actually design and realize three mechanical vias, the last design is chosen to build the prototype.

3.1.3 THREE VIAS PATCH ANTENNA REALIZATION

3.1.3.1 STEPS OF REALIZATION

The first step in realization mode is to machine each substrate with its metal layout: the down ground plane, the substrate containing metal discs, the substrate with the stripline, the upper ground plane and finally the substrate with the patch.

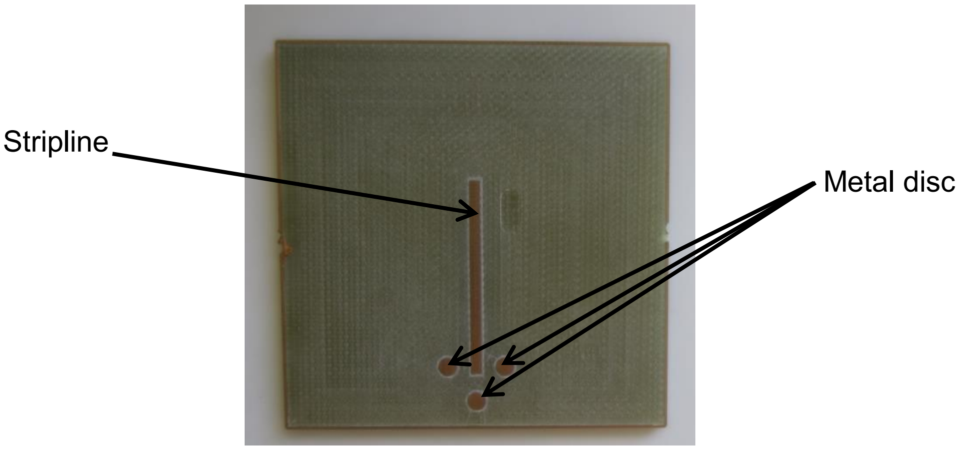

Figure 51: Striple + Metal discs

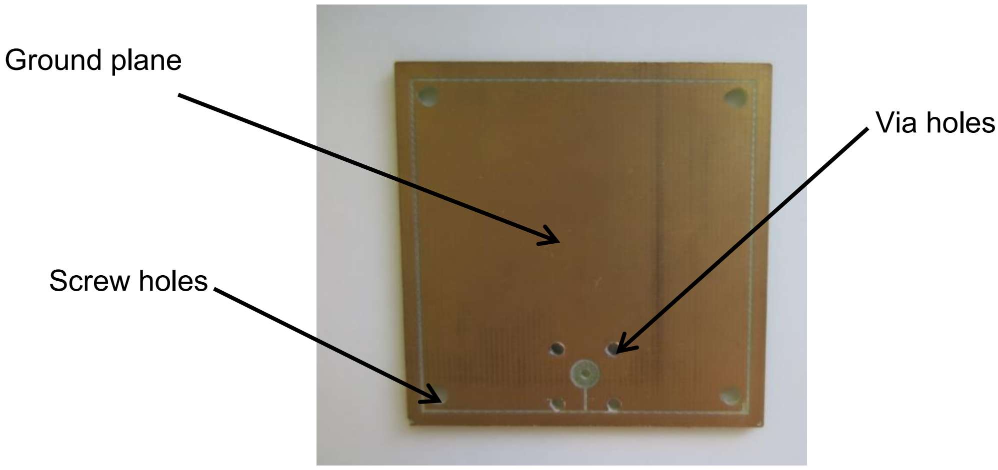

Figure 52: Down ground plane with holes

In the picture above there are four via holes, the goal here is only to show how the ground plane is made. With three vias it would have been the same design.

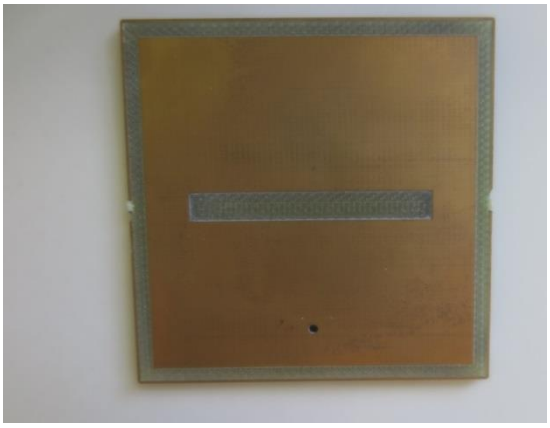

Figure 53: Upper ground plane with aperture

Then, it needs to make the mechanical vias by crimping them on each three down substrate.

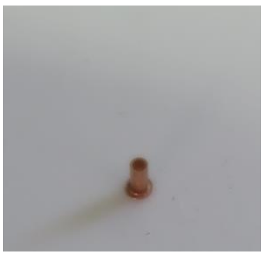

Figure 54: Via alone not crimped

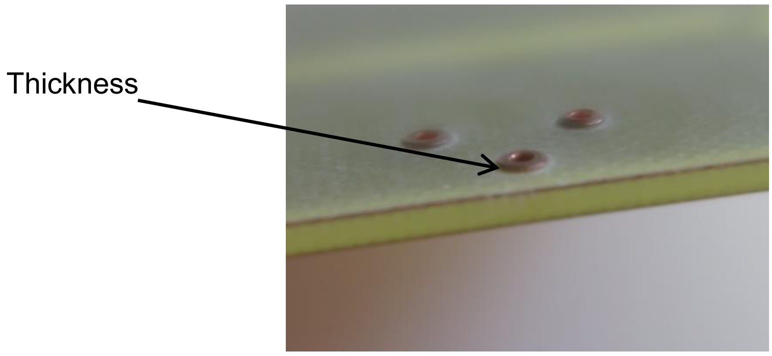

Figure 55: Crimped vias

As seen on the figure 65, when vias are crimped there is still a non negligible and embarrassing thickness.

The next step is the soldering of the SMA core with the stripline: it creates the contact between the core and the stripline.

Then, the SMA connector is soldered to the down ground plane: it enables the contact between the SMA and the ground plane and it also allows to properly fixing the SMA to the whole structure.

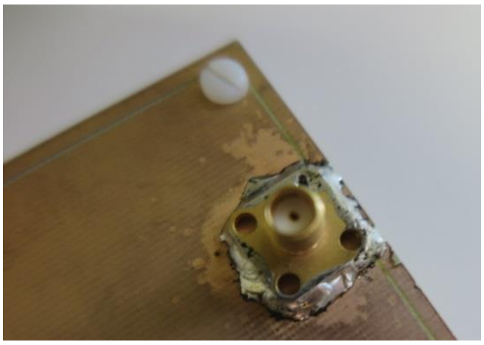

Figure 56: Soldered SMA connector on the ground plane

Finally, the last step is to build the whole antenna by assembling the three down substrates helping with nots and nylon screws and then positioning the patch substrate still using nots at the right thickness.

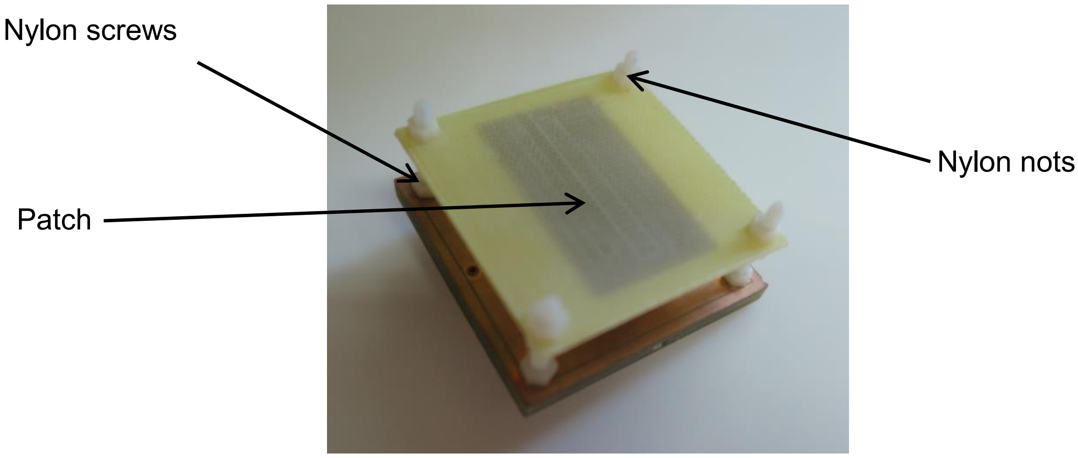

Figure 57: Antenna with 3 vias - Final realization

3.1.3.2 FIRST RESULTS – COMPARISON WITH SIMULATION

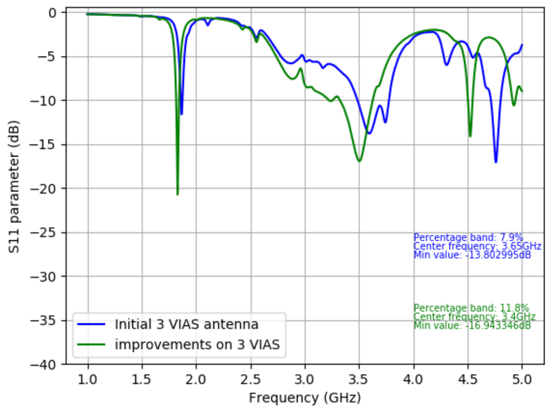

Figure 58: S11 parameters for 3 vias antenna

The picture is showing the S11 parameter without any improvements and with some feasible improvements. Therefore, the blue curve represents the initial produced antenna and the green curve means the 3 vias antenna with improvements. These improvements due to some defects are detailed later on.

Between these two steps, the bandwidth as well as the center frequency is improved. The bandwidth passes from 8% to 12%, and the center frequency goes from 3.65 GHz to 3.4 GHz.

The next picture shows the comparison between the two previous realizations with the simulation one.

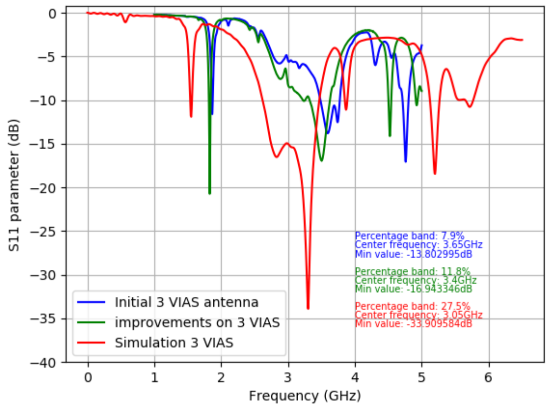

Figure 59: S11 parameter - comparison realization and simulation

The result shows that simulation and realization are completely different. In fact, the bandwidth in simulation is equal to 27% whereas in realization it is found a 12% bandwidth. The blue and green colors in the above picture represent the realization results.

These differences are explained in the following paragraph.

3.1.3.3 ENCOUNTERED ISSUES

3.1.3.3.1 Loop effect

When the engraver is machining a substrate it may happen it adds a copper line all around the substrate. This copper line may create a loop effect and this affects the electromagnetic radiation and therefore the S11 parameter as well.

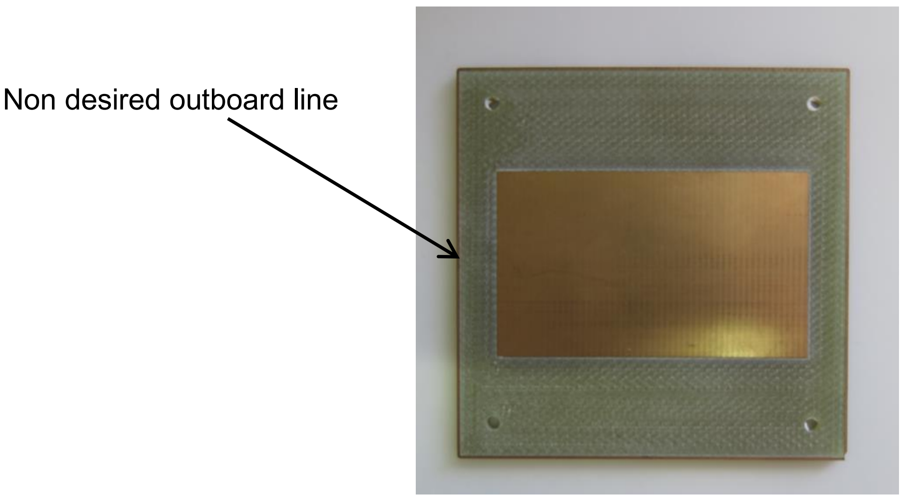

Figure 60: Outboard line

3.1.3.3.2 Via fabrication

As previously said by crimping the vias and then putting the two substrates together using the nylon screws it creates an air gap which deteriorates the S_{11} parameters.

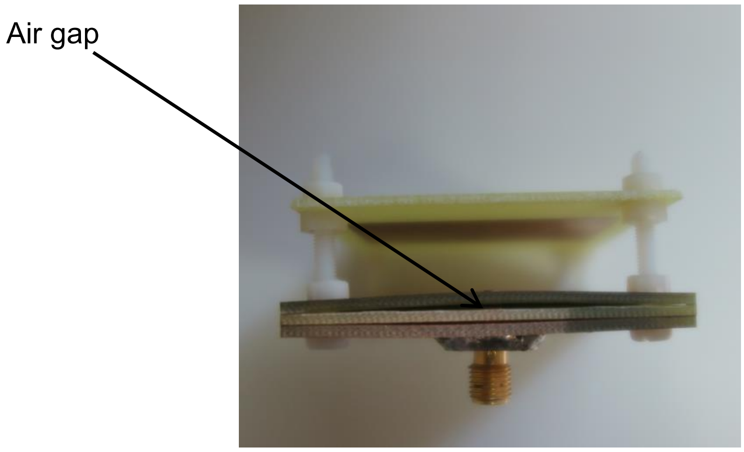

Figure 61: Air gap due to the thickness vias

3.1.4 CORRECTED PATCH ANTENNA: SCREW VIAS

Consequently, all these defects caused by this realization affect the radiation result as well as the S11 parameter. The solution is to use the SMA holes to put 4 metal screws which play the role of the vias and ensure the contact between both ground planes.

3.1.4.1 CORRECTION IN SIMULATION

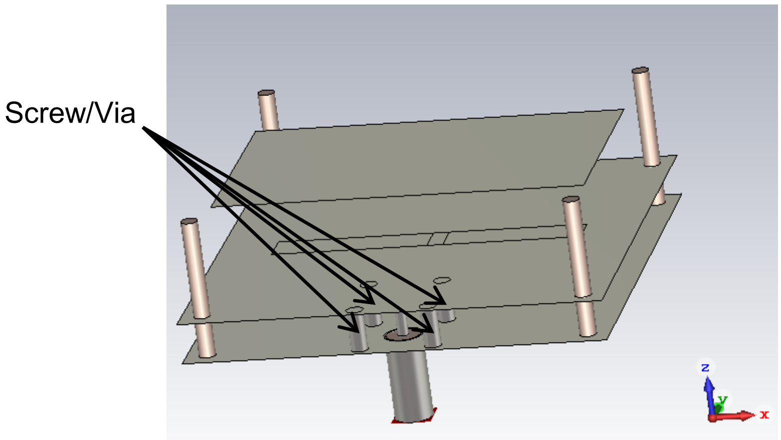

Figure 62: Screw/via patch antenna

Compared to the previous prototype, in this case the SMA's holes are used to put screws from the down ground plane to the upper one. Therefore, the whole structure remains the same and it only needs to solder the core to the feedline and not the SMA anymore. These screws are made with metal and fixed using metal nods. This latter material allows conducting the current and hence the electromagnetic field.

Moreover this new design does not have any air gap as the previous one due to the fact these screws enable to tighten substrate each other.

Finally, the loop effect in this case is deleted; in fact precautions were made to avoid machining again the metal line on the board edges.

The following graph displays the result for the S_{11} parameter in simulation.

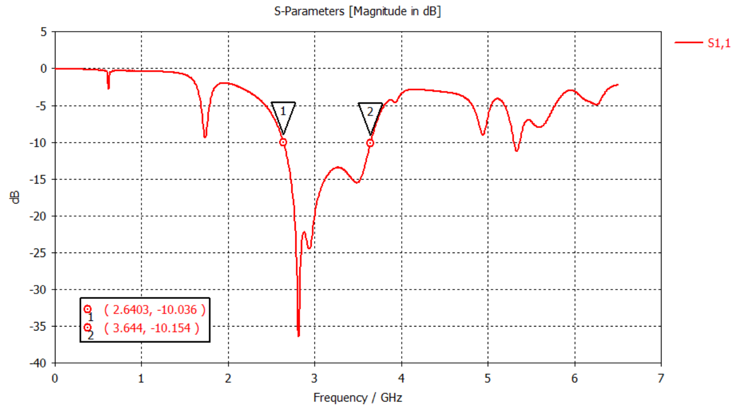

Figure 63: S11 parameter

In simulation with the improvements, the bandwidth goes from 2.6 GHz to 3.6 GHz which corresponds to 1 GHz and then it represents 32% of the center frequency.

The radiated pattern at 3.1 GHz is given below.

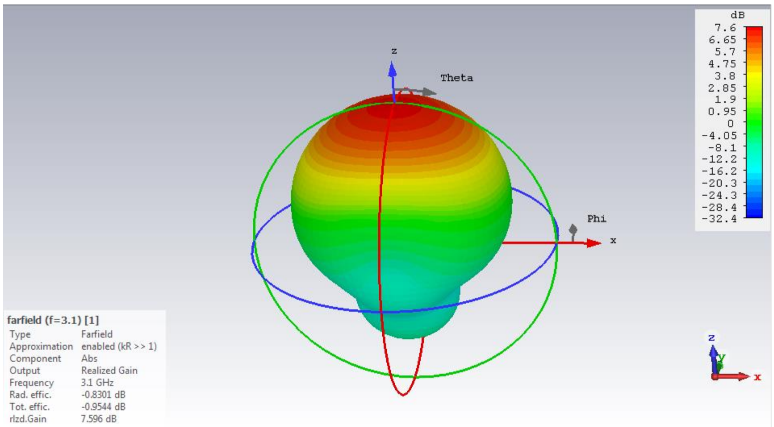

Figure 64: Farfield diagram at 3.1 GHz

The radiated diagram is still correct at the center frequency with a value of 7.6 dB. The radiation is located in the propagation axis.

3.1.4.2 REALIZATION NEW DESIGN

3.1.4.2.1 Realization steps

The steps for the new design are little bit different from the previous design. It still needs to produce the different substrate with their own characteristics. However, instead of making the mechanical vias in this case as it is not necessary. The only thing to do is to tighten the nots.

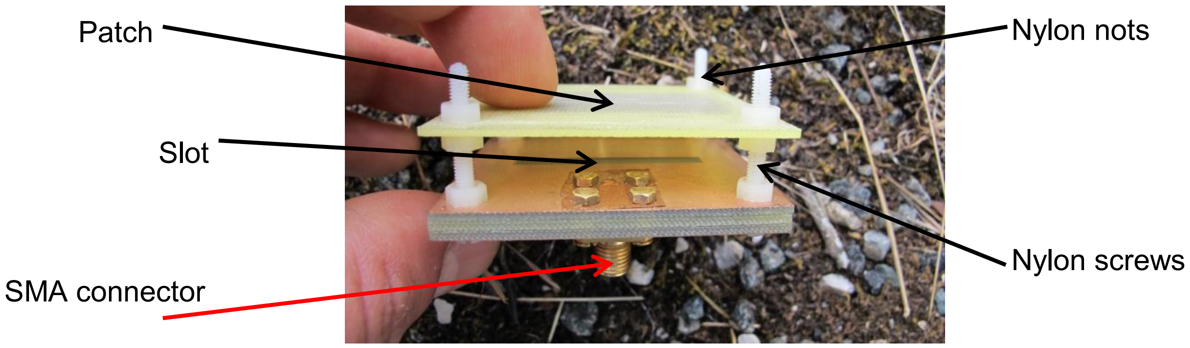

Figure 65: Image of the realized antenna

3.1.4.2.2 Comparison with simulation

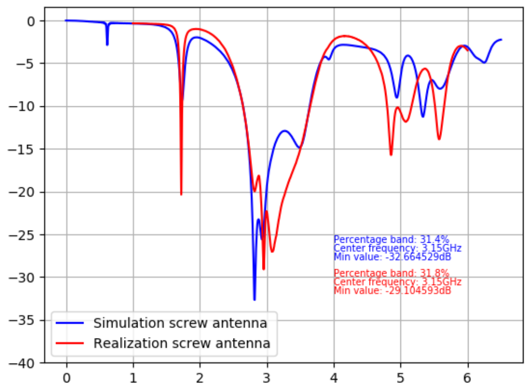

Figure 66: Comparison simulation and realization

The realization and the simulation are similar in terms of S_{11} parameters. The bandwidth in realization is little bit higher than the one in simulation which is a positive point so far.

The following picture shows the radiated pattern of the realization.

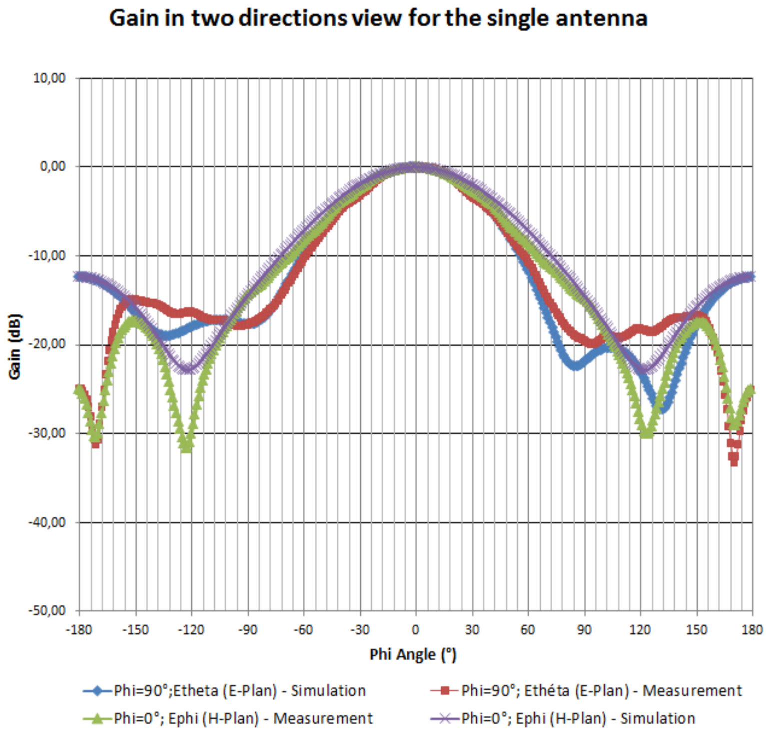

Figure 67: Gain in two directions for the single antenna

The aperture coupled patch antenna with screws assimilated as vias is the right solution for the target. The simulation and the realization of this antenna are similar. Consequently by realizing the simulated product its realization is totally truthful.

The following figure shows the comparison between all correct designs for the S_{11} parameters: from the simulation to the realistic test in anechoic chamber.

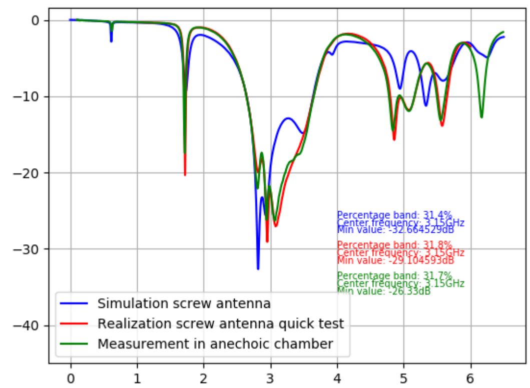

Figure 68: Final comparison

The center frequency and the percent of bandwidth from the simulation to the realization are similar. Therefore the possible bandwidth which can be obtained is equal to 31% which moreover corresponds to 960 MHz of bandwidth. The only little difference may be observed for the minimal value where the best one is in simulation.

3.1.5 CONCLUSION ABOUT SINGLE PATCH ANTENNA

The solution where the vias are replaced by screws is the best one. The next idea is to compare the simulation results to the measurements for the antenna array. To do so, the antenna which is going to be in array disposition is the one called “aperture coupled patch antenna”.

3.2 PATCH ANTENNA ARRAYS

3.2.1 ANTENNA ARRAY REQUIREMENTS

The array composed with an amount of antennas which can vary depending on the type of processing operations. The minimum required number of antenna is five. The antennas inside the array are disposed in a cross way.

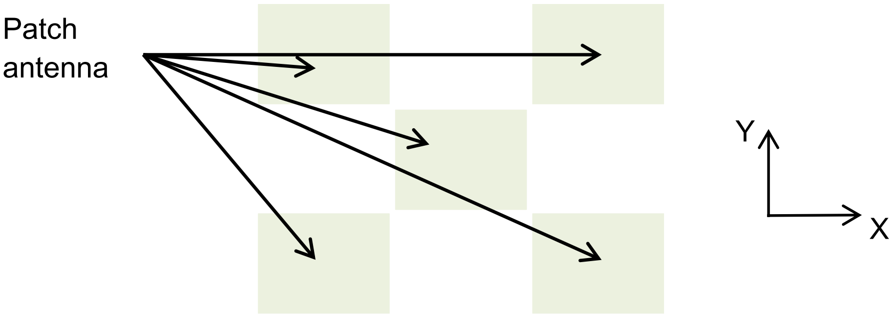

Figure 69: Disposition of the array

The distance between two patches in the x direction is settled at 50 mm as well as in the y direction.

The interesting to look at while testing and doing the antenna array is the coupling in E and H planes between two patches. As the study only focuses on the center patch, it needs to check the coupling between the others. This coupling determines whether the close antennas may disrupt the functioning of the center one.

Consequently, the previous designed single patch antennas are transformed in array form in order to be simulated and realized. Then, the simulation and the realization for the array are compared as for the single patch antennas.

3.2.2 SIMULATED ANTENNA ARRAYS

The previous patch antennas are designed in arrays. Results are observed in simulation and it is discussed in the 2.5.3 part.

In this part there are two views: the first one is about to find the right array to be produced and the second one is to analyze the array behavior for the statistical study.

3.2.2.1 THE STUB PATCH ANTENNA ARRAY

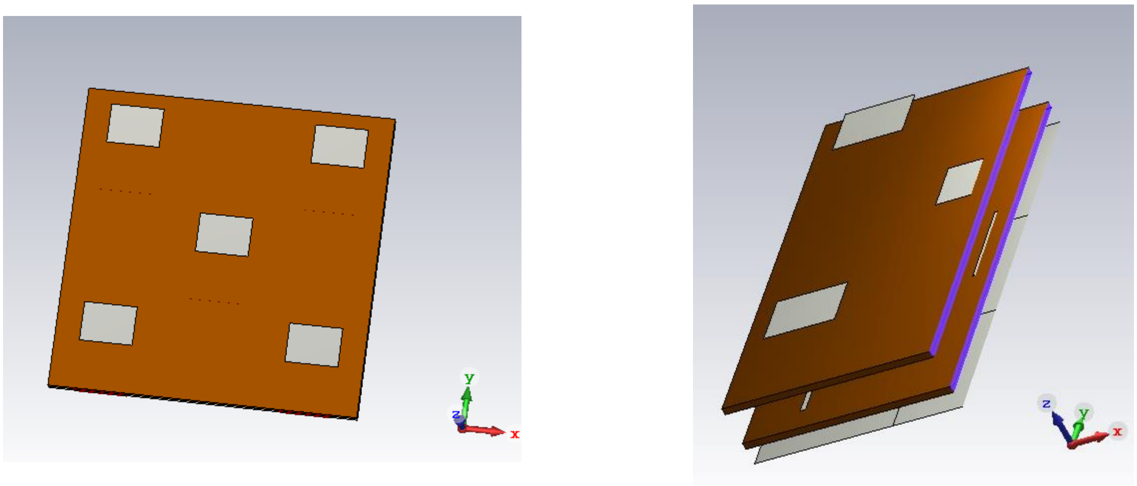

Figure 70: Design of the stub patch antenna array

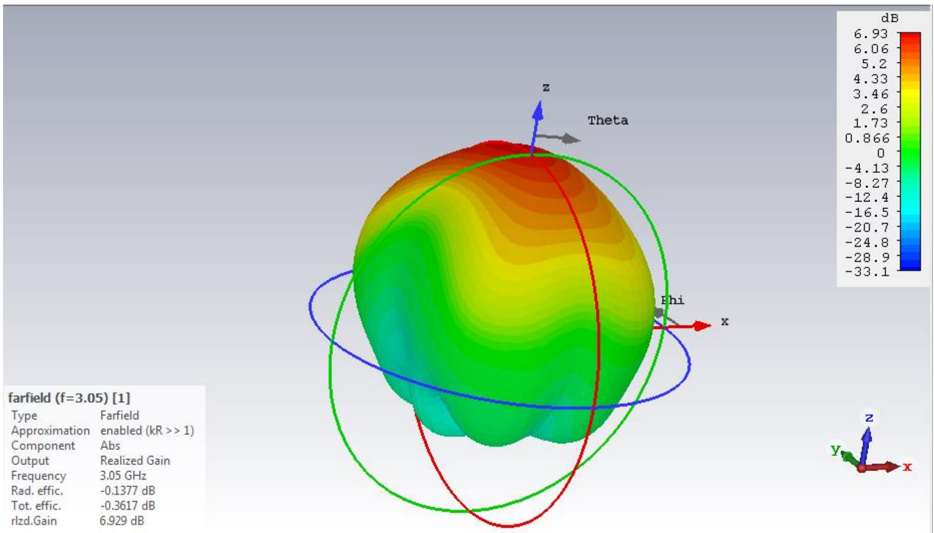

Figure 71: Farfield stub patch antenna

The realized gain for this array is equal to almost 7 dB. For the required application this gain is a wholesome value.

3.2.2.2 THE DOUBLE PATCH WITH APERTURE GROUND PLANE ARRAY

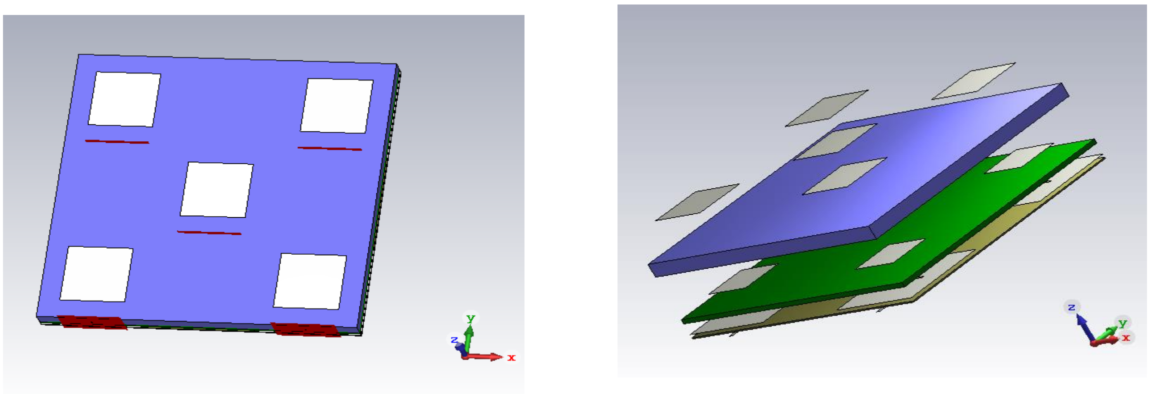

Figure 72: Design of the double patch with aperture ground plane array

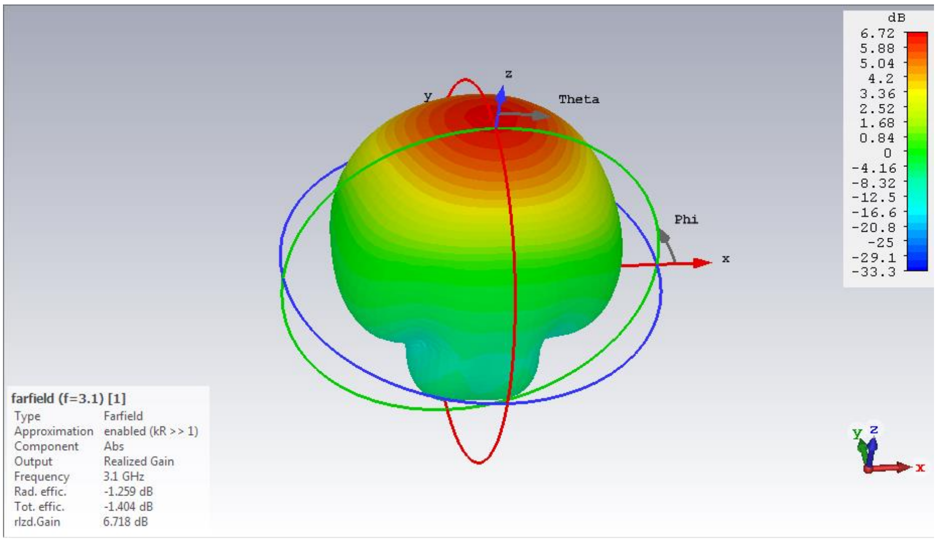

Figure 73: Farfield of the double patch with the aperture ground plane

In this case the realized gain is almost 7 dB. This value is really useful for the needed application.

3.2.2.3 THE DOUBLE PATCH FEEDING BY COAX PROBE

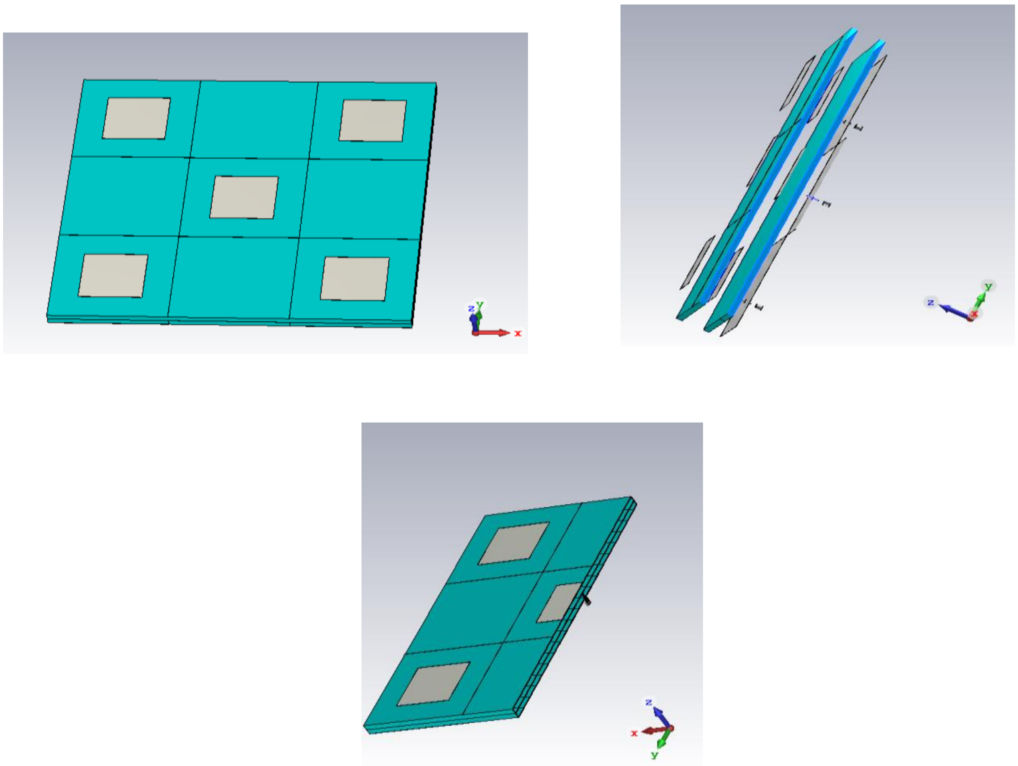

Figure 74: The double patch feeding by coax probe

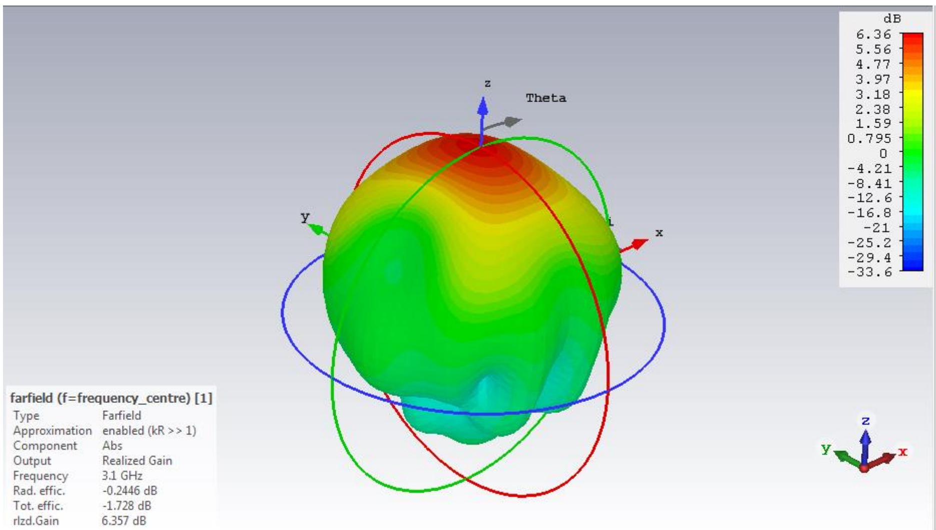

Figure 75: Farfield for the double patch feeding by coax probe

The realized gain for the double patch feeding by coax probe is almost 6.5 dB. Even though this value is less than the others it is still acceptable for the application.

The antenna which has been chosen for the realization is not presented is the precedent list; a deeper study indeed about it is completed in the next paragraph by highlighting one issue.

Therefore, the following picture shows for the previous designed antenna arrays all the S_{11} parameters.

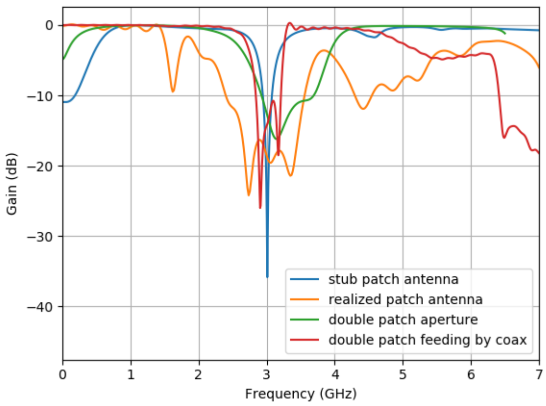

Figure 76: S11 parameters for every designed array

The next figure is showing the coupling between each patch antenna in the array. The coupling does not have to be high otherwise the behavior of the center patch antenna radically changes. The expected value for this coupling should be at least lower or equal to -20 dB.

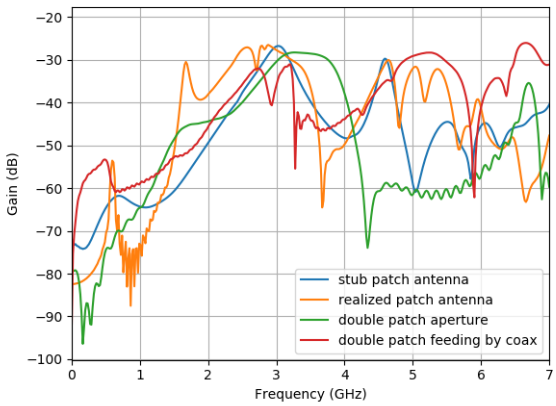

Figure 77: S12 for every designed array

3.2.3 SOLVING THE APERTURE GROUND PLANE ISSUE

The coupled aperture patch antenna has encountered problems while putting it in array disposition. The ground plane containing the apertures (which is called "the aperture ground plane") is responsible of S_{ii} parameter degradation.

Around the center frequency within the desired bandwidth there is a peak higher than $-10\,dB$ which deteriorates the S_{11} shown by the Figure 81. This peak seems to disappear when the ground plane with apertures is discontinuous which means each ground plane is independent. Therefore, the coupling between the close antennas near the center one radically affects the S_{11} parameter.

The following pictures show the different design and the results for the S_{ij} and S_{11} parameters.

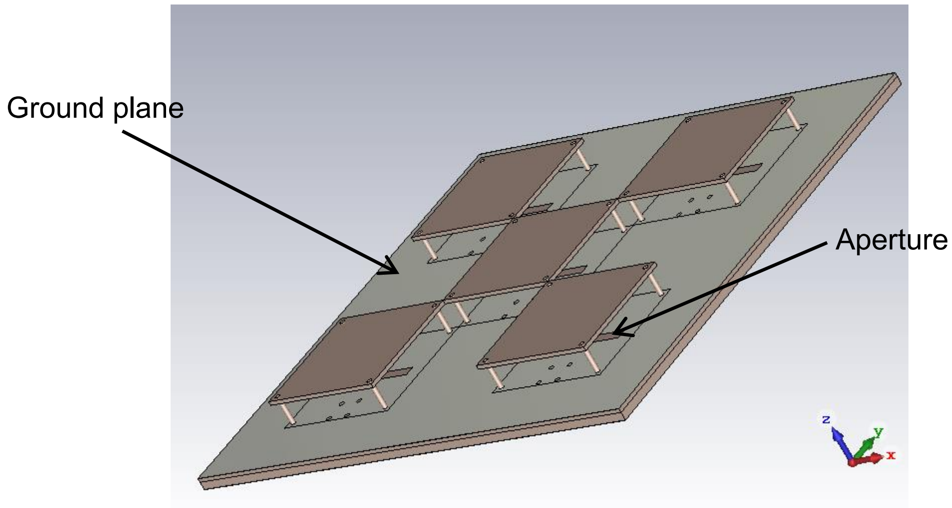

Figure 78: Continuous aperture ground plane

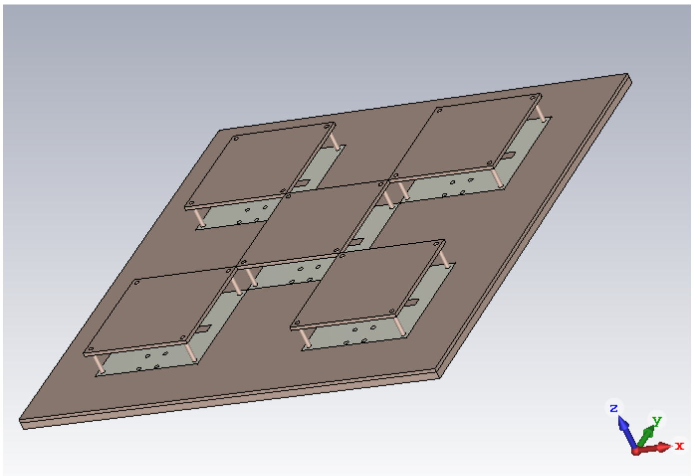

Figure 79: Discontinuous aperture ground plane

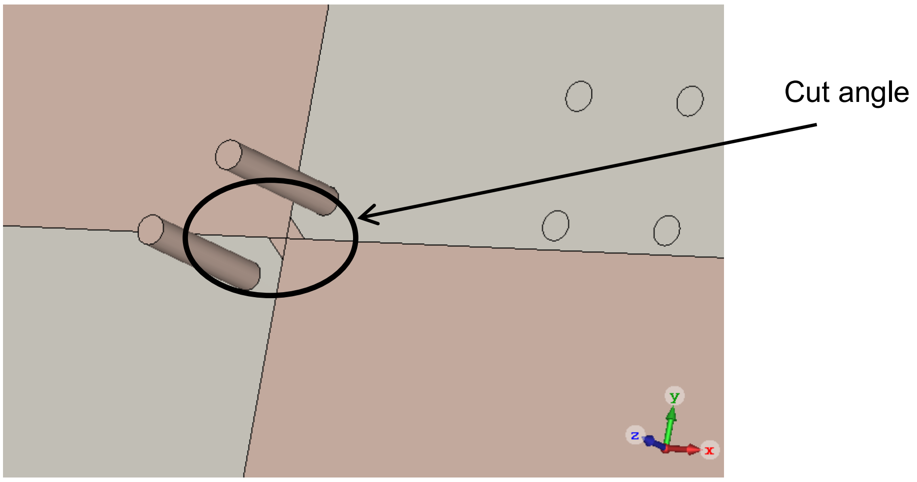

Figure 80: Cutting angles

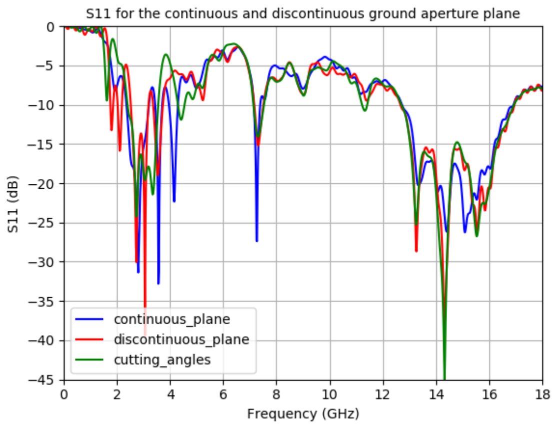

Figure 81: S11 parameter for the three previous cases

In one hand by cutting the angles of each ground aperture plane, the S_{11} comes back to the expected one. The uniform ground aperture plane can hence generate surface currents on the ground plane. Thus by eliminating this regularity, these surface currents are limited to a small area which is the same when the antenna was not in array disposition.

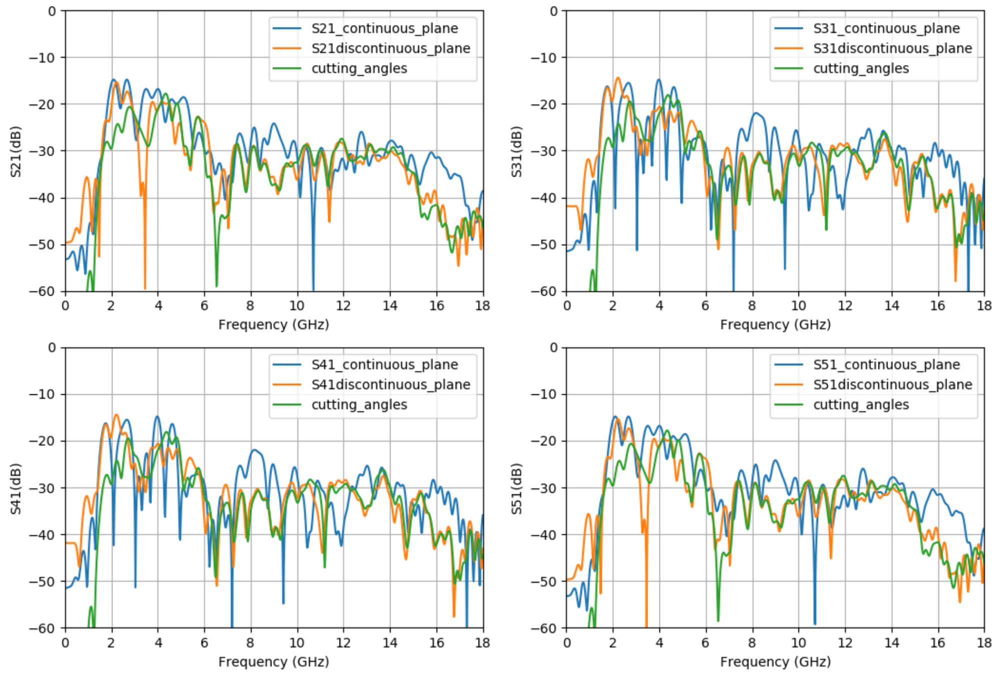

Figure 82: Sij parameters for the three previous cases

In the other hand by cutting the angles from the single ground plane from each patch antenna, the coupling is drastically improved. It is less than -20 dB which is widely acceptable. Furthermore, regarding the S_{11} parameters, the interested bandwidth is significantly improved. In fact the result for the single antenna is identical to the array disposition. Moreover, the previous pike around the center frequency has completely disappeared.

Consequently, the ground plane containing the apertures is responsible for the bad coupling and the wrong S_{11}. When the angles of this plane are not cut, the surface currents are establishing on the ground plane and hence create parasites.

3.2.4 THE REALIZATION: INDEPENDENT APERTURE GROUND PLANES

The realization has been made after the whole simulations. Hence, the only good antenna was the one known as “coupled aperture patch antenna”. This antenna indeed offers the greatest results in the single case and in array disposition. The methodology for making the antenna array is the same used for the single antenna realization. The engraver with the provided DXF files was used to machine each substrate.

The intention here is still to focus on the patch antenna in the middle of the array. Immediately after doing the realization a quick test has been done to check if the S-parameters were correct. In case those parameters weren't appropriate it needs to redesign the array.

Hence, the following pictures show the comparison regarding the S_{11} parameters from the simulation to the realization. As said before a quick test was made to verify the S_{11} parameter and then the antenna was checked in anechoic chamber where there are fewer losses.

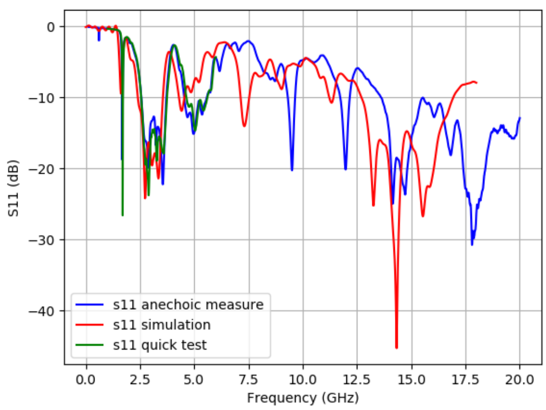

Figure 83: S11 parameter comparison for the array

The quick test was only made from 1 GHz to 6 GHz. In that band the idea is to check the bandwidth for the antenna and not the specific behavior outside its bandwidth.

The next chart shows the same comparison only from 0 GHz to 6 GHz;

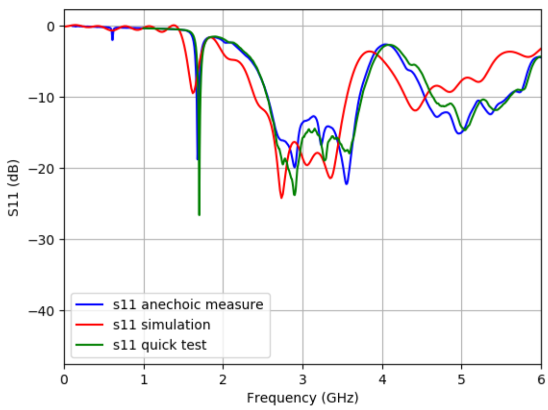

Figure 84: Comparison from 0-6 GHz

Despite the frequency shift for the simulation curve – the red one in the figure – every S_{11} parameter has the same shape. Hence, the simulation gives the same results compared to the realization.

3.2.5 CONCLUSION ABOUT PATCH ANTENNA ARRAYS

The different tested arrays offer acceptable results in terms of S_{11} parameter and realized gain. Therefore they are kept for the statistical study.

However during the array realization of the aperture coupling antenna problems have been encountered in particular on the aperture ground plane. Those problems deteriorated the S_{11} parameter.

The last antenna which is called “the aperture-coupling antenna array” is the one to be applied for the statistical study. Its simulation and measurement results are similar. In the following part this similarity is really appreciated. In fact the statistical study is yielded in simulation and experimental ways.

4. STATISTICAL STUDY: BEHAVIOR OUTSIDE THE BANDWDITH

4.1 INTRODUCTION

Under electromagnetic perturbations an antenna array may be affected. This array could receive a certain amount of gain inside a frequency band. But usually an array only receives energy from its functional bandwidth. Furthermore, the outside bandwidth behavior for an antenna array is generally unknown. Hence, it may happen the antenna is able to capture piece of gain outside its functioning bandwidth.

Therefore, the following part is aiming to study the planar antenna array behavior under electromagnetic waves. The antenna array is reciprocal which means the transmitting gain and the receiving gain are strictly equal. Accordingly to reduce the time of simulation the solution is to set far field probes all around an antenna array. This is used to measure the gain instead of using plane wave probes and measuring the received gain on the antenna. Only one simulation is necessary with the far field probe method.

4.2 PRESENTATION OF THE SIMULATION SETUP

The probes are set front of the array only on a demi-sphere. The array is indeed symmetrical. This positioning is showing on the figure below.

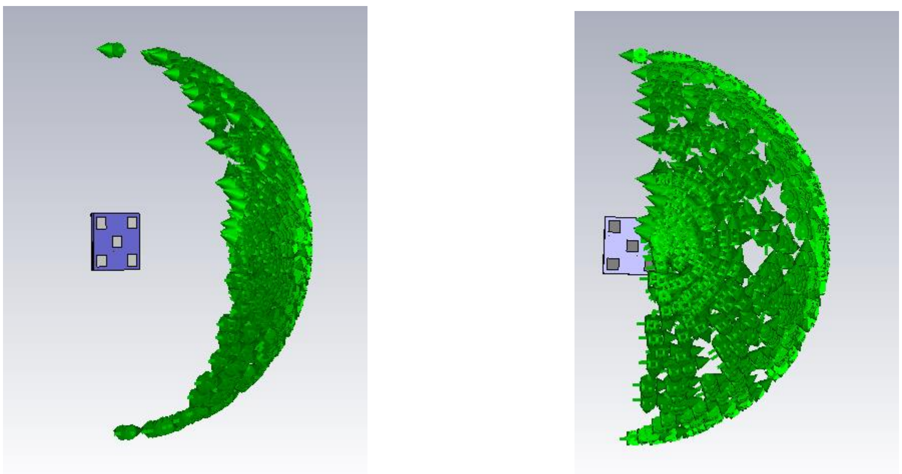

Figure 85: Random positioned probes

A probe in simulation is defined with three parameters: the theta angle, the phi angle and its position. Moreover, a probe is able to measure the electric field with those fixed previous parameters.

These two angles are defined as the figure below shows.

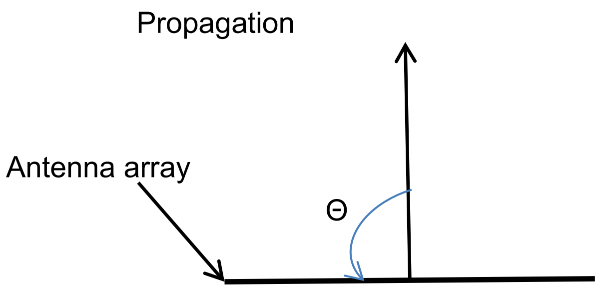

Figure 86: Top view of antenna array

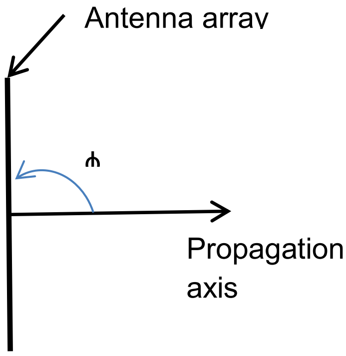

Figure 87: Side view antenna array

Due to the symmetrical planar antenna array the theta angle is defined from 0° to 90° and the phi angle is set from -90° to 90°.

Moreover, the electromagnetic wave aggression locations are unknown. Hence probes are positioning randomly around the array. The arising question is consequently: how many probes are needed?

To fill the space around the array a maximum number of probes can be chosen. The first idea was to set thousand random probes. Nevertheless the simulation time and number of meshes is very high. Thus, the second idea is to decrease the number to six hundred probes and three hundred probes. Consequently, between these two kinds of number of probes, which one is enough to run the right statistical study?

To answer to this question by using the final statistical method the comparison between these two numbers of probes has been done.

This comparison is exposed on the figure below.

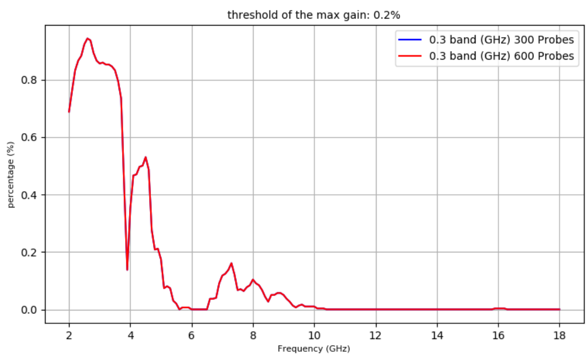

Figure 88: Comparison 300/600 probes

Each shape of curve referring of 300 or 600 probes is similar. Therefore, the number of probes is fixed at 300.

4.3 CONTENT OF THE STATISTICAL STUDY

This sub-part deals with the content of the statistical study. It explains how the statistic is made. The measuring gains are coming from each probe at each frequency from 0 GHz to 18 GHz and each angular positions (representing by phi and theta angles). The 0 GHz and 18 GHz frequencies include both the functional bandwidth and the out band frequencies.

Once all measurements coming from probes are collected the idea is to compute a probability. This probability represents the coupling percentage which symbolizes the piece of gain captured or not by the antenna.

The probability is computed as follow:

- Inside the frequency band from 0 to 18 GHz, it needs to select a sweep frequency band for the aggression with a variable size. Five sizes have been selected: 100, 200, 300, 400 and 500 MHz. Larger bands could have chosen.
- Then it needs to fix a threshold of the potential received gain. The threshold is defined as a percentage of the maximum gain in the functional bandwidth of the antenna. Again five thresholds have been taken: 10%, 20%, 30%, 40 and 50%. Not higher threshold have been used to simplify the study.

After choosing the frequency band and the maximum gain threshold a probability is calculated. This latter is estimated within the selected frequency band. Consequently this likelihood is obtained where the gain of each probe is higher than the fixed threshold. Therefore, the probability defines the percentage of the coupling at one threshold and one frequency band for every probe.

However, the interesting thing is to limit the theta angle. In fact a theta angle equal to 0° represents the propagation axis whereas the theta angle equal to 90° may define the side of the antenna. Therefore, the statistic is to measure the coupling percentage while limiting the theta angle (either in propagation axis or not) and fixing a frequency band and a threshold maximal gain.

4.4 STATISTIC ON EACH PATCH ANTENNA ARRAY

The previous explained statistic is proceeded on every designed previous antenna arrays following the same procedure.

The next curves are displaying the coupling percentage for the realized patch antenna array in the propagation axis (for theta angle equal to 10°) and for every threshold.

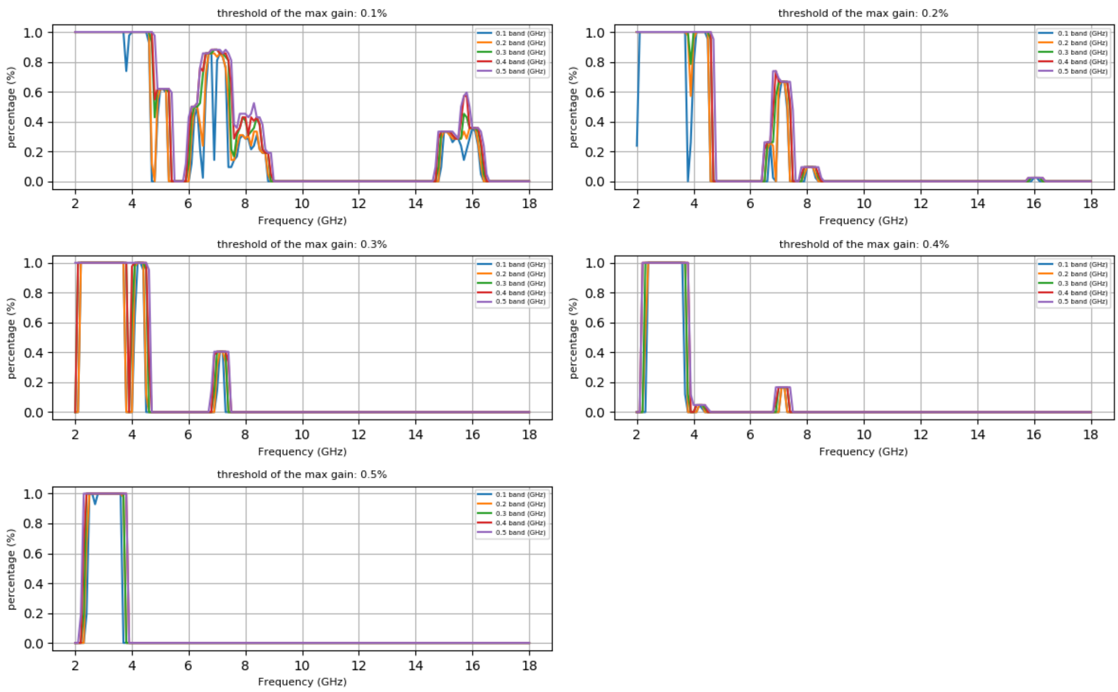

Figure 89: Coupling percentage for theta equal to 10 degrees for the realized antenna array

The table 7. is obtained following the statistical procedure as previously described and by analyzing all curves as the one showing in figure 91.

By looking at the Figure 89 it is clear the curve's shape for every kind of sweep frequency is the same; that is why in the table 7. the sweep 500 MHz is only considered.

			THETA (Θ in degrees)								
Antennas	Threshold (%)	Center Frequencies	10	20	30	40	50	60	70	80	90
Stub antenna	10	8-9 GHz	1	0.99	0.97	0.95	0.95	0.95	0.95	0.95	0.95
	50	8-9 GHz	0.98	0.4	0.35	0.35	0.35	0.35	0.35	0.35	0.35
Double patch antenna	10	8-13 GHz	1	0.95	0.85	0.80	0.80	0.75	0.65	0.6	0.6
	50	9-12 GHz	0.95	0.7	0.55	0.4	0.40	0.35	0.3	0.3	0.25
Double patch with coaxial	10	7-8 GHz	1	0.98	0.98	0.97	0.98	0.99	0.98	0.98	0.98
	50	7-8 GHz	1	0.8	0.7	0.6	0.55	0.45	0.4	0.35	0.3
Realized antenna	10	6-8 GHz	0.85	0.85	0.8	0.8	0.75	0.7	0.65	0.6	0.55
	50	/	/	/	/	/	/	/	/	/	/
Mean values	10	8-10 GHz	0.9625	0.9425	0.9	0.88	0.87	0.8475	0.8075	0.7825	0.77
	50	8-10 GHz	0.7325	0.475	0.4	0.3375	0.325	0.2875	0.2625	0.25	0.2225

Table 7: Table of coupling percentages

The table is displaying there is a special frequency band where the coupling can be maximum depending on the type of antennas. It also shows there are four different tested antenna arrays. The chart only indicates two kind of threshold, the little and the big one (10% and 50%) which represent the worst and the best case.

4.5 STATISTIC CONCLUSION

By looking at the table it clearly appears when the threshold is equal to 10% of the maximum gain, the coupling percentage is very high for each antenna array whatever the probe positioning is. However, this observation can be balanced, in fact in most observed cases while increasing the theta angle (from 0° to 90°) the coupling percentage of every antenna array is decreasing.

Moreover by taking a theta angle of 10° which represents the propagation axis for the radiation (and whatever the threshold is) the coupling probability is almost equal to 1 (around 0.95) for every antenna array. It means if the electromagnetic wave is guided by the propagation axis the center patch antenna will surely received the maximal gain (within the special frequency band).

Then by computing the average of the coupling percentage for each antenna array and for each angular position at fixed threshold it appears for the 10% threshold the percentage is lightly decreasing passing from 95% to 80% respectively from 0° to 90° of theta angle. Besides for the 50% threshold the percentage is strongly decreasing and goes from 73% to 22% still from 0° to 90° of the theta angle.

Finally the last observation is concerning the realized patch antenna array: by taking a threshold of 50% there is any chance to couple with the antenna; there is indeed any frequency band where the percentage is greater than zero.

Conclusion

The objective of the internship was to study the impact of electromagnetic perturbations on planar antenna arrays.

In one hand a sizeable bibliography has been done. It aimed at finding the antenna's theory and the potential patch antennas compatible with study. Then, for all those existed antennas several simulations have been proceeded. Moreover, realizations have also been produced. The most preferable solution has consequently been realized for measurement. Finally the comparison between the simulation and the realization of the design showed good agreement between the different kinds of antennas.

The best candidate as patch antenna has been then integrated into an array of 7 elements.

Those arrays have been simulated related to the array requirements: the position of the single antenna and the total realized gain. Hence an antenna array has been selected regarding to the results in terms of coupling and realized gain to be fabricated. Afterwards, its simulation and its realization have been compared and results exhibited good agreement.

In the other hand a statistical study has been done aiming at evaluating the filtering capability of an antenna array (based on the previous selected designs). The behavior has been studied within larger frequency band to include the *out-of-the-band* frequencies. Then, the coupling percentage under electromagnetic waves has been computed for each kind of antenna array and depending on the probe positions.

Finally, the statistical study outcomes the fact that an antenna may receive power not only inside its functional bandwidth but also outside of it (depending on parameters such as the indicent angle or the maximum gain of the array). This result offers the answer to the question that has motivated this internship.

Glossary

CEA: French Alternative Energies and Atomic Energy Commission

Index of Figures

Index of Tables

References

John L. Volakis, "Antenna Engineering Handbook (Fourth Edition)", chap. 7: Microstrip Antennas, 7-1.

John L. Volakis, "Antenna Engineering Handbook (Fourth Edition)", chap. 16: Wideband Microstrip Antennas, p16-1.

John L. Volakis, "Antenna Engineering Handbook (Fourth Edition)", part 1: Introduction and Fundamentals, p 1-1.

Robert Plonsey, and Robert E. Collin, "Principles and applications of Electromagnetic Fields", chap. 9: Time-dependent Fields, p 299.

Frederic Croq, and Albert Papieraik, "Stacked Slot-Coupled Printed Antenna", IEEE Microvave a,d guided wave letters, Vol. 1, NO. 10, October 1991.

T Balakrishman, G Ravikanth, A Vengadarajan, and Bhaskar Gupta, Senior Member, IEEE, "A Wide Band Proximity Coupled Antenna with Slot in the Microstrip Feed and the Ground Plane".

Dan Sun, Wenbin Dou, and Lizhi You, "A Wideband Aperture-Coupled Microstrip Antenna with Backed Cavity of Dielectric".

Y. T. Lo, and S. W. Lee, "Theory, Applications, and Design; Antenna Handbook"

John D. Kraus, and Ronald J. Marhefka, "Antennas for all Applications, Third Edition, International Edition".

Constantine A. Balanis, "Antenna Theory, Analysis and Design, Third Edition", Edition Wiley.

Constantine A. Balanis, "Modern Antenna Habdbook", Edition Wiley.

Appendixes

Appendix 1: Farfield Electromagnetic Fields

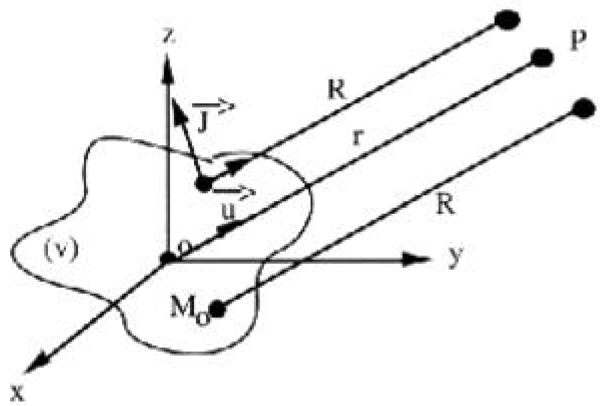

Figure 90 : Antenna for farfield computations

For a spherical distribution

$$\vec{E}(P) = \frac{jk}{4\pi}\eta\Psi(r)\iiint(\vec{J}(M_0) \wedge \vec{u}) \wedge \vec{u}e^{+j\vec{k}\overrightarrow{OM_0}}dV$$

$$\vec{H}(P) = \frac{jk}{4\pi}\Psi(r)\iiint(\vec{J}(M_0) \wedge \vec{u})e^{+j\vec{k}\overrightarrow{OM_0}}dV$$

Where $\Psi(r) = \frac{e^{-ikr}}{r}$; $k = \frac{\omega}{v} = \omega\sqrt{\mu\varepsilon}$ and $\eta = \sqrt{\frac{\mu}{\varepsilon}} = 377\ \Omega$

For a surface distribution

$$\vec{E}(P) = \frac{jk}{4\pi}\eta\Psi(r)\iint\left((\vec{J_s} \wedge \vec{u}) \wedge \vec{u}\right)e^{j\vec{k}\overrightarrow{OM_0}}\,dS$$

For a line distribution

$$\vec{E}(P) = \frac{jk}{4\pi}\eta\Psi(r)\int((\vec{u_c} \wedge \vec{u}) \wedge \vec{u})I(l_0)e^{j\vec{k}\overrightarrow{OM_0}}\,dl_0$$

Appendix 2: Kind of feeding for a patch antenna

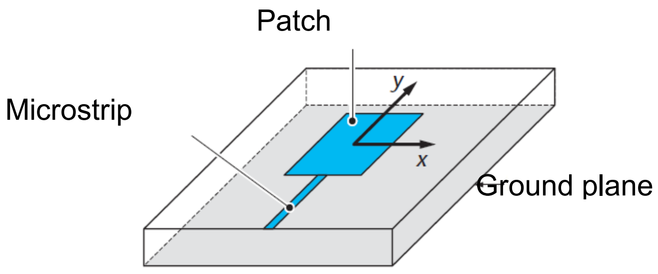

Figure 91 : Microstrip

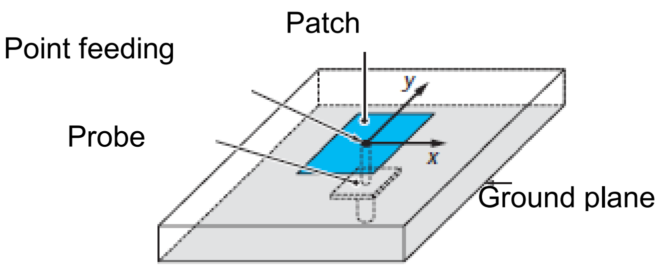

Figure 92 : Coaxial probe feeding

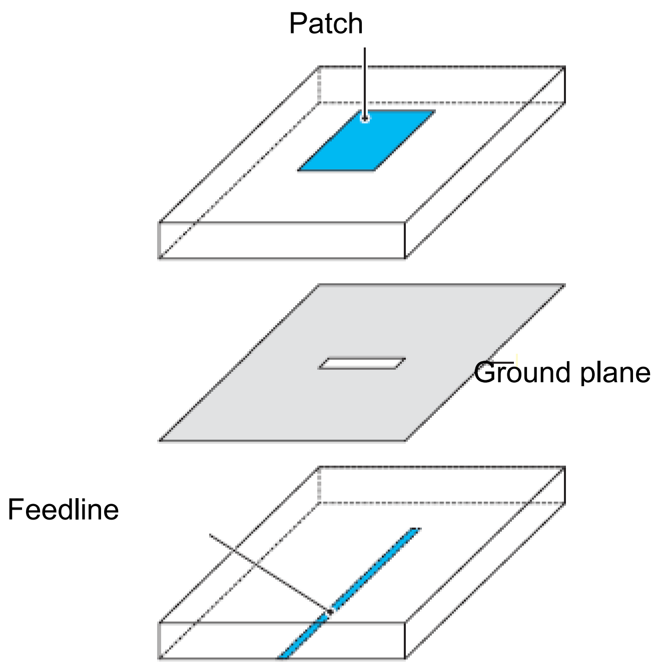

Figure 93 : Coupled aperture and microstrip

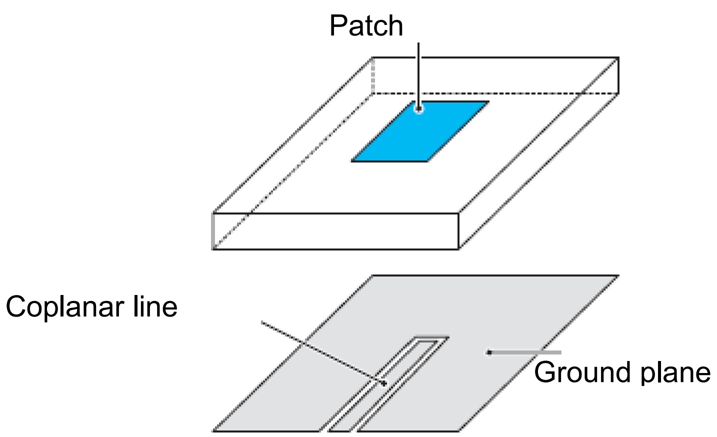

Figure 94 : CPW - Coplanar Waveguide

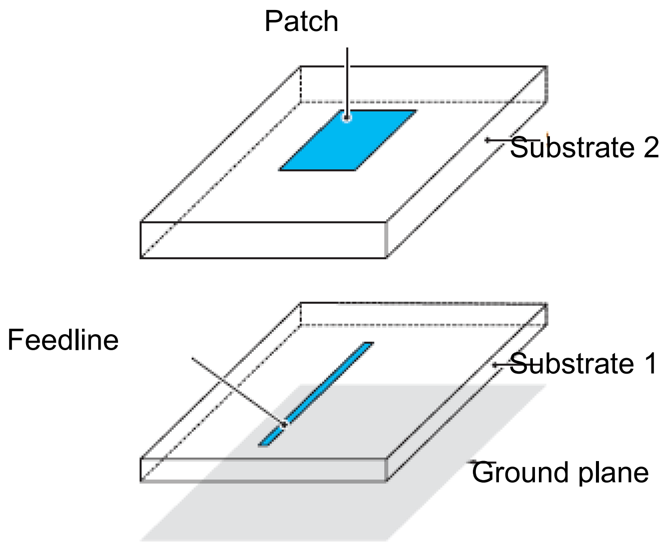

Figure 95 : Stripline

Appendix 3: Optimization 5 vias patch antenna

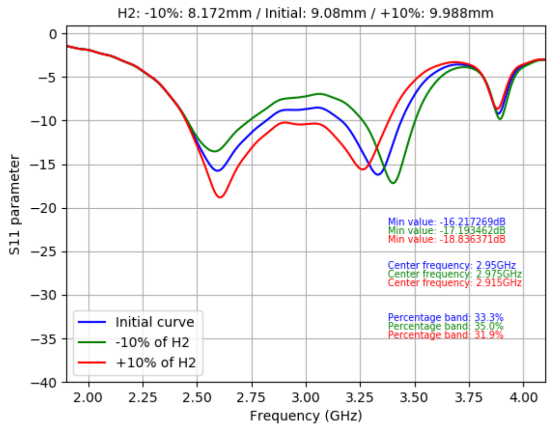

Figure 97: H2 parameter - 5 vias patch antenna

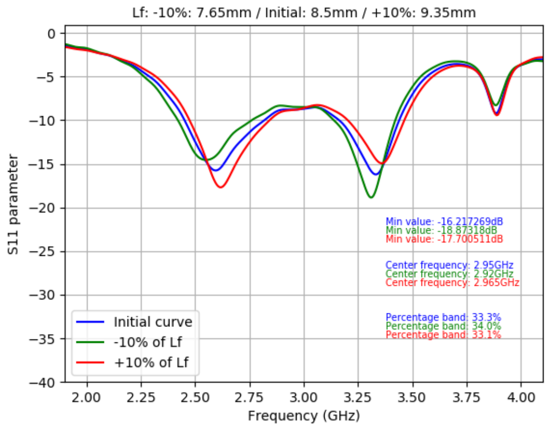

Figure 96: Lf parameter - 5 vias patch antenna

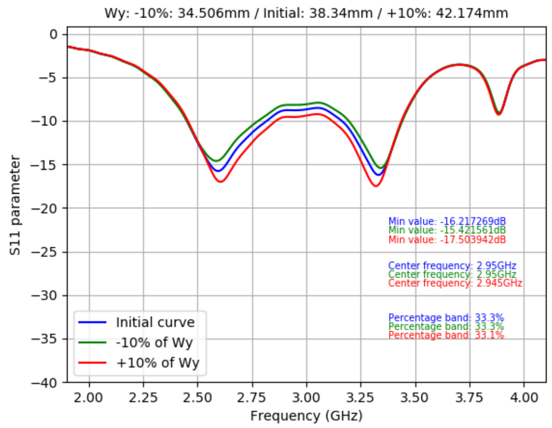

Figure 99: Wy parameter - 5 vias patch antenna

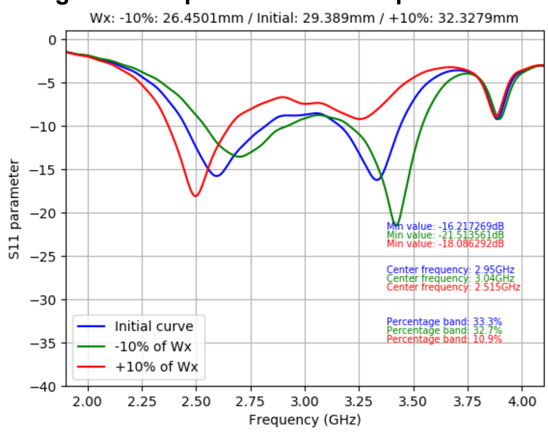

Figure 98: Wx parameter - 5 vias patch antenna

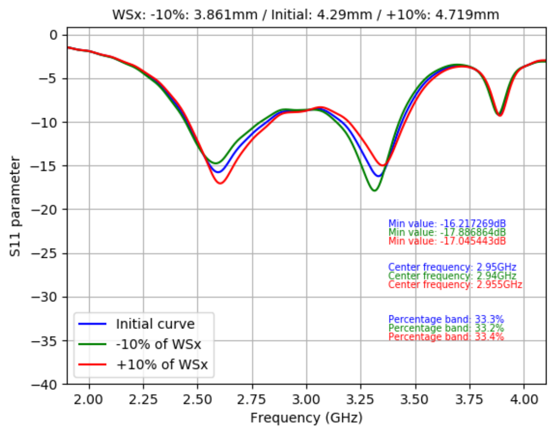

Figure 101: WSx parametr - 5 vias patch antenna

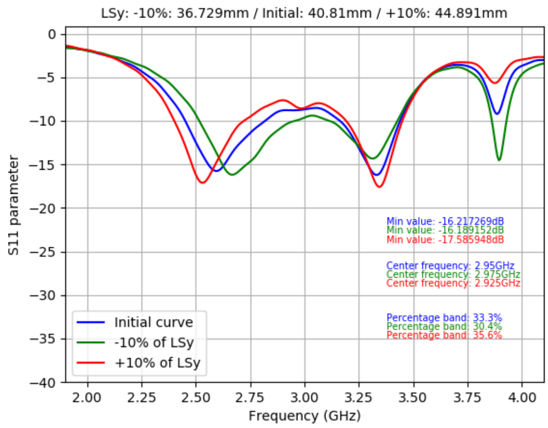

Figure 100: LSy parameter - 5 vias patch antenna

Appendix 4: Optimization 3 vias patch antenna

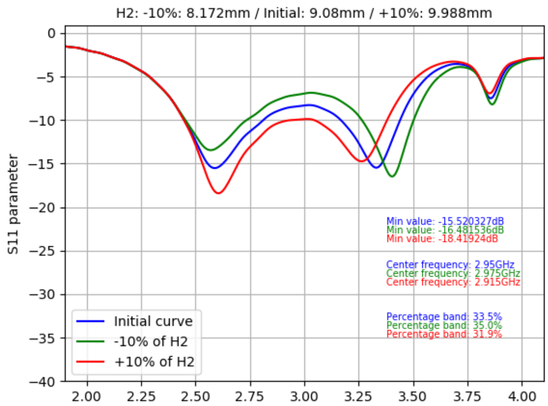

Figure 102: H2 parameter -3 vias patch antenna

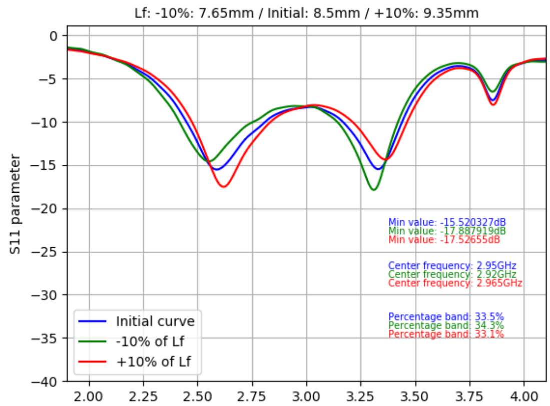

Figure 103: Lf parameter - 3 vias patch antenna

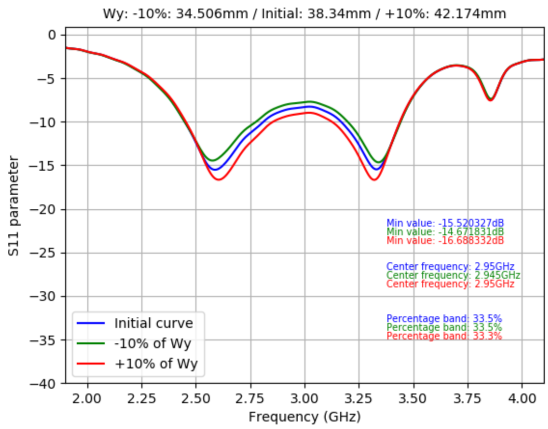

Figure 104: Wy parameter - 3 vias patch antenna

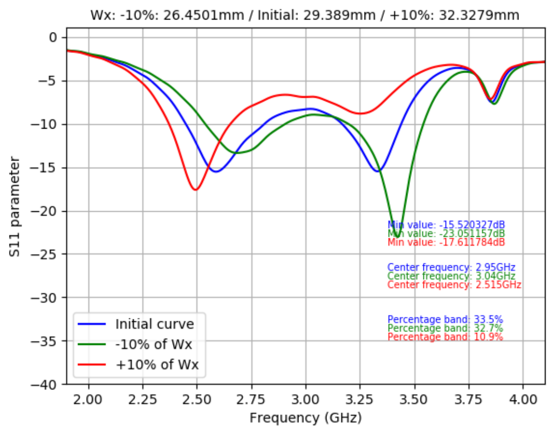

Figure 105: Wx parameter - 3 vias patch antenna

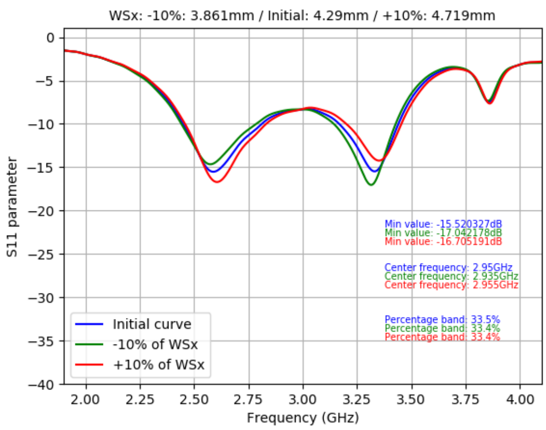

Figure 107: WSx parameter - 3 vias patch antenna

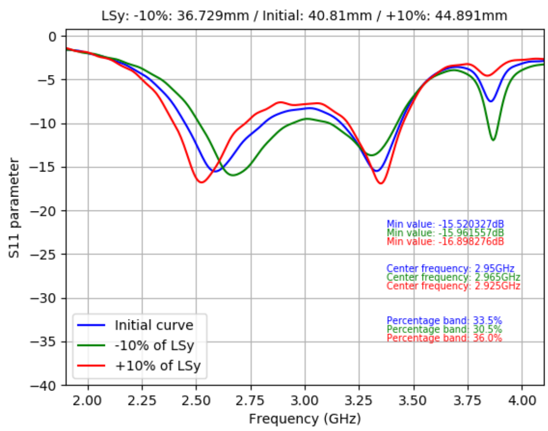

Figure 106: LSy parameter - 3 vias patch antenna

Appendix 5: Optimization on simulation for the realized antenna without vias.

This appendix is here to show what it has been obtained for the optimization on the realized antenna without any via.

First parameter H2:

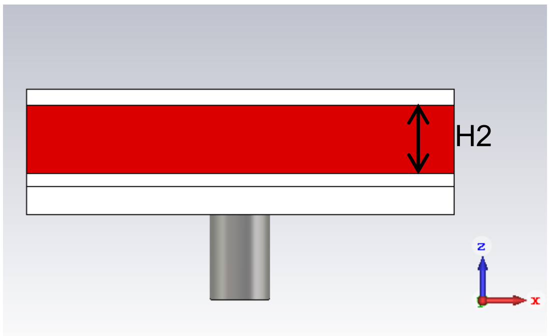

Figure 108: H2 parameter

Second parameters Wx/Wy – dimension of the patch:

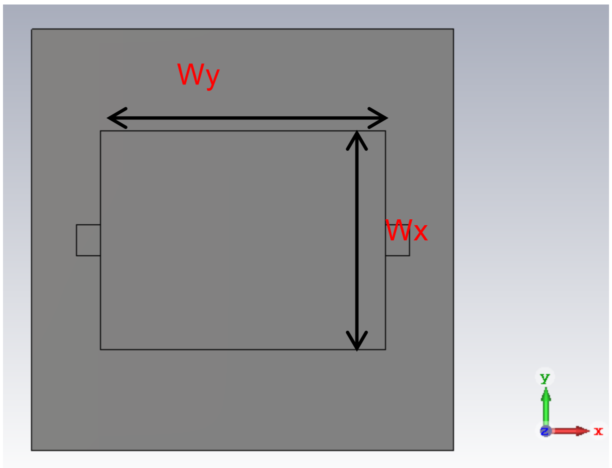

Figure 109: Wx/Wy parameter

Third parameters Lsy/Wsx – dimensions of the slot:

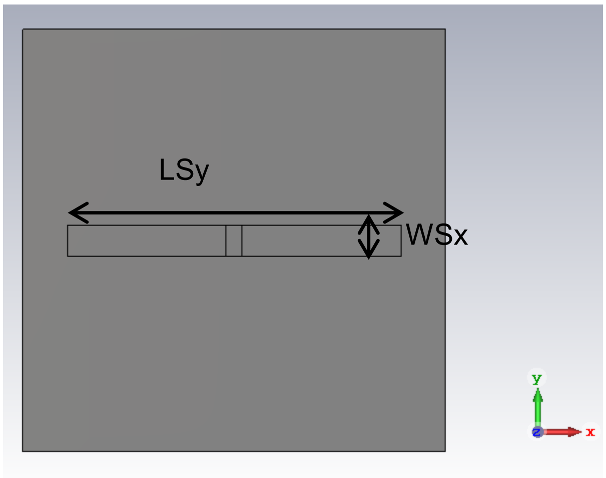

Figure 110: LSy/WSx parameter

Fourth parameter Lf:

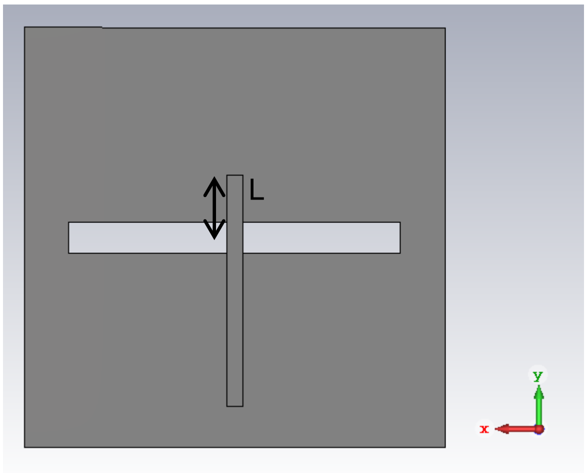

Figure 111: Lf parameter

Therefore these 6 parameters play a huge role in the influence of the S_{11} parameter.

The simulation of each parameter is done by taking for each parameter more or less 10 percent of their values.

During the simulation only three characteristics will be studied: the center frequency, the percentage of the bandwidth and the minimum value within this bandwidth. Analysing those three characteristics the influence of each parameter is thus defined.

The first parameter H2:

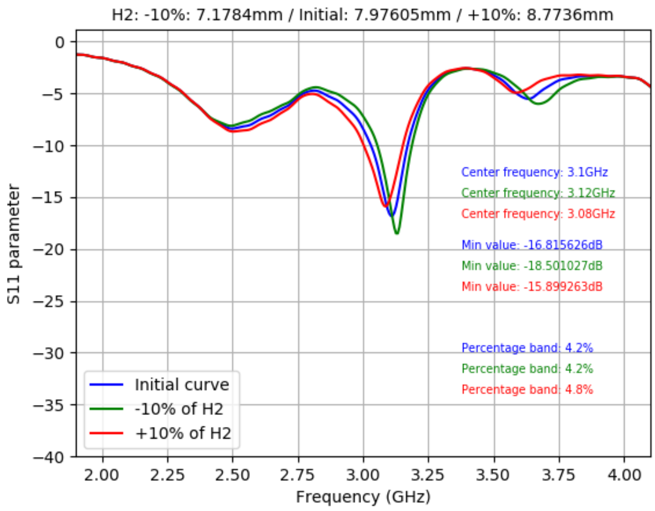

Figure 112: H2 parameter

The center frequency is shifting from 3.08 GHz to 3.12 GHz which corresponds to a 40 MHz scale frequency. Then, the minimum value within the bandwidth is more or less constant; it is around -15 dB. Finally, the bandwidth percentage is moving from 4.2% to 4.8% so there is a variation of 0.6% which is very low.

Globally the H2 parameter has a low influence of the three interested characteristics.

The second parameter Lf:

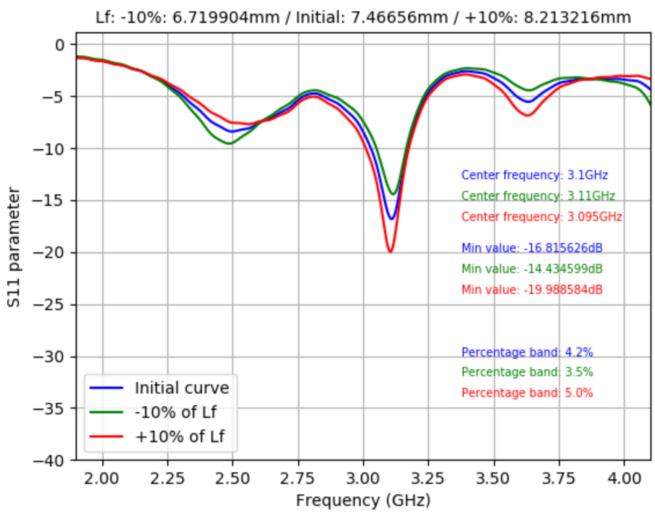

Figure 113: Lf parameter

Regarding the center frequency, the Lf parameter does not have any influence; in fact the value remains the same. However, the minimum value varies from -14 dB to – 19 dB, therefore the Lf affects the minium value within the bandwidth. Moreover, the bandwidth passes from 3.5% at -10% to 5% to +10% which corresponds to an increase in terms of frequency of 50 MHz.

Consequently, the Lf parameter affects both the bandwidth and the minium value. Increasing the Lf parameter will increase both the bandwidth and the minimum value.

The third parameter Wy:

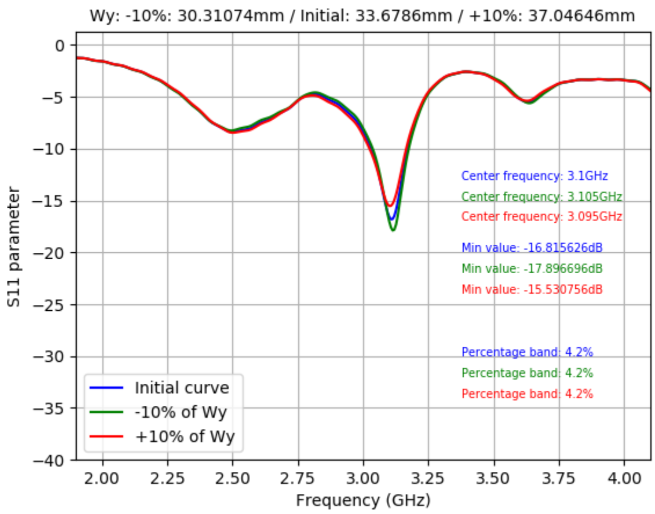

Figure 114: Wy parameter

As can be seen in the above picture the Wy parameter will only affect the minimum value which means, this parameter will better adapt the antenna an the center frequency.

Generally the Wy parameter does not any major influence on the three characteristics. Both the bandwidth and the minimum value remain constant.

The fourth parameter Wx:

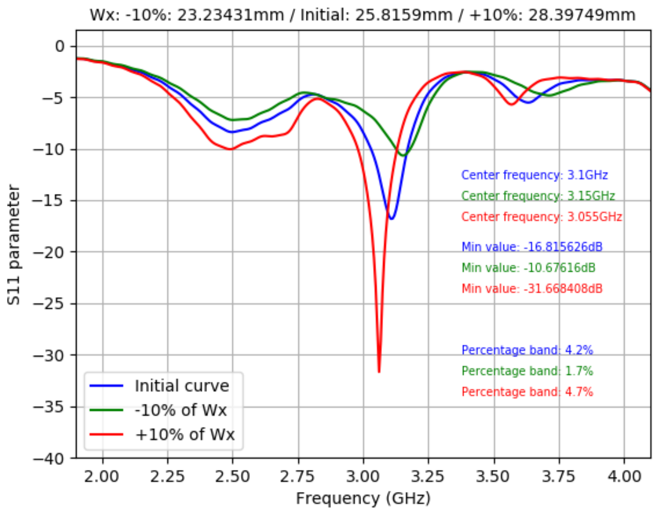

Figure 115: Wx parameter

Increasing the parameter Wx by 10 percent the center frequency is scaling from 3.1 GHz to 3.055 GHz, moreover the major influence is seen for the minimum value. From the initial value to the plus 10 percent value, the minimum value within bandwidth varies from -16 dB to 31 dB. The same observation as done for the minimum value can be seen for the bandwidth. There is a little increase of it.

So far the Wx parameter has the major influence on the three characteristics. It affects mainly the minium value at the center frequency by increasing its value.

The fifth parameter WSx:

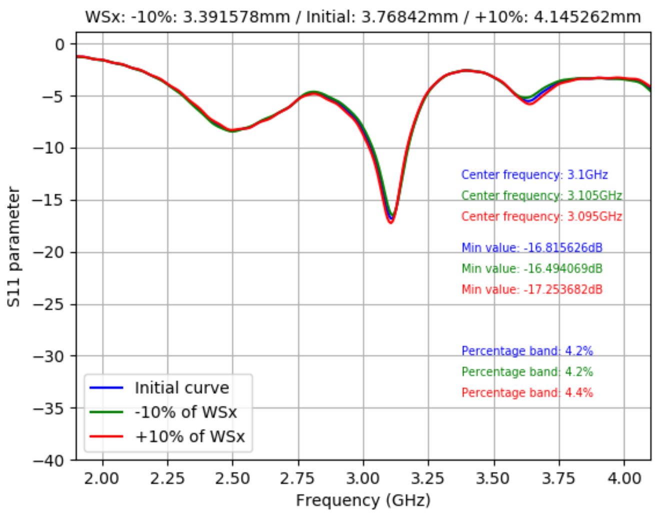

Figure 116: WSx parameter

Each curve for different value of WSx are merging. Therefore, the WSx parameter which is the width of the aperture does not affect the three interested characteristics at all.

The sixth parameter Lsy:

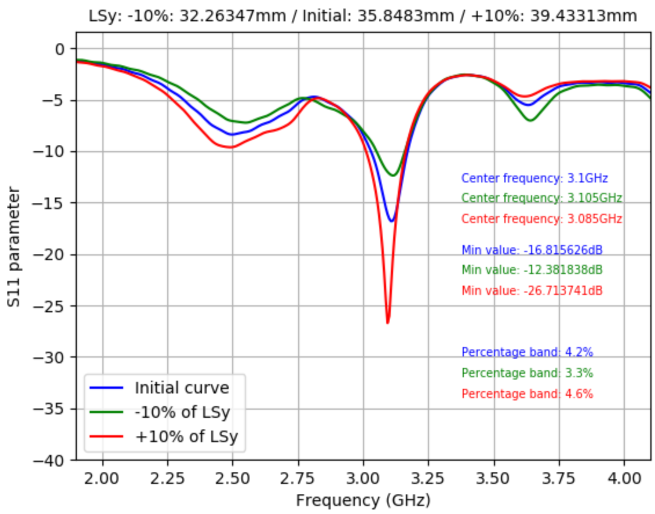

Figure 117: LSy parameter

The LSy parameter mainly affects the minimum value at the center frequency. In fact, it passes from -12 dB to -26 dB. By taking +10 percent of LSy the antenna is better adapted. Regarding the bandwidth it evolves around 0.5% from the initial while increasing the LSy length by 10%.

The LSy parameter is the second major influencer parameter. It affects mainly the minimum value at the center frequency and poorly the bandwidth.

Appendix 6: The different kind of used arrays.

Stub patch antenna

This antenna is made with a stub on its feedline.

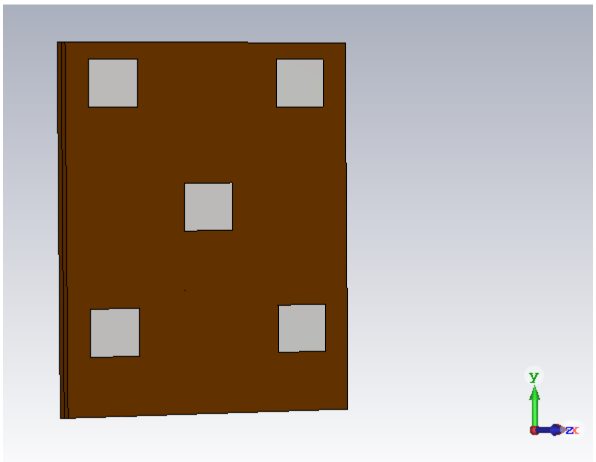

Figure 118: Stub patch antenna

This is the S_{11} parameter to summarize what it has been found in the previous chapters.

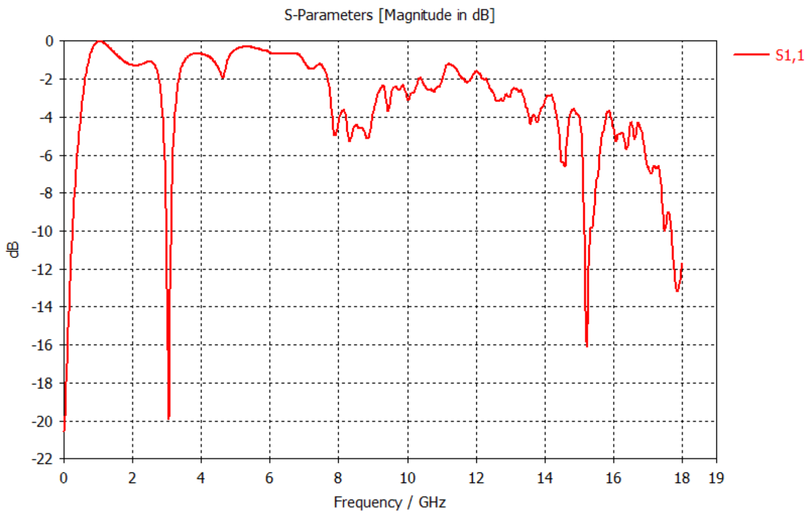

Figure 119: S11 parameter stub patch antenna

When the probe is set in propagation axis, the coupling is very high within several bandwidths; its percentage indeed is equal to 100 percent whatever the band frequency for a threshold equal to 10 percent of the total gain. It means when the antenna receives only 10 percent of the total gain the coupling is very high.

However, when the probe for the theta angle is set on the antenna's side the percentage decreases from 90 percent to 20 percent while the threshold is passing through 10 percent to 50 percent.

The double patch wih aperture antenna

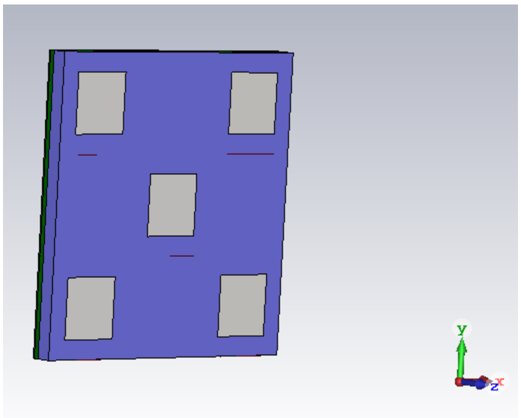

Figure 120: The double patch with aperture array

This is the S_{11} parameter to summarize what it has been found in the previous chapters.

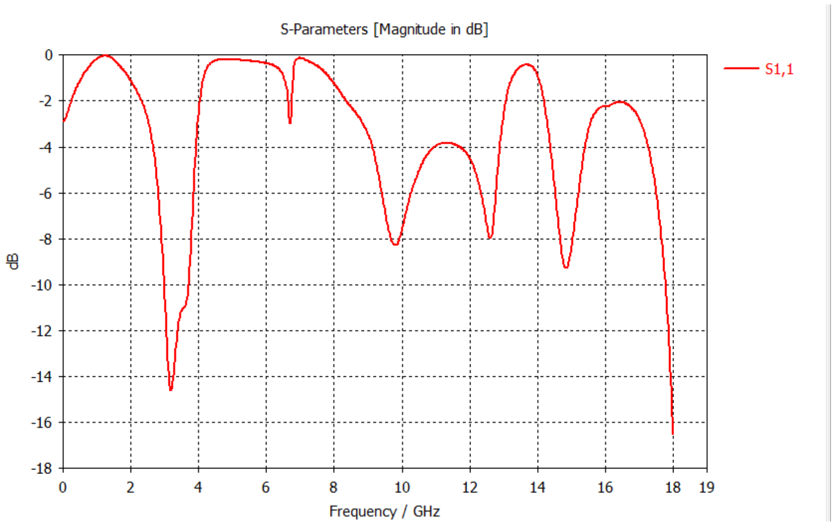

Figure 121: S11 for the double patch with aperture

When the probe is set in propagation axis, the coupling is very high within two main bandwidths; its percentage indeed is equal to 100 percent whatever the band frequency for a threshold equal to 10 percent of the total gain.

Instead when the probe for the theta angle is set on the antenna's side the two previous observed bandwidths are still visible however the coupling percentage decreases from 90 percent to 20 percent while the threshold is passing through 10 percent to 50 percent.

The double patch feeding by coaxial probe array

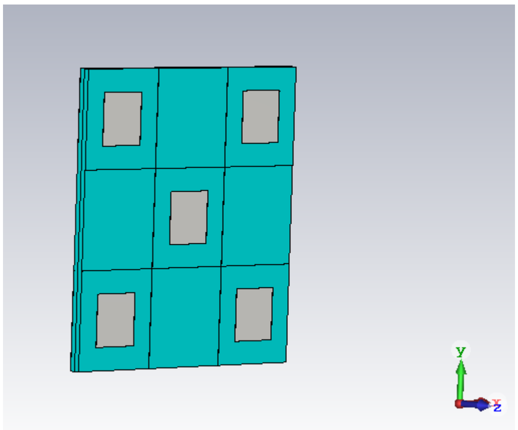

Figure 122: The doube patch feeding by coaxial probe array

This is the S_{11} parameter for the double patch antenna feeding by coaxial probe.

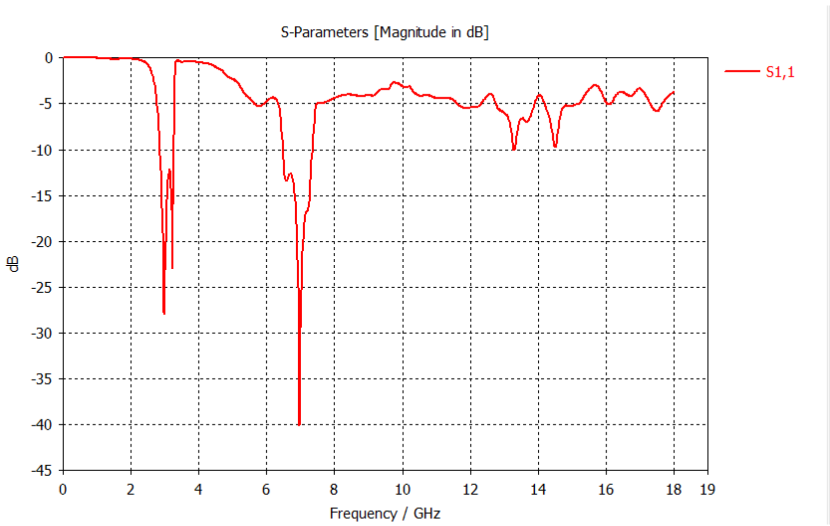

Figure 123: S11 parameter for the double patch feeding by coaxial probe array

When the probe is set in propagation axis, the coupling is very high within three main bandwidths; their percentages indeed are equal to 100 percent except for the third one which is equal to 80 percent whatever the band frequency for a threshold equal to 10 percent of the total gain.

Instead when the probe for the theta angle is set on the antenna's side the first bandwidth is still visible however from 6 GHz to 18 GHz there is always a percentage at least equal to 20 percent for the coupling while the threshold is passing through 10 percent to 20 percent.

Annexe 7: Ethique/Développement durable/Santé et sécurité au travail.

La qualité du CEA Gramat, son environnement, la santé et la sécurité de ses employés fait l'objet d'un service dédié. Pour veiller au bon fonctionnement de l'entreprise, il est obligatoire de suivre certaines règles.

Ethique/Qualité

Le CEA Gramat utilise la norme ISO 9001 v2015 afin d'organiser les activités de soutien et de production. Cette méthode a pour but de « travailler efficacement et de façon homogène », mais aussi d'éviter les dysfonctionnements, les éventuelles pertes de temps et d'argent ». La finalité est donc de s'améliorer continuellement.

La méthode s'applique sur toutes les activités du centre et sur son impact environnemental.

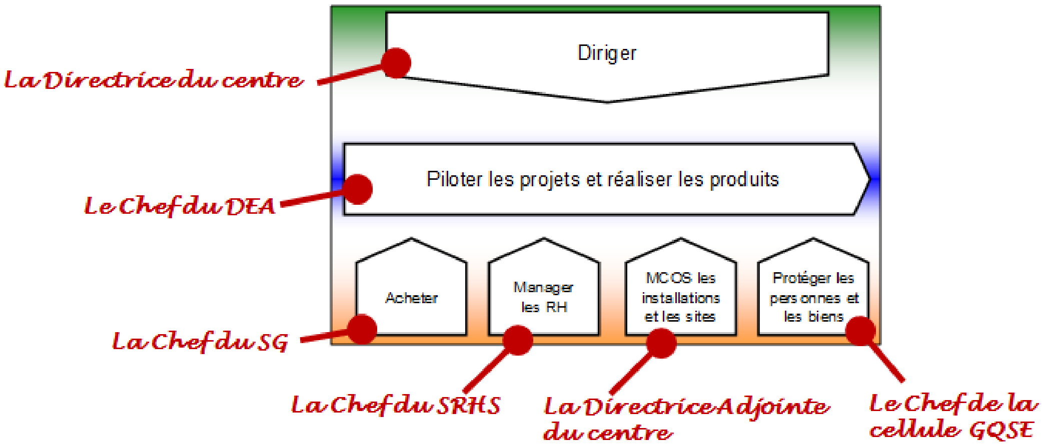

Figure 124: Les acteurs du processus qualité

Développement durable

Le tri sélectif est respecté au CEA Gramat afin de trier les déchets produits par le centre. En effet, le plastique, le papier et les déchets ménagers sont séparés.

Le CEA Gramat est un SIENID c'est pourquoi il dispose d'un Plan de Surveillance de l'Environnement. Il s'agit là de surveiller l'impact sur l'environnement des installations présentes sur le site : cela permet de vérifier l'absence de marquage et de pollution.

Santé et sécurité au travail

La santé au CEA Gramat

« Le Service de Santé au Travail a pour mission première exclusive d'éviter toute altération de la santé des travailleurs du fait de leur travail ».

Au CEA Gramat, une infirmière et une assistante sociale sont disponibles pour répondre aux demandes des employés et notamment les urgences. Elles sont également là pour prévenir les risques professionnels, de faire en sorte d'améliorer les conditions de travail et enfin de contribuer au maintien dans l'emploi des travailleurs.

La santé des travailleurs est surveillée en parallèle avec la sécurité du site, en effet chaque employé est soumis à des règles de sécurité à respecter qui pourraient le cas échéant nuire en son intégrité.

Sécurité au CEA Gramat

La sécurité au CEA Gramat est effectué à l'aide de plusieurs acteurs, ceux-ci gravitent tous autour de la directrice qui coordonne les opérations de ses acteurs. Le lien entre les acteurs et la directice du centre sont deux types : soit fonctionnelle soit hiérarchique.

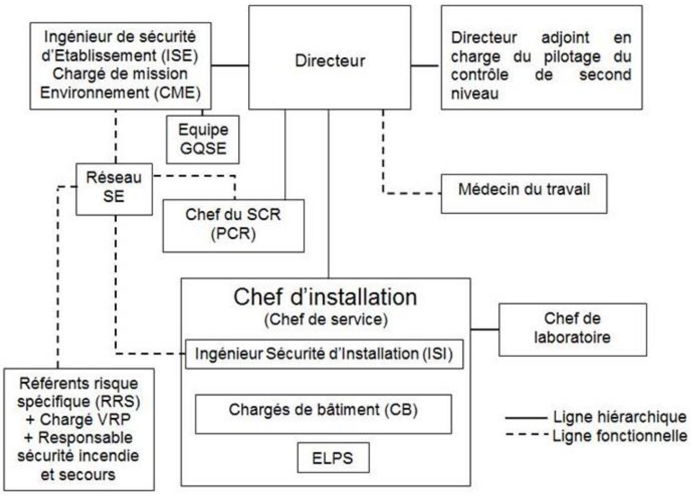

Figure 125: Schéma de l'organisation sécurité du CEA Gramat

Pour chaque manipulation sur un site, une fiche de sécurité est faite par le responsable technique (celui qui demande la manipulation). Cette fiche, après analyse des éventuelles risques, est validée par le chargé du bâtiment, l'ingénieur sécurité d'installation et enfin le chef d'installation.

Cette fiche de sécurité décrit l'expérience à venir, avant les moyens et les outils utilisés pour la réaliser.

Glossaire

GQSE : Groupe Qualité Sécurité Environnement

SIENID : sites et installations d'expérimentations nucléaires intéressant la défense